UNIVERSITA' DEGLI STUDI DI PADOVA

Sede Amministrativa: Università degli Studi di Padova

Dipartimento di Innovazione Meccanica e Gestionale

SCUOLA DI DOTTORATO DI RICERCA IN INGEGNERIA INDUSTRIALE
INDIRIZZO: INGEGNERIA DELLA PRODUZIONE INDUSTRIALE
CICLO XXIII

STUDY ON THERMAL AND RHEOLOGICAL PARAMETERS OF HIGH STRENGTH STEELS IN HOT FORMING CONDITIONS

Direttore della Scuola: Ch.mo Prof. Paolo F. Bariani
Supervisore: Ch.mo Prof. Paolo F. Bariani

Dottorando: Daniele Pellegrini

Table of contents

Abstract

Hot stamping of high strength steels is one of the technological processes, in the field of sheet stamping, that is achieving a major increase in popularity among manufacturers due to the capability of obtaining higher quality products while reducing costs. Its adoption is particularly intense in the automotive industry, where it has enabled to increase the strength-to-weight ratio of several components, thus enabling to reduce vehicles emissions, improving environmental friendliness, and enhance their performance and crash safety, reducing meanwhile the needed material quantities.
In this process, the sheet is heated over austenitization temperature and maintained at that temperature until a fully austenitic microstructure is achieved. Then it is transferred from the furnace to the press and there formed and quenched at the same time using cooled dies. Forming at elevated temperature enables to improve formability and reduce springback while obtaining a final shape with particularly elevated mechanical performances.
The relatively late increase in popularity of this process has however limited the number of experimental studies performed about it. More than this, the use of elevated temperatures adds a layer of complexity to the process analysis, which therefore requires the design of specific tests.
The aim of this work is to analyze and improve the knowledge about two main issues regarding a stamping operation performed at elevated temperatures: the assessment of material formability and the study of the thermal evolution of the sheet under the dies.
The analysis of formability is one of the most pressing issues since its proper evaluation is vital for the correct design of a process. Methods using continuum damage mechanics are still too complex for a useful employment in an industrial environment and the more advanced experimental methodologies for formability assessment, such as Nakajima and Marciniak tests, doesn't take into account sheet temperature and its influence on material properties. In this work an experimental equipment has been specifically developed to perform Nakajima tests at elevated temperatures, recreating on the specimen conditions similar to those achieved during hot stamping. Then an experimental campaign has been performed using such equipment in order to assess the formability of a commonly used ultra high

strength steel.
Another major issue relative to the analysis of an hot stamping process is the evaluation of the thermal evolution of the sheet inside the dies. The vast majority of studies performed as of today on that purpose were aimed at assessing the process parameters that enabled to reach a fully martensitic microstructure at the end of the stamping operation. This work is aimed at improving such knowledge extending the analyses to the whole spectrum of cooling rates achievable. The possibility of exploiting such knowledge to obtain functionally graded sheets, locally lowering the cooling rates to a point where martensitic transformation is inhibited, has also been investigated, theorizing the use of ceramic die inserts in order to locally reduce the heat transfer coefficient. Two analytical models have been developed on that purpose to individuate the most influencing factors, whose effects were then studied through experimental testing. Finally, the results of the experimental tests were used to validate the numerical results and assess the feasibility of such technique, underlining its limits and its field of application.

Sommario

Lo stampaggio a caldo di acciai alto resistenziali rappresenta uno dei processi tecnologici, nel campo dello stampaggio di lamiere, che sta riscontrando un sempre maggiore interesse tra i produttori grazie alla capacità di ottenere, attraverso il suo impiego, prodotti di qualità superiore, riducendo nel contempo i costi. La sua adozione è particolarmente significativa nel campo dell'industria automobilistica, dove ha di fatti permesso di aumentare il rapporto resistenza-peso di molti componenti, consentendo quindi di ridurre le emissioni prodotte dai veicoli, riducendone l'impatto ambientale, e di migliorarne performance e sicurezza in caso di impatto, riducendo contemporaneamente le quantità di materiale richiesto.

In questo tipo di processo il materiale è riscaldato oltre temperatura di austenizzazione e mantenuto in tali condizioni fino a che una microstruttura completamente austenitica si sia sviluppata nel pezzo. Questo viene quindi trasferito dalla fornace alla pressa e lì formato e temprato contemporaneamente attraverso l'uso di stampi raffreddati. Lo stampaggio a tali temperature permette di migliorare la formabilità e ridurre i fenomeni di ritorno elastico ottenendo a fine stampaggio un pezzo dalle elevate caratteristiche meccaniche.

Il relativamente tardo aumento di interesse per questo processo ha limitato tuttavia il numero di studi sperimentali condotti al proposito. Oltre a ciò, l'utilizzo di temperature elevate introduce una serie di complessità relativamente alle analisi sperimentali necessarie per una adeguata comprensione del processo, per la quale è quindi necessario progettare test specifici.

L'obiettivo del presente lavoro è l'analisi e il miglioramento delle conoscenze riguardo due problematiche fondamentali relative ad un'operazione di stampaggio effettuata ad elevate temperature: lo studio della formabilità del materiale e dell'evoluzione termica del pezzo all'interno degli stampi.

L'analisi della formabilità costituisce uno dei problemi di maggior rilievo in quanto la sua corretta valutazione è un elemento fondamentale per la corretta progettazione del processo. I metodi basati sulla meccanica di danneggiamento del continuo sono ancora troppo complessi per un loro uso proficuo in campo industriale e i più avanzati test per l'analisi della formabilità, come i test Nakajima e Marciniak, non considerano la temperatura della lamiera ne tanto meno la sua influenza sulle proprietà del materiale. In questo lavoro è stato specificatamente

sviluppato un apparato sperimentale per l'esecuzione di test Nakajima ad elevate temperature, in modo da ricreare sul provino condizioni simili a quelle reali di processo. Tale apparato è stato quindi utilizzato per condurre una campagna di test al fine di verificare la formabilità di un acciaio alto resistenziale in condizioni di stampaggio a caldo.
L'altra problematica considerata è relativa all'analisi dell'evoluzione termica della lamiera all'interno degli stampi. La pressoché totalità degli studi eseguiti ad oggi al proposito ha mirato a valutare i parametri di processo che consentano di ottenere una microstruttura totalmente martensitica a fine processo. Questo lavoro si propone di migliorare la conoscenza degli effetti dei parametri di processo sui profili di raffreddamento ottenibili, proponendo di utilizzarla al fine di ottenere lamiere a gradiente di proprietà meccaniche, andando a ridurre localmente la velocità di raffreddamento e quindi inibendo la formazione di fase martensitica. A tal fine si è valutata l'opportunità di utilizzare inserti ceramici negli stampi in modo da ridurre il coefficiente di scambio termico all'interfaccia. Due modelli numerici sono stati sviluppati in modo da analizzare i fattori più influenti, che sono poi stati studiati attraverso una serie di campagne sperimentali. Infine, i dati ottenuti sono stai comparati con quelli predetti dai modelli numerici e si è valutata la fattibilità di tale tecnica, valutandone i limiti per l'applicazione in campo industriale.

Chapter 1

Introduction

1.1 Context

The needs of modern automotive industry define some of the most critical areas on which researches on manufacturing technologies are being focused as of today. The impact of such industry on a global scale is very heavy indeed and as such, every step forward in cost reduction and improvement of the quality of the final products can have huge repercussions, both on the manufacturers and on the final costumers. In particular, many advancements are being achieved relatively to the manufacturing of structural parts of car bodies through sheet metal forming. Many new materials are gaining more and more popularity, therefore broadening the spectrum of alternatives and solutions that can be followed for the design of such structures. Every one of the used materials has to be chosen as the most appropriate for the specific functions that it will be going to satisfy, taking into account and trying to compromise manufacturing necessities and the desired specifications of the final product. In this light, the adoption of high strength steel is becoming one of the most prominent interests among car manufacturers.
These materials features elevated mechanical properties that make them particularly suitable for many critical structural parts. The manufacturing process needed to take advantage of their unique properties, the hot stamping, was developed and patented in 1977 but it wasn't until 1984 that it was adopted for the manufacturing of a structural component in a standard mass production vehicle[1]. Since then, the adoption of these materials has seen a rapid increase, coming from the 3 millions parts per year produced in 1987 to the 8 million parts per year produced in 1997 to the approximately 107 million parts per year as of 2007[2]. This corresponded also to an increase of the number of the different structural parts manufactured using these materials and, as of today, their role in the

production of car bodies is particularly prominent, as visible in Figure 1.1, and it's still constantly gaining increasing importance.

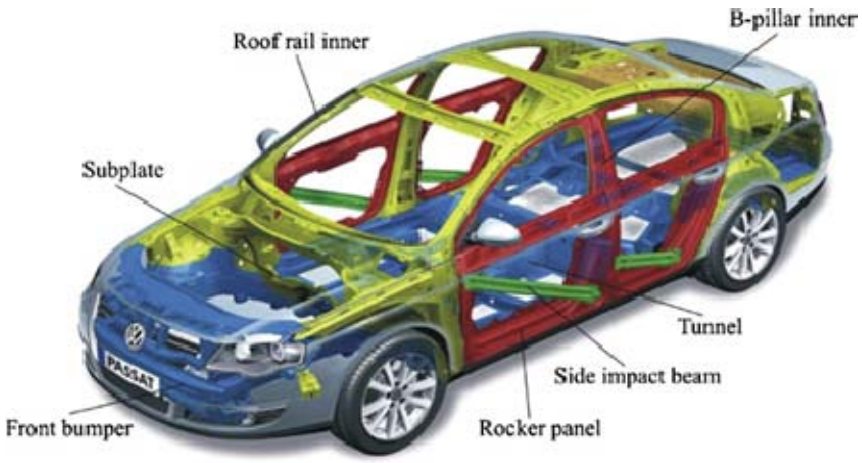

Figure 1.1: Parts manufactured using hot stamped parts in a modern vehicle[3]

These materials possess indeed very peculiar characteristics. Their high stress resistance and consequently their elevated strength-to-weight ratios enables to employ less material, lightening the overall structure, while maintaining structural integrity, especially in critical situation such as crash impact absorption[4]. Less material needed also implies that significant cost reductions can be achieved[5]. Moreover, lighter vehicles have reduced emissions and fuel consumption, thus improving environmental friendliness[6]. However, these steels can prove to be challenging to use in manufacturing processes were the forming operations performed with the same methodologies used for standard steel grades.
Their microstructure, indeed, before appropriate heat treatment, is not that different from those of other commonly used materials, being basically ferritic-perlitic, thus possessing similar mechanical properties and not constituting a particularly attractive choice. However they distinguish from other steel grades from the fact that they are particularly quenchable and therefore, once at elevated temperature and possessing a fully austenitic microstructure, they don't require particularly elevated cooling rates in order to achieve a complete martensitic final microstructure[7]. After quenching the formability is particularly low, and that's why the stamping must be performed before or together with the quenching itself.
In this process, known as hot forming, the sheet gets heated over austenitization temperature in a furnace, undeformed or already stamped, left there for the time needed to develop a completely austenitic microstructure and then rapidly transferred to the press and formed or calibrated in cooled dies, simultaneously quenching the sheet. At the end of the pressing operation the final shape achieves good geometrical accuracy and possesses a fully martenistic microstructure. The elevated temperatures at which the sheet gets pressed greatly reduce the stresses needed to achieve plastic deformations, thus reducing the forming forces needed, and greatly reducing springback phenomena[8][4]. Formability also improves in a

significant way, extending the range of geometries achievable.

1.2 The industrial problem

It is clear that hot forming constitutes a very attractive process due to all its different obvious advantages both relatively to process productivity and to the quality of final products. However, the use of elevated temperatures adds a completely new layer of complexity in the evaluation and design of pressing operations and in the estimation of the final properties of the stamped parts. In the light of using numerical analysis tools to predict sheet behavior during forming, the change in material properties due to temperature and microstructural evolution has to be taken into account. Also, microstructural evolution itself depends on many different factors, first of all on temperature profiles achieved along the piece.
In this context, the correct assessment of material properties at different temperatures while in austenitic phase is a very critical step for the correct analysis of hot stamping processes. Many different studies have been recently published in order to fill these gaps, both in terms of experimental data and in terms of proposal of analysis tools and methodologies[9]. However there are still major shortcomings in different fields, one of which is the analysis of the formability of these materials. This is due both to the complexity of the test needed and to the necessity of taking into account all the major influencing factors during the test themselves.
Another major issue derives from problems that are eventually encountered when finishing operations such as trimming and cutting are necessaries. These are performed, in the vast majority of cases and for obvious practical reasons, after the forming operations, with the component having its final martensitic microstructure. This implies that those operations requires high loads and produce elevated stresses and wear were they performed using cutting tools[10]. This in turn induce low geometrical accuracy and in some cases even early failure of the tools themselves[11]. Other technologies can be adopted that can overcome those issues, such as laser cutting techniques, but they imply additional and usually not negligible costs. Therefore many researches are being aimed at obtaining different final microstructures in different areas of the same piece, thus achieving functionally graded shapes where softer microstructure could be located in correspondence of the areas that should be cut, reducing shear stresses. This could also prove to be very useful in improving the impact resistance if those softer microstructures are reached in critical spots were energy absorption is to be preferred over structural integrity.
In order to achieve such results, however, the development of proper methodologies is necessary and this requires a deep and sound knowledge of the thermal evolution of the piece inside the dies and of its driving physical

phenomena. This type of study in reference to hot stamping processes has only be marginally considered in literature since the major problem, as of today, was to assure a cooling rate elevated enough to achieve quenching throughout the piece.

1.3 The objective of work

The present work has been focused in analyzing what were deemed to be as two fundamental issue about hot forming processes. These are the evaluation of the forming limit of employed steels and the achievement of functionally graded pieces at the end of a forming operation.
In order to evaluate the forming limits of an UHSS sheet it has been decided to specifically develop an experimental equipment designed in order to be able to perform the tests needed to evaluate such limits with an accurate control of the influencing parameters. After proper calibration and testing, it has been chosen to analyze the formability in dependence of temperature of one of the materials most commonly used in hot stamping operations, the 22MnB5.
For the analysis of the feasibility of obtaining functionally graded shapes, it has been decided to evaluate the possibility of imposing, during the forming operation, different cooling profiles in different areas of the same piece, thus achieving different final microstructures. This highlighted the need to perform an analytical study of the thermal evolution of the blank, individuating the driving physical phenomena involved and developing two different numerical models in order to spot the most interesting cases to be analyzed through experiments. These were eventually performed and the feasibility and the limit of application of such methodology were assessed. Finally, the results obtained through experimental testing were compared to those of the analytical model in order to assess their accuracy.

Chapter 2

Literary review

2.1 The hot stamping process

The hot stamping process can be considered in two main iterations, direct and indirect hot stamping, as visible in Figure 2.1. In the direct stamping method, the sheet is heated in a furnace over austenitization temperature, then extracted and transferred to a press where it is, at the same time, formed and quenched in cooled dies. In indirect hot stamping, near net-shape cold preformed parts are used instead of undeformed blanks, which are heated and then quenched and calibrated in a pressing operation, also performed with cooled dies.

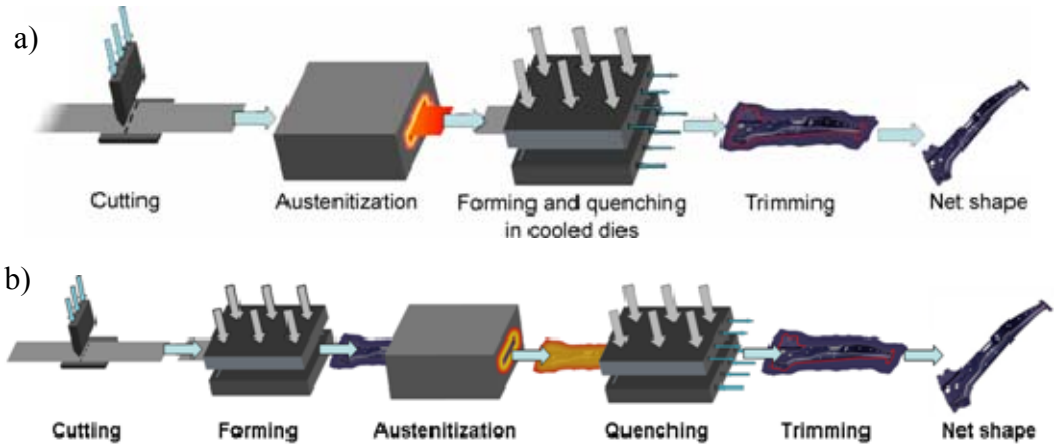

Figure 2.1: Two main iterations of the hot stamping process: a) direct hot stamping, b) indirect hot stamping

The materials used in these process, denominated Ultra High Strength Steels, can achieve elevated mechanical properties after quenching, reaching up to 1500 MPa of final tensile strength in spite of the about 600 MPa of the same steels before being heat treated. This enables to maintain or improve the mechanical resistance of final products while greatly reducing the thickness of the metal sheets used. Their mechanical properties after quenching are visible in Figure 2.2 in comparison to those of other common steel grades.

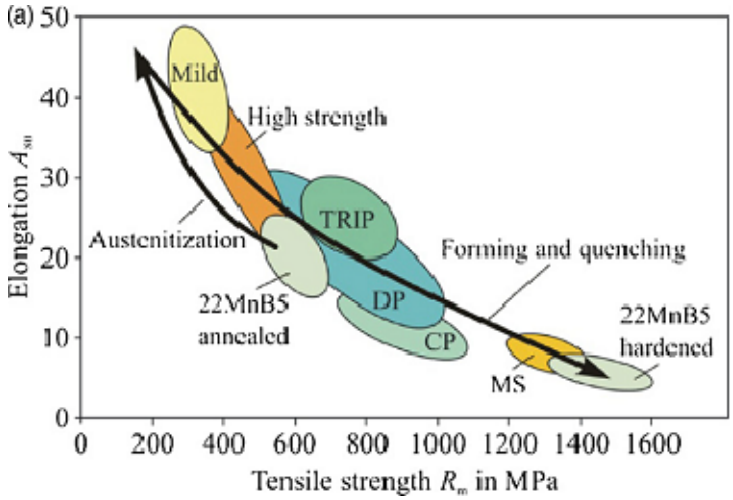

Figure 2.2: Classification of High Strength Steels in relation to maximum elongation and tensile strength at fracture[12][9]

If the forming operation is performed along with quenching at elevated temperatures, the advantages brought by this process extends over the achievement of elevated mechanical properties as process performances gets improved as well. As a matter of fact, the specific thermal conditions of the sheet enhance formability lowering flow stresses. This has a direct impact on the obtainable geometries and on the loads required in order to form the blank. More than this, the springback effects are also greatly reduced improving geometrical accuracy.

As of today, only three steel grades have exhibited the capacity of reaching a fully martensite microstructure at the end of a quenching process performed with cooled dies, all of them being boron alloys: 22MnB5, 27MnCrB5, 37MnB4. The mechanical properties before and after quenching of these are visible in Table 2.1[9]. In this work the attention is focused on the 22MnB5 alloy which is one of the most widely used in hot forming operations.

Material	Martensite start temperature [°C]	Critical cooling rate [°C/s]	Yeld Stress [MPa]		Tensile strength [MPa]	
			As delivered	Hot stamped	As delivered	Hot stamped
20MnB5	450	30	505	967	637	1354
22MnB5	410	27	457	1010	608	1478
37MnB4	350	14	580	1378	810	2040

Table 2.1: Mechanical and thermal properties of high strength steels

Four main phases can be distinguished in a typical hot forming process: cutting of the blank from the batch, heating in a furnace over austenitization temperature, forming and quenching in cooled dies and trimming.
During the cutting from the batch operation, the sheet is usually cut from a coil in order to obtain the needed dimensions and profiles for the blanks.
After cutting, the thermal treatment begins to be applied to the sheet as illustrated in Figure 2.3, which shows a typical temperature profile applied on a blank.

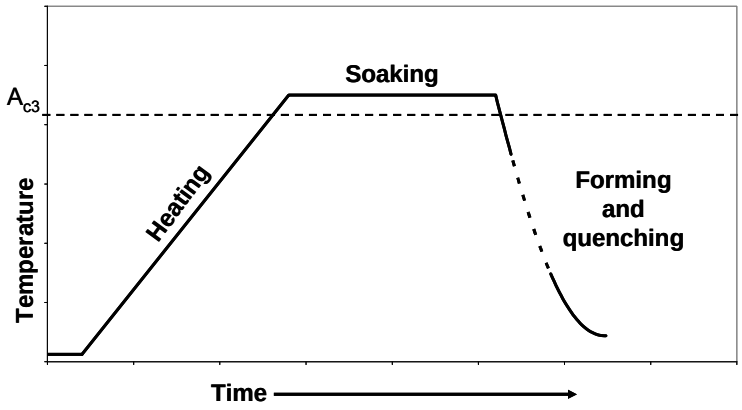

Figure 2.3: Typical temperature profile applied on a sheet in a hot stamping process

The heating is one of the most critical operations for an hot forming process. Here the blank is heated over austenitization temperature, which is of 830°C for a 22MnB5 alloy, and maintained at such temperatures in order to assure that a fully austenitic microstructure is achieved. Different studies have been performed in order to analyze the dependency of heating temperature and sheet thickness on the minimum dwell time needed to obtain a fully martensitic microstructure. These studies, their results visible in Figure 2.4, have shown that a minimum of 3 minutes are needed for heating performed at 950°C, which is a temperature commonly used in actual manufacturing processes, in order to obtain a fully austenitic microstructure before stamping and therefore a fully martensitic microstructure at the end[13].

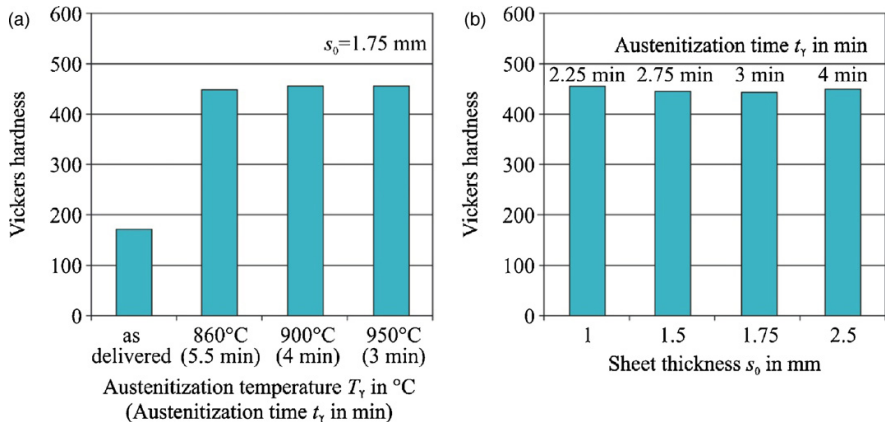

Figure 2.4: Hardness of a sheet after hot stamping in dependence of austenitization temperature, austenitization time and sheet thickness. Values over 400 HRV indicates a fully martensitic microstructure

Moreover, slow heating times are frequently needed in order for one of most commonly used coating, an Al-Si coating developed by Arcelor, to be effective due to its dependence on iron atoms diffusion from steel to coating itself[14]. The use of this type of coating therefore also put an upper limit to the time that the blank can spend in the furnace since coating layer thickness must be contained under 40μm to ensure accurate enough weldability[9]. As of today, roller hearth furnaces are the only type of heating furnaces employed, but these imposes the need for large volumes since a furnace be as long as 40m. More than this, they also has low energy efficiency. This has brought at analyzing alternative heating methods, such as conduction and induction heating, which are currently being developed[15], in order to make them suitable for industrial applications.

The forming phase is where actual forming and quenching take place. In order to avoid unwanted microstructural transformations and therefore be able to achieve a fully martensitic microstructure in the final pieces, the temperature drop due to transferring from furnace to press must be contained as much as possible. To that extent, usually, automated system are employed which enable to achieve transferring times as low as 3s. Also, in order to avoid quenching of the blank due to blank holders contact, distance blank holders are frequently used.

An investigated possibility for the improvement of this kind of processes is the use of working media. These methodologies are actually being developed and will hopefully increase the application field of these materials. The working medias considered as of today are nitrogen and air. These are used to form the blank after the closing of the tools and therefore freeform of the piece takes place in the initial phases of the forming operation. Lower contact times of the piece on the dies are also obtained, thus achieving a more uniform temperature profile on the piece itself which therefore has more homogeneous mechanical properties throughout its geometry[16][17].

In order to achieve a complete martensitic microstructure and to avoid the possibility that thermal distortions could arise during cooling after forming, the

blank is usually maintained in the closed dies until it reaches 150°C, which reflects in closing times of about 10s. This has been proved to be reducible up to 2s in case that particular steels, with improved thermal conduction, are used for the tools[18].

One of the most critical aspects in this process is also the proper design and production of the dies. Since the thermal aspect is a key issue, the opportune placement and geometrical definition of the cooling ducts is a matter of uttermost importance. Currently, three manufacturing options are available. The first consider drilling the holes directly into the tools, where limitations due to machining operations have to be taken into account, thus limiting the range of geometries achievable and therefore limiting the effectiveness of the cooling system. Another option involve the use of ducts placed directly into the casting mould of the dies, enabling a total control of their geometry, but with the arise of other technological problems. The third and final option consider using packs of laser cut die segments screwed together. While being the most cost effective option, this also limits the geometrical accuracy achievable at the end of the stamping process[9].

After the extraction from the press, the blank is usually cut and trimmed to obtain the net shape. The use of standard hardened cutting tools is frequently avoided in favor of laser cutting techniques, which are considerably less cost effective. The elevated shear rate of the martensitic microstructure can indeed greatly lower tool wear resistance, thus lowering the quality of the trimmed piece, and in some cases even bring the tools to anticipated failure. Several studies have been conducted, relatively to cutting with hardened tools, in order to analyze the effects of the different process parameters on the quality of the sheared surface and on the geometrical accuracy achievable. No influence of punch speed on blanking forces and obtained geometries has been seen, while the rollover increase with the increase of the clearance of the punch on the die, whether the blanking angle considered. Also, the influence of the clearance on burr formation has been investigated[11]. Particular attention has been also given to the choice of die materials, where studies have shown that an optimal compromise of toughness and hardness must be found to improve the performances of cutting operations[19].

Due to all the aforementioned disadvantages, laser cutting techniques are therefore frequently preferred. Even if the equipment costs for such process are usually higher, wear and failures of the cutting tool are avoided, while having the possibility of easily cutting complex shapes maintaining the same geometrical accuracy throughout time.

2.2 Material properties

2.2.1 Chemical and thermal properties

As stated in Chapter 2.1,only three steel grades are suited for an hot stamping process: 22MnB5, 27MnCrB5, 37MnB4. Their chemical composition can be seen in Table 2.2.

Material	Al	B	C	Cr	Mn	N	Ni	Si	Ti
20MnB5	0.04	0.001	0.16	0.23	1.05	-	0.01	0.40	0.034
22MnB5	0.03	0.002	0.23	0.16	1.18	0.005	0.12	0.22	0.040
37MnB4	0.03	0.001	0.33	0.19	0.81	0.006	0.02	0.31	0.046

Table 2.2: Chemical composition of Ultra High Strength Steels in percentages[9]

When these boron alloys are cooled after austenitization, at cooling rates over about 27°C/s, a diffusionless transformation involves their microstructure which becomes martensite starting from about 425°C, the so called martensite start point, and completes at about 280°C, the martensite finish temperature. In these materials, the mechanical properties after quenching are directly dependent on the carbon content of the alloy and so different mechanical properties can be achieved varying that value. Chromium and Manganese have little effect on the final mechanical strength, but are of vital importance in improving the hardeanability of the steels. However, the element that has the major effect in improving that feature is the Boron, which slows the transformation into softer microstructure[20].
One of the major issue in the use of these steels for an hot stamping process is the prevention from oxidation. Since they have to be heated at elevated temperatures and maintained at those temperatures for a certain amount of time while remaining in an oxidizing atmosphere, due to manufacturing reasons, the use of a proper coating layer is mandatory.
One of the most commonly used coating is the Al-Si coating provided by Arcelor-Mittal, as it proved to be an optimal protection agent against oxidation. This costing has an initial thickness of 23μm to 32μm. During heating, the Fe in the steel substrate diffuse into the Al-Si layer, thus preventing scale formation. The coating has its melting point at about 500°C but during heating the diffusion of Fe form Al-Si-Fe alloys that have a higher melting point, thus enabling the formation of an homogeneous protecting surface. Being diffusion a thermally activated process, that therefore evolves throughout time, the heating rate must be kept reasonably low in order for this phenomena to properly develop. The optimal heating rate value has been evaluated as being about 12°C/s[21]. This coating has however low forming limits and is therefore not indicated for use in indirect hot stamping processes.
Other coatings have been considered in literature, such as hot-dip galvanized zinc layers, which offers cathodic protection but, in order to minimize microcracks

propagation from coating to the base material, it is mainly used in indirect hot stamping, and x-tec, which can be used both in direct and indirect hot stamping processes, offers active corrosion protection, substitute the role of lubricants in cold forming operations and is based on a combination of μm-scaled materials applied with a sol-gel process[22].
The steel considered in this work is 22MnB5 with Al-Si coating, produced by Arcelor-Mittal under the commercial name of USIBOR 1500P.
Due to the thermal properties of this steel, during the heating phase of a hot stamping process the sheet is heated over A_{C3}, which is at about 830°C, usually at temperatures around 900°C, and then it's left at that temperature for about 5 minutes. The minimum cooling rates needed to obtain a fully martensitic microstructure in this material, as visible from its characteristic CCT curves which can be seen in Figure 2.5, is 27 °C/s.

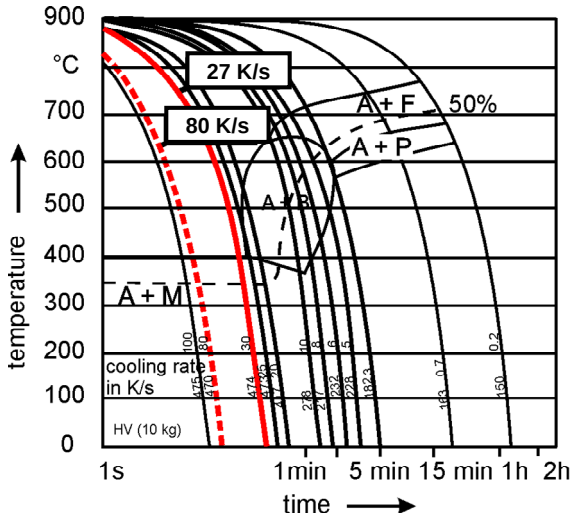

Figure 2.5: CCT diagram of USIBOR 1500P

2.2.2 Rheological properties

The evaluation of the rheological properties of these steel grades plays a fundamental role for the proper understanding of material flow during hot stamping operations and therefore in the ability to correctly design this type of processes. Many different studies are therefore being aimed at obtaining a deep and sound understanding of the mechanical behaviour of such steels in the particular thermal conditions in which they are stamped.
In fact, most of the stamping operations are nowadays carried at ambient temperature or at warm forming conditions at best. The use of high temperatures diminish the effects of parameters are usually important in cold forming operations such as rolling direction, defining anisotropy, whereas other parameters, such as strain rate, assume a more prominent role.

Specific attention has been given in the last few years to the evaluation and modelling of the flow behaviour of 22MnB5 in dependence of temperature and strain rate when it has a completely austenitic microstructure, since the vast majority of deformations happen when the material temperature is still well above martensite start temperature. In order to study this dependences, a number of authors have performed numerous monoaxial traction tests with a particular attention to the thermal profile applied to the specimen and to the lasting of the deformation phase itself, in order to avoid phase changes during test. The applied thermal cycles usually mimics those founded in a real hot forming process, such as that visible in Figure 2.6a. Examples of the flow curves obtained through these tests are visible in Figure 2.6b.

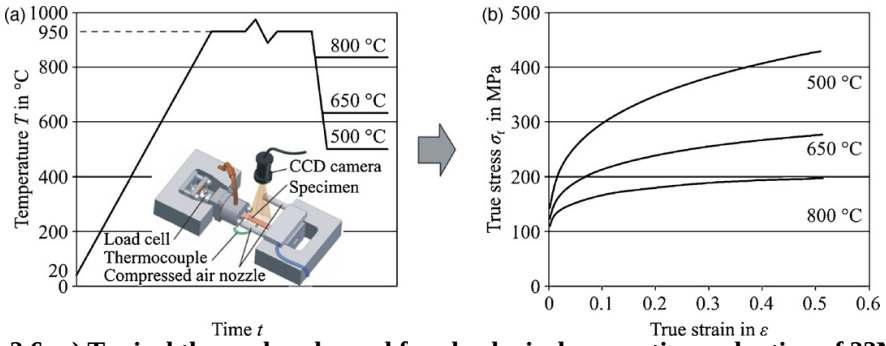

Figure 2.6: a) Typical thermal cycle used for rheological properties evaluation of 22MnB5; b) Flow behaviour of 22MnB5 at different temperatures[7]

It is clear from these figures that temperatures variations have a great effect on material behaviour and that at the increase of temperature the plasticity of the material increase significantly and the slope of the initial material work hardening decrease as well. This behaviour is mainly attributed to the increased dislocation mobility achieved at the rise of temperature, that lowers the stress needed to apply a plastic deformation. The effects of strain rate have also been analyzed and an example of that influence is exemplified in Figure 2.7.

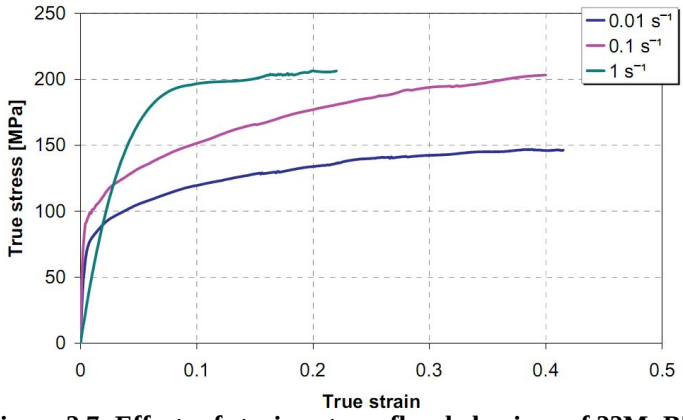

Figure 2.7: Effects of strain rate on flow behaviour of 22MnB5[4]

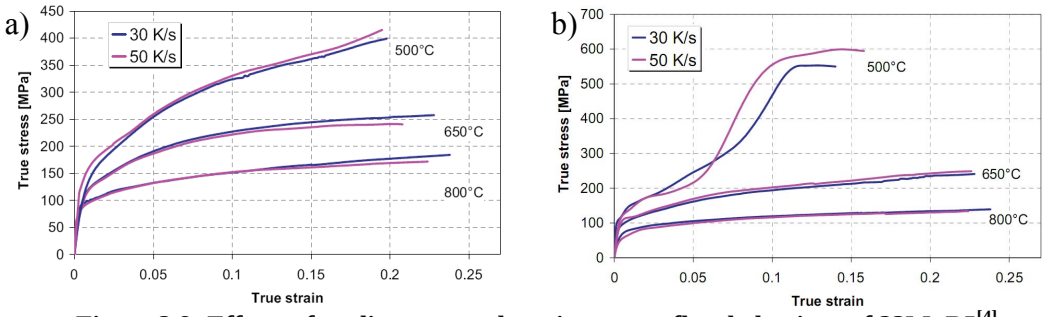

Figure 2.8: Effects of cooling rate and strain rate on flow behaviour of 22MnB5[4]

It is clear from these results that lower strain rates lead to a lowering of the flow stresses due to occurring of dynamic recovery processes balancing the strain dependent hardening.
The dependence on cooling profile has also been investigated. A broad range of cooling rates have been applied to the specimen after the austenitization and before the actual traction test. Examples of the results from these tests are visible in Figure 2.8a and Figure 2.8b.
These test showed that cooling rates as low as that achievable with cooling in calm air, quantified in 15 °C/s, don't affect the material behaviour as long as the deformation temperature is over 650°C.
On the other hand, at 500°C, the flow curve exhibit a sudden increase of the flow stress due to beginning of bainitic transformation[4].
Plastic anisotropy was also analyzed in relation to temperature and the results showed that at a temperature of about 800°C-850°C the material exhibits an almost isotropic behaviour. In fact, the austenitization procedure, and the consequent change in microstructure, reduce the influence of the rolling direction to a point that its effect can be not considered in the material analyses[23].
The number of information regarding UHSS behaviour at different temperatures is quite sound and accurate, but their importance in process design directly depends on the possibility of employing such data in FEM codes. The same reasons that limited the number of studies performed on hot forming processes also limited the reliability and availability of these. To this end, a number of codes have been considered and their suitability analyzed by different authors.
It is clear that the classic material models cannot describe sufficiently well the mechanical behaviour of the material due to the fact that many different parameters, thermal, microstructural and mechanical, have to be taken into account for a correct prediction of the material flow. As such, different models, semi-empirical and physically based, have been investigated in literature.
One of the models considered is the Voce model with the inclusion of Kocks model for the evaluation of the saturation stress in dependence of temperature and strain rate. This has been used to predict rheological results and has been compared with the Molinari-Ravichandran model, which features the ability to account for history effects thanks to the evolution law of the internal parameter.

The latter can be linked to the characteristic length scale of the microstructure that develops in the material throughout the test. These models shown a good capacity to predict the behaviour of 22MnB5 in hot forming conditions, as visible in Figure 2.9.

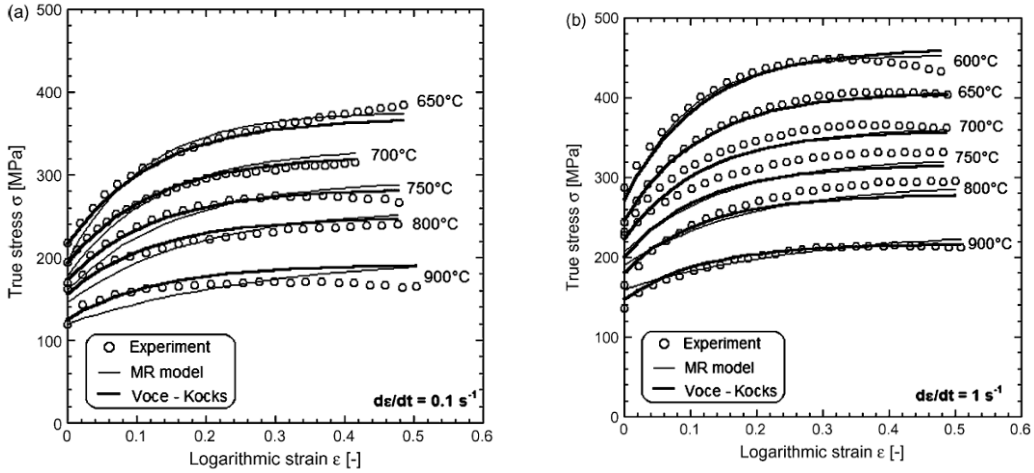

Figure 2.9: Experimental data and numerical predictions comparison of 22MnB5 flow behaviour evaluated using Voce-Kocks and Molinari-Ravichandran models at a) 0.1s^{-1} and b) 1s^{-1} of strain rate

The Voce-Kocks model produced slightly better results and uses less parameters than the Molinari-Ravichandran model, which in turn is more flexible due to its ability to account for history effects[24].
Other analyzed models are the ghost model, which shows a good agreement up to a plastic strain of 0.05, the Nemat-Nasser and Norton-Hoff models, which however cannot accurately predict the saturation of the flow tress at high values of plastic strain, the Tong-Whalen, which have shown to be one of most capable of accurately fit the experimental data, and Johnson-Cook model, which is incapable of correctly represent the flow stress at relatively large plastic strains[25].

2.3 Formability evaluation

The correct numerical formulation of a model capable of correctly predict the rheological behaviour of the material doesn't constitutes the only necessary factor needed for a exhaustive analysis and design of a hot stamping process. In order to possess a comprehensive knowledge of the limits of the process, in terms of maximum applicable deformation on the blank, a formability analysis has also to be performed.
The determination of formability is a major issue in the analysis of a hot stamping process due to its dependence on a number of different parameters. In fact, both

material mechanical, thermal and microstructural characteristics and the considered process conditions plays a decisive role in its definitions. More than this, numerical methodologies usable to predict failure in sheet metal forming at elevated temperatures, such as continuum damage mechanic, are still in an early stage of development and adoption, thus making the availability of exhaustive experimental data a pressing issue.

Different methodologies have been proposed throughout time in order to evaluate formability. These comprise different levels of completeness, which is usually achieved at the increase test complexity, and range from the analysis of simple monoaxial traction tests, to more accurate tests such as cupping and bulging, to even more complex procedures such as Nakajima and Marciniak tests.

Monoaxial traction tests are able to evaluate the values of stress and strains that bring the specimen to failure for a single strain condition. They feature the ability to perform the test in highly controlled environment and the possibility to analyze a wide variety of test parameters. However, they can't consider complex stress states and therefore can only be used for preliminary analyses.

Cupping and bulging tests uses a punch, in the case of the cupping test, or a working medium, in the case of the bulging test, in order to apply a more complex stress state on the sheet. The one analyzed through these tests is close to the planar deformation case. The results are given in terms of maximum punch displacement and load or maximum pressure before failure. They are relatively simple and fast but, even if they consider a strain condition more similar to those achieved in a real stamping process, they are also limited, due to the fact that only a generic evaluation of material formability can be achieved[26].

Some of the most important tests in order to correctly analyze the formability of sheet metals are those that enables to draw the FLC diagram of the material. The latter, a representation of which is visible in Figure 2.10, has been introduced by Keller[27] and Goodwin[28] and has been widely adopted both in industrial and academic context alike. It represent the formability limit for different strain paths for a given material, describing the area and therefore the couples of principal strains that are likely to conduct to the onset of instability.

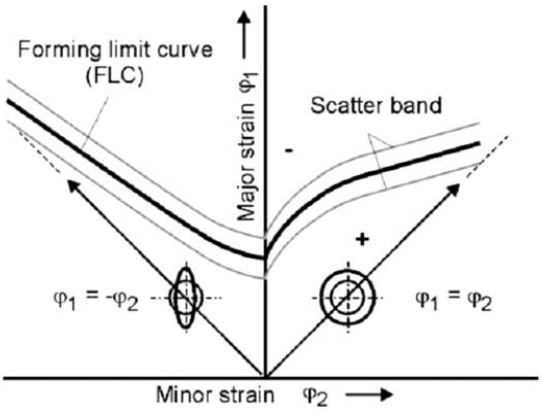

Figure 2.10: Generic FLC diagram with indication of its most important features

The tests that are most commonly used in order to trace an FLD are the Nakajima and the Marciniak ones.
Typical Nakajima and Marciniak test setups are visible in Figure 2.11a and Figure 2.11b.

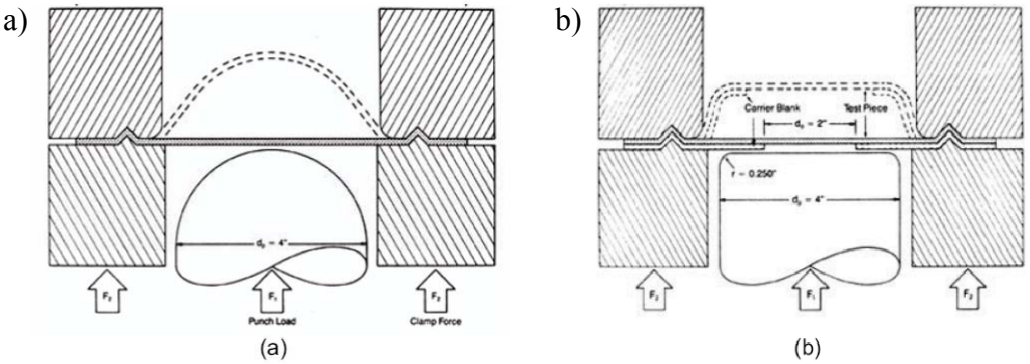

Figure 2.11: Schematic representations of a) a Nakajima test and b) a Marciniak test for formability evaluation

A Nakajima setup features a clamping equipment, on which the specimens are fixed, and an hemispherical punch. The punch, moving at a constant speed, deforms the specimen until it fractures. Then the strains on specific sections on the surface of the specimen are evaluated so that values of major and minor strain are obtained. These two values defines a strain conditions that brings the sheet to failure. Using different specimen geometries, different strain fields could be imposed on the specimen, thus obtaining two sets of major and minor values that describe the Forming Limit Curve of the given material[29].
Since the obtained values of major and minor strains depend on the punch-sheet interaction it is vital, in order to obtain accurate values, that sheet deformation is as close as possible to a free forming case. Therefore, particular attention has to be given to lowering as much as possible the friction at the punch-sheet interface and usually very low punch speeds are also adopted[30]. More than this, since slipping of the specimen in the clamping equipment has to be absolutely avoided in order to not alter the material flow during testing, the die holders usually features specifically designed drawbeads.
The Marciniak test setup uses the same working principle of the Nakajima test, being a bit more complicated but enabling to avoid the effects of friction through the use of a carrier blank that function as an interface, avoiding the direct contact of the punch, which is flat in a Marciniak setup, with the specimen[31].
The evaluation of the Forming Limit Curve through experimental testing is a costly and time consuming process. Therefore through time different numerical model have been proposed in order to evaluate those results considering material rheological data. These were formulated on the basis of classical or modified Swift and Hill instability criteria[32],[33],[34]. One of the most accredited models is

the one proposed by Marciniak and Kuczynski and is based on the assumption that, in biaxial strain conditions, the strain is localized in an area of geometric non homogeneity. These mathematical representations, even the Marciniak-Kuczynski model, lack however the ability to predict the FLC with sufficient accuracy due to the fact that many different factors, such as anisotropy, grain size, material imperfections, affect their shape[35] and most of the models start from not experimentally justifiable assumptions. More than this, the mathematical models are strongly dependent on the evaluation of the yield locus, which also is a costly and time consuming task.
The standard evaluation procedure for the assessment of major and minor strain values to be used in an FLC diagram for a given specimen is usually performed etching a repeating pattern of geometrical features with known dimensions, an example of which is illustrated in Figure 2.12a, throughout its surface and measuring, after the test, how these features changed shape along three parallel sections normal to fracture direction. Then, in accordance to ISO12004, both major and minor strain values obtained along these sections are selected and fitted with inverse parabolas in order to evaluate the strains that brought to failure avoiding considering post-necking deformations[36]. This procedure is time consuming since every single feature has to be measured singularly by an operator. More than this the resolution of the strain profile depends on feature dimensions which in turn affects the quality of the evaluations: an higher number of points means that their analysis can be performed with a greater accuracy, but the dimensions of a single feature would diminish as well, lowering the accuracy of the single strain measurement.
Optical measuring systems are therefore being employed with increasing frequency. These enable an inline evaluation of the strain profiles along the whole surface of the specimen, with increased accuracy and on a large number of point. They use two cameras in order to obtain a stereoscopic view of the test area and therefore evaluate the displacements in all three dimensions. A stochastic pattern has to be impressed on specimen surface and the analysis system will proceed, during the test, to analyze how this pattern deforms, evaluating the strain values accordingly. A typical setup for the analysis of deformations with an optical measuring system for a Nakajima test is illustrated in Figure 2.12b.

a) b)

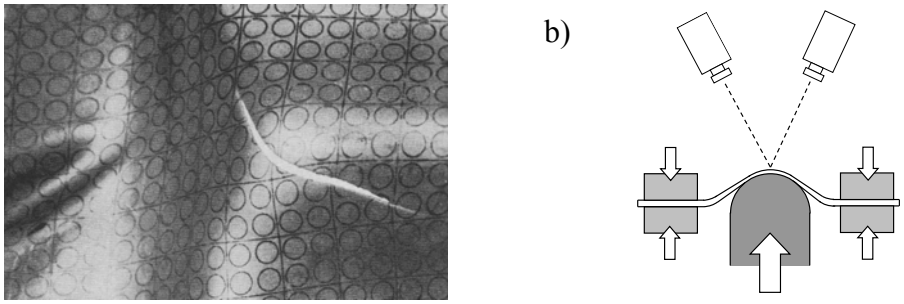

Figure 2.12: a) Example of a circular pattern painted on a surface for strain evaluation through classical means and b) schematic diagram showing optical measurement of strains in a Nakajima test

2.4 Graded microstructures

The achievement of hot stamped parts with tailored properties is one of the emerging topics on which a lot of experimental studies are being aimed. The reasons for this increase in popularity can be found in two main issues that the increased adoption of ultra high strength steels in modern automotive industry has made particularly prominent. On one hand, as already mentioned, the use of standard and therefore economic cutting methodologies such as hard cutting is limited by the elevated mechanical properties achieved in the stamped shape, with consequent increase of wear of tools. Local softer microstructures can therefore extend tool life and final geometrical accuracy. On the other hand, the use of these materials to produce structural automotive components has made the issue of improving impact absorption a particularly critical matter. Grading the mechanical properties of the stamped part along its profile enable to control the way the piece reacts in such critical situation, allowing to improve vehicle safety.
Different approaches have been analyzed in literature in order to obtain hot stamped parts with tailored properties.
One of the first attempt to realize these was through the use of tailor welded blanks, a technology already commonly used in sheet metal forming at room temperatures. In this case, blanks of heat treatable steels grade are laser welded with others that are not, and then hot stamped to the final shape[5]. Lamprecht et al.[37] analyzed the possibility of using H340LAD steel grade in order to complement the use of UHSS USIBOR 1500P, characterizing its mechanical properties in dependence to temperature and evaluating the properties of the weld seam. The study proved the feasibility of such methodology with good results relatively to the measured hardness profiles, as visible in Figure 2.13. Different practical issues arise however from the use of this technique: the coating has to be removed in the welding area, thus exposing part of the blank to oxidation, and the formability is particularly low in the area of the welding seams, thus narrowing down the type of shapes achievable.

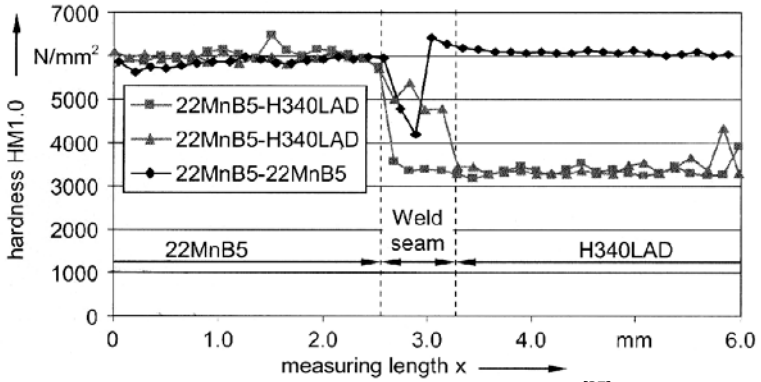

Figure 2.13: Hardness profile as measured by Lamprecht et al.[37] across the weld seam of a tailored welded blank

Partial hardening has also been evaluated by Saeglitz et al.[38], where a temperature difference is applied to the blank prior to hot forming, thus applying different cooling profiles on different areas of the stamped part. Both mechanical and microstructural analyses have been performed, verifying that UTS values up to 1500MPa are found in the hardened areas, with corresponding martensite phase, while values as low as 550MPa are evaluated in the so called high ductility section. The transition zone between the two areas is however particularly broad and characterized by a continuous and smooth change of mechanical properties, as visible from the measured hardness profile of Figure 2.14. This methodology is limited by the difficulty of applying in a industrial environment such particular heating treatment.

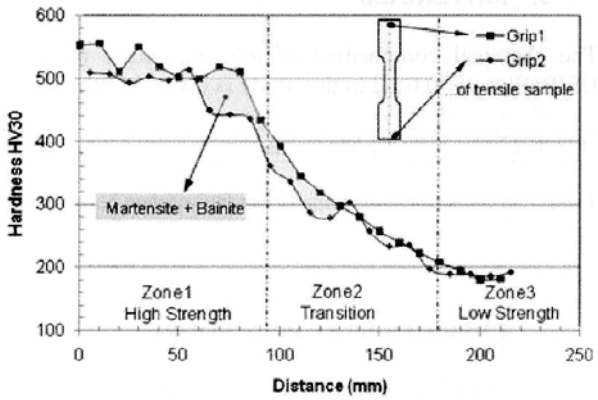

Figure 2.14: Hardness profile measured along the transition zone of a partial hardened central pillar

The opposite approach has been followed by Lenze et al.[39], who evaluated the possibility of using heated dies in order to locally reduce the cooling rate in the MBW1500 high strength steel. The results of this analysis showed that die temperatures over martensite start, hence over 400°C, are necessary in order to avoid martensite transformation in the blank.
Mori et al.[40] evaluated the possibility of using grooved tools in order to selectively quench different areas of a blank during hot forming. This same approach was also investigated numerically by George et al.[41]. In the analyses performed by Mori et al., a simple final hat shape has been considered. The blank has been heated through using resistance heating on the blank already fitted on the dies. These had grooves in order to avoid direct contact with the blank in selected areas, as visible from the test setup of Figure 2.15a.

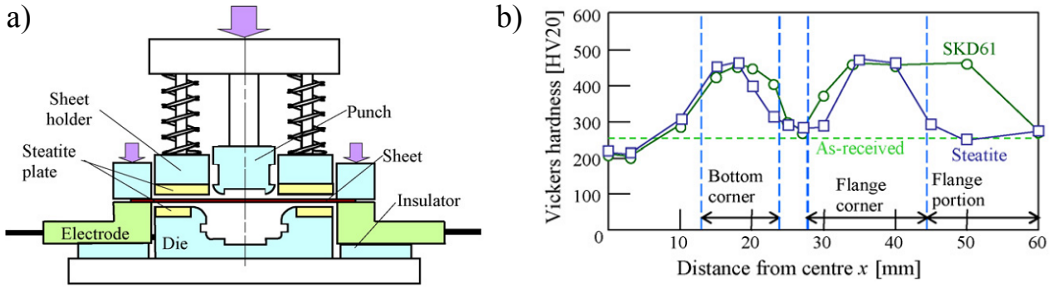

Figure 2.15: a) Equipment setup and b) Hardness profile measured on a hat-shaped part as described by Mori et al.[40]

In this study, the hardness profile of the hat-shaped piece was evaluated after extraction from the die, verifying an evident decrease in hardness, meaning that martensite formation has been inhibited to some extent in the areas where the grooves were placed, as visible from Figure 2.15b. This methodology is however limited by the fact that in the areas of the grooves no deformations can be applied to the blank.

Another analyzed approach was considering different tool materials in order to locally control the cooling profiles and therefore the phase transformation kinetics of different areas of the same shape. Casas et al.[18] evaluated the feasibility of using tool materials with thermal conductivities ranging from 55.2 W/mK to 6.1 W/mK. The study also showed that nanocasting could represent a basis for the development of such materials and evaluated this methodology as having very promising possibilities. These analyses where also used as a starting point by Laumann et al.[42], who evaluated, using numerical analysis methodologies, the effects of the different die materials considered in the aforementioned study and of different cooling techniques in the obtainable material properties at the end of the forming operation. The results of this work shows that significant improvement can be achieved in the final cutting operation if the dies are properly designed.

2.5 Approach

The main aim of this work is to achieve a number of information on the mechanical and thermal behaviour of an ultra high strength steel, the 22MnB5 and in particular the commercial version USIBOR 1500P, in a hot stamping process in order to complement the data already available in literature.

The major lack of information about these material is relative to their formability and this is, in fact, one of the most pressing issues for the proper design of a stamping operation. This is due to the major difficulties that arise in performing the standard formability tests taking into account thermal conditions close to those found in a real hot forming process. Also, some test parameters that at ambient temperature don't significantly influence the results plays a major role at elevated

temperatures and have to be properly considered. To this end, an experimental equipment was specifically designed, prepared, calibrated and tested. This was then used in order to perform Nakajima test campaigns on 22MnB5 steel and evaluate its formability at different temperatures while still in austenitic phase, thus reproducing the conditions in which it is deformed during hot stamping.
The other major issue considered was the possibility of obtaining tailored properties on the final shape as extracted from the press. After the evaluation of the different approaches already considered in literature, a mixed approach has been chosen, where the combined use of different die materials, heating of the dies and correct choice of process parameters has been analyzed. This should enable to locally reduce the cooling rate up to a point where martensite transformation could be inhibited while reducing the drawbacks typical of every single approach.
In order to evaluate the effects of the different process parameters on the obtainable thermal profiles, two numerical models have been developed. These enabled to individuate different viable methodologies, which in turn led to the definition of the experimental campaign.
Evaluating the possibility of using different die materials with different thermal properties in order to locally reduce the cooling rate, two different ceramic materials were chosen as candidate. Their tribological properties were evaluated in order to individuate the most appropriate for the particular application.
The experimental plan defined through analytical modelling was then performed with a specifically designed experimental setup using, when necessary, ceramics inserts made of the chosen ceramic material. Figure 2.16 shows the cooling rate fields considered for these analyses in comparison to that used in a standard hot stamping process.

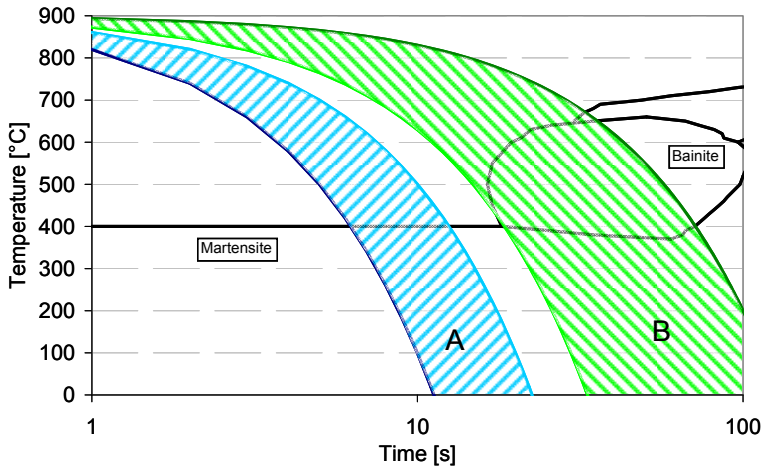

Figure 2.16: Cooling rate field usually employed in a standard hot stamping process (A) and fields usable for the stamping of functionally graded shapes (A and B)

The experimental campaign led to the individuation of the most promising

methodology and of its limits of applicability. It also enabled to analyze the impact of the different process parameters on the achievable thermal evolution of the blank.
Finally, the numerical results obtained through the analytical models were validated through direct comparison with the thermal profiles obtained in the experimental campaigns.

Chapter 3

Analytical modelling

3.1 Case study

To analyze the effects of the different process parameters on the thermal profiles obtainable on a blank, it has been decided to refer to the most simple and controllable case. Therefore a particular system was considered where the influences of the different aspects affecting the thermal profile evolutions could be analyzed singularly. The base configuration is visible in Figure 3.1.

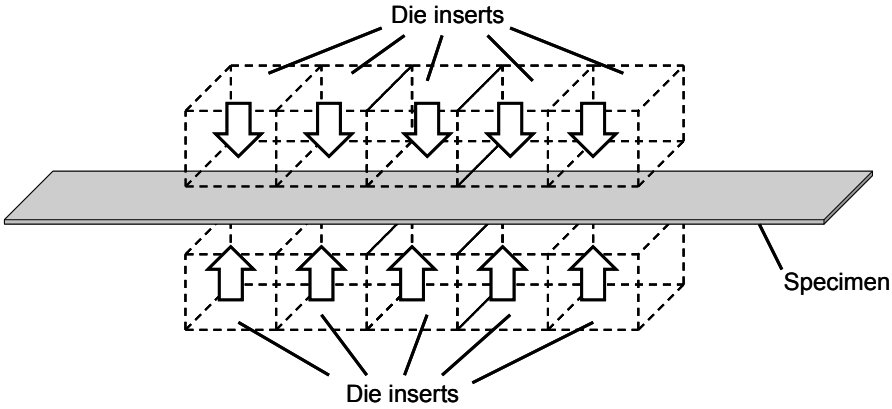

Figure 3.1: Base configuration for the analysis of thermal behaviour of a strip of UHSS steel in hot forming conditions

It has been decided to use flat dies in order to make the effects of plastic deformation on the onset of phase transformation negligible and to consider an homogeneous pressure along the specimen length. More than this, this

configuration enables to easily use dies insert of different materials in order to study different geometrical configuration.
To understand the basic dynamics involved in the thermal evolution of the specimen and how the different parameters interact with each other, two analytical models of different complexity were developed. They also enabled to estimate process limits and to individuate the most interesting cases to be analyzed with further experimental analyses.
The two different numerical models were developed using the numerical analysis program Matlab from Mathworks. The approaches used in the two models are exemplified in Figure 3.2a and Figure 3.2b.

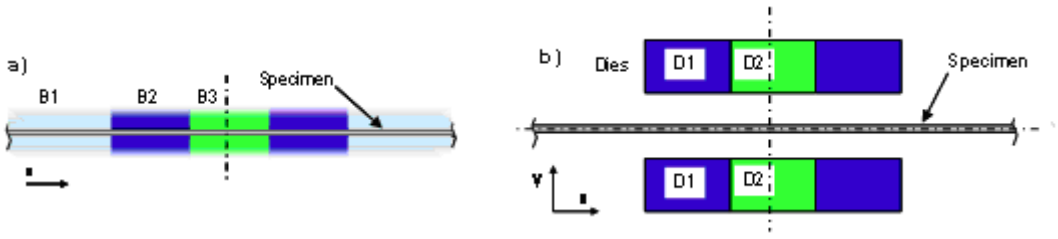

Figure 3.2: a) Monodimensional and b) bidimensional model domains representations

The models differs in the way the environment surrounding the specimen is considered.
In the first one a monodimensional approach has been preferred. Therefore, only the specimen is modelled, while the boundary conditions, even if variable through time and along specimen length, are considered unaffected by the thermal profile achieved on the specimen itself.
The second model uses, on the other hand, a bidimensional approach. In this case both the dies and the specimen are fully modelled, therefore enabling not only to evaluate the heat flux exchanged at the interfaces but also its effect on the thermal profile achieved on the dies. This model is more accurate than the first one, particularly if heated dies are used. However, its much greater complexity reflects in a great increase, two to three orders of magnitude high, of the computational time needed to obtain a solution. It is therefore possible to analyze a much smaller number of different cases. This model also enables, if necessary, to evaluate the latent heat generated by martensite phase transformation, at the expense, however, of even more computational time.
Both the approaches considers some sort of symmetry in order to reduce the number of equations that needs to be solved. They also both consider two main different interactions of the specimen with the surrounding: the exposure to the air of the environment, where convection and radiation are the most significant physical phenomena, and the contact with the dies, where thermal conduction plays a major role in dependence of die material thermal properties and local temperatures at the interfaces.
For both the approaches, the same process has been considered in order to mimic a real hot forming process. This is visible in Figure 3.3.

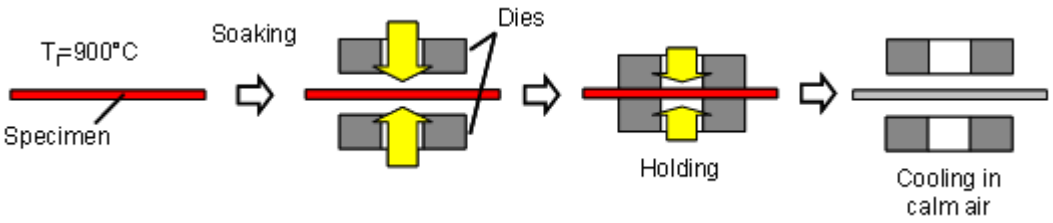

Figure 3.3: Stamping procedure considered for numerical analyses

The specimen has been initially considered at a fixed uniform temperature as taken out of the furnace. A soaking time has been imposed in order to account for the temperature drop due to transferring from the furnace to the press. The specimen is then closed in the dies for a determined closing time and, after that, extracted and let cooling in calm air.
Different configurations, pictured in Figure 3.4 have been analyzed in order to achieve a complete perspective on the problem. These can be grouped into three main categories: cooling in calm air without forming, cooling in dies with air gap and cooling in dies with inserts of different materials. All these configuration have been considered with a mirror symmetry along the middle axis parallel to the x coordinate. More than this, they all share the same initial conditions, which imposes the specimen at a constant initial temperature of 920°C as extracted from the furnace.

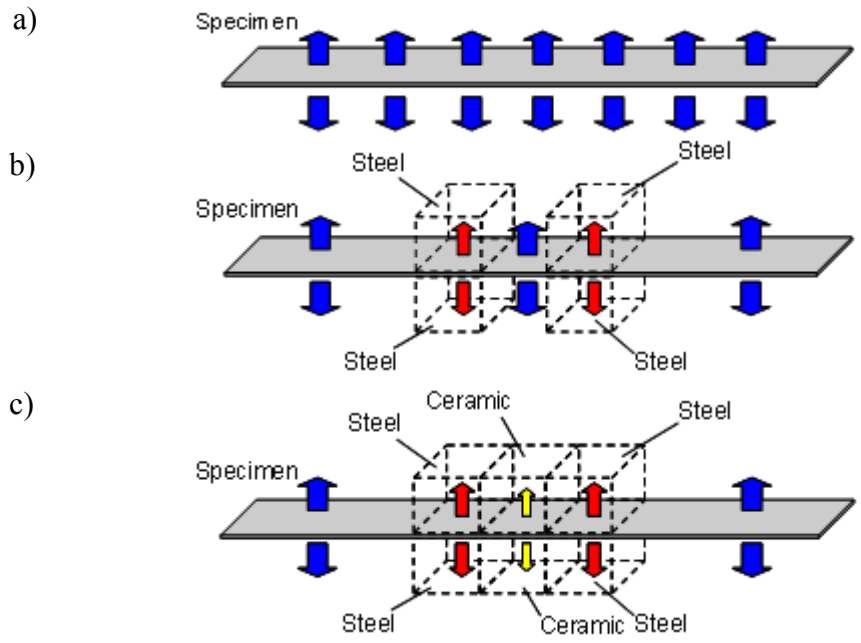

Figure 3.4: Configuration analyzed with the numerical models: a) cooling in calm air, b) cooling with air gap on dies, c) cooling with ceramic insert on dies

The monodimensional model has been used to analyze all the three different

configurations while only the third one has been used in the numerical studies performed with the bidimensional model. This was due to the fact that the latter can bring a significant contribute only if full dies are used.

3.1.1 Monodimensional model

As stated, the monodimensional models have been used for the evaluation of the thermal profiles achievable on the blank in all the three different configurations.
In the cooling in calm air category, the specimen has been considered left cooling outside the dies. The geometrical configuration is pictured in Figure 3.4a. A single case has therefore been studied. The results of this analysis helped evaluating the minimum cooling speed achievable, and therefore the theoretical limitations of the approach. For the specimen material, values obtained from literature illustrated in Table 3.1 have been used. The specimen, as in all subsequent analyses, is considered having a thickness of 1.5mm.

Material	Thermal conductivity	Density	Specific heat capacity
Usibor 1500P	42 W/m K	7750 Kg/m^3	460 J/Kg K

Table 3.1: Thermal properties of USIBOR 1500P used in numerical analyses

In the cooling in dies with air gap category, a geometrical configuration as the one presented in Figure 3.4b has been imposed.
The first set of analyses where prepared in order to evaluate the effects of air gap width and closing time on the obtainable thermal profiles. Thanks to the computational efficiency of the monodimensional model, a large number of solutions have been evaluated changing the values relative to those factors in small steps. The values considered are presented in Figure 3.5, along with the other parameters used in the model. A soaking time of 3s has been imposed for every solution.

	Value
Air gap width (L) [mm]	1 – 201 at step of 5
Closing time [s]	0.1 – 10.1 at step of 0.5
HTC [W/(m^2°K)]	3175
Soaking time [s]	5
Steel die width [mm]	25
Length outside dies [mm]	87.5

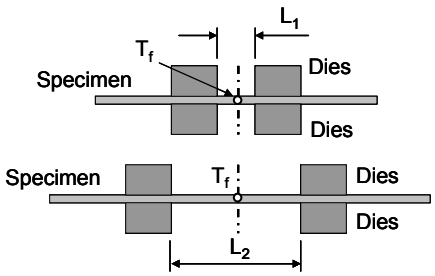

Figure 3.5: a) Parameters and b) geometrical configurations used for air gap width influence analyses

Due to both the elevated number of analyses performed and the fact that latent heat due to martensitic phase transformation was not evaluated in these analyses,

the considered output was the temperature just after pressing, evaluated in the centre of the air gap zone (T_f of Figure 3.5). If that latent heat can indeed be considered negligible when pressing, if compared to the heat fluxes involved, the same cannot be said after that.
The HTC values have been chosen in accordance to literature[43]. The geometry of the specimen was changed in conjunction with the change of the air gap width, thus maintaining the geometrical characteristics of the areas at the sides of the air gap, changing therefore its total length, as exemplified in Figure 3.5.
Two analyses have also been performed in order to evaluate the influence of different steel dies and specimen geometries for different closing times on the thermal profile in T_f. The air gap width was considered fixed. The significant parameters used these analyses are visible in Figure 3.6 and Figure 3.7.

	Value
Air gap width [mm]	25
Closing time [s]	0.1 – 10.1 at step of 0.5
HTC [W/(m^2°K)]	3175
Soaking time [s]	5
Steel die width (L) [mm]	0.5 – 100.5 at step of 2.5
Length outside dies [mm]	87.5

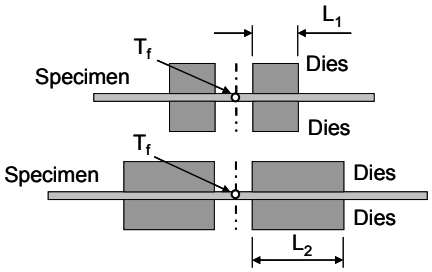

Figure 3.6: a) Parameters and b) geometrical configurations used for steel die insert width analyses

	Value
Air gap width (L) [mm]	25
Closing time [s]	0.1 – 10.1 at step of 0.5
HTC [W/(m^2°K)]	3175
Soaking time [s]	5
Steel die width [mm]	25
Length outside dies (L) [mm]	0.5 – 200.5 at step of 12.5

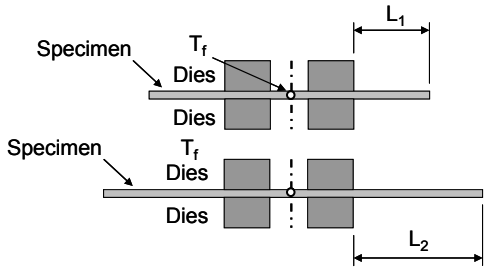

Figure 3.7: a) Parameters and b) geometrical configurations used for outer length influence analyses

In the last configuration category, the effects of the presence of a ceramic insert placed in at the centre of the dies have been evaluated. That insert is placed among two steel inserts to mimic its presence in a hot stamping die. The value of the heat transfer coefficient for the specimen-ceramic interface has been imposed from literature considering a Zirconium dioxide insert. As for the previous case, the influence of the ceramic insert width and of the closing time have been evaluated as visible in Figure 3.8, which sums up the used model parameters. The final temperature has been evaluated in the same way as well, considering the temperature calculated in correspondence of the symmetry line right after pressing.

	Value
Ceramic insert width (L) [mm]	0.5 – 100 at step of 2.5
Closing time [s]	0.1 – 10.1 at step of 0.5
HTC steel [W/(m^2°K)]	3175
HTC ceramic [W/(m^2°K)]	497
Soaking time [s]	5
Steel die width [mm]	25
Length outside dies [mm]	87.5

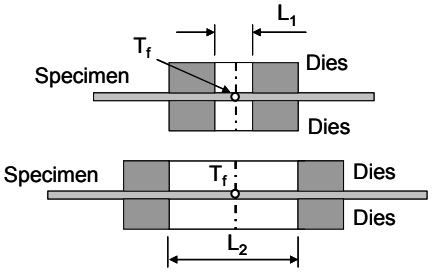

Figure 3.8: a) Parameters and b) geometrical configurations used for ceramic insert length and closing time influence analyses

3.1.2 Bidimensional model

In order to analyze the mutual influence of different die temperatures and closing times, the bidimensional model has been used. The configuration considered is therefore the third one, were a ceramic insert 75mm wide has been taken into account. The used model parameters are illustrated in Table 3.2., while the geometrical configuration employed is illustrated in Figure 3.9

Parameter	Value
Soaking time [s]	5
Closing time [s]	3 – 10 at step of 2
Cooling time [s]	35
Dies temperature [°C]	25, 50 – 400 at step of 50

Table 3.2: Process parameters used in bidimensional analyses

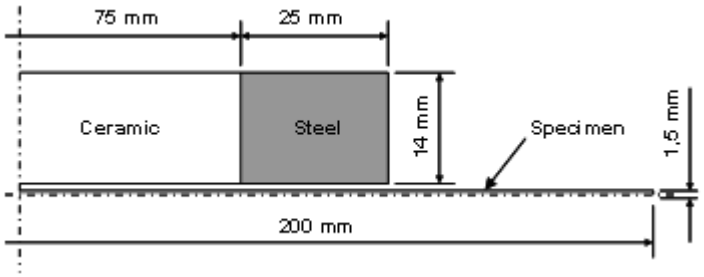

Figure 3.9: Geometrical configuration used in the analyses performed with the bidimensional model

Since in this case the die inserts are also modelled, their different thermal properties have been evaluated from literature and implemented in the model itself. These are illustrated in Table 3.3

	Die steel	Ceramic	Specimen
Density [Kg/m^3]	7750	6000	7750
Thermal conductivity [W/mK]	42.2	2.70	42
Heat capacity [J/Kg K]	460	400	460
Thermal expansion [10^{-6}/°C]	13.3	10.3	13.5

Table 3.3: Material properties used in the analyses performed with the bidimensional model

Finally, the effects of heat generated due to martensite phase transformation have been evaluated in selected cases of the bidimensional model.
In the following chapters, the two different models are illustrated and the results of the performed numerical analyses presented and commented.

3.2 Monodimensional model definition

3.2.1 Analytical definition

Even if this model is more simple than the bidimensional one, it still take into account the majority of the effects involved in determining the temperature profile of the blank in a forming operation. Only the specimen has been fully modelled, while the presence of the dies is defined as imposed boundary conditions that can vary through time, but aren't affected by the thermal evolution of the blank. For an infinitesimal section of the specimen along its length, the different heat fluxes involved can be identified as explained in Figure 3.10.

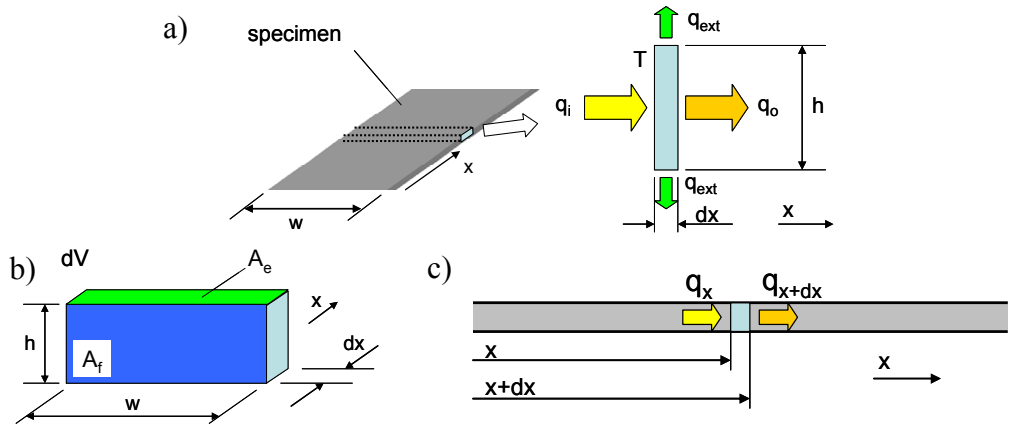

Figure 3.10: a) Thermal fluxes through an infinitesimal section, b) geometric relations ofr an infinitesimal volume, c) thermal fluxes along specimen length for an infinitesimal section

Being the slab at uniform temperature T, two main kind of fluxes can be recognized: the heat exchanged with the environment, q_{ext}, and the thermal fluxes

along the specimen length, q_i and q_o.
Considering the general thermal conduction equation[45], and not taking into account phase transformation kinetics, the local temperature of the slab can be described as a function of the heat fluxes as:

$$\rho c_v \frac{\partial T}{\partial \tau} dV = q_{dx} A_f + q_{ext} dA_e$$

Where ρ and c_v are density and specific heat capacity of the specimen material, τ the time, q_{dx} the net heat flux across the specimen length relative to the infinitesimal slab, q_{ext} the heat exchanged with the environment, dV, A_f and dA_e respectively the volume, the section transversal area and the upper or lower area.
The net heat flux q_{dx} can be expressed as the difference of the ingoing heat flux q_i with the outgoing heat flux q_o, therefore:

$$q_{dx} = q_o - q_i = q_{x+dx} - q_x = \lambda \frac{\partial}{\partial x}\left(T + \frac{\partial T}{\partial x} \partial x \right) - \lambda \frac{\partial T}{\partial x} = \lambda \frac{\partial^2 T}{\partial x^2} \partial x$$

Where λ is the thermal conductivity of the sheet material.
To evaluate the heat exchanged with the environment, two different cases must be distinguished. When exposed to the air, the effects of radiation and convection have been taken into account, therefore:

$$q_{ext} = q_{conv} + q_{rad} = \alpha(T)\left(T - T_a\right) + \sigma\varepsilon\left(T^4 - T_a^4\right)$$

Where q_{conv} and q_{rad} are the thermal fluxes due to convection and radiation respectively, α(T) the convection coefficient evaluated for the local temperature T of the slab, T_a the temperature of the environment, considered constant, σ and ε the Stefan-Boltzmann constant and the emissivity coefficient as expressed by the Kirchoff law.
When pressed on the dies, the heat exchanged through radiation and convection can be considered minimal, and instead the thermal fluxes relative to direct contact with die surfaces needs to be accounted for[46]. The equation for the evaluation of the heat exchanged at the interfaces then becomes:

$$q_{ext} = q_{cont} = HTC\left(T - T_d\right)$$

Where q_{cont} is the heat exchanged due to direct contact, HTC is the heat transfer coefficient, and is mainly a function of the die and sheet material and contact pressure, and T_d is the temperature of the die considered constant through time. Since up to two different die inserts have been taken into account, in a symmetrical setup, up to two different values of T_d have been considered, and the

temperature of the die has been imposed constant in the whole contacting surface.
It is possible to see that both the equations describing the heat exchanged with the surroundings share the same analytical form and are represented by the same equation, while representing different physical phenomena. Therefore, a single equation has been used for the model:

$$q_{ext} = A(T - T_e) + B(T^4 - T_e^4)$$

where
$A = \alpha(T)$
$B = \sigma\varepsilon$
$T_e = T_a$
when considering the slab exposed to the air and
$A = HTC$
$B = 0$
$T_e = T_d$
when considering the contact with the dies.
From geometrical consideration it is also possible to evaluate dV, A_f and dA_e as
$dV = w\,h\,dx$
$A_f = w\,h$
$dA_e = w\,dx$
Where w is the specimen width and h the specimen height.
Substituting the obtained equations in the general thermal conduction equation:

$$\rho\, c_v \frac{\partial T}{\partial \tau} w\,h\,dx = \lambda\left(\frac{\partial^2 T}{\partial x^2}\right)\partial x\, w\,h + \left[A(T - T_e) + B(T^4 - T_e^4)\right] w\,dx$$

Which becomes:

$$\rho\, c_v \frac{\partial T}{\partial \tau} = \lambda\left(\frac{\partial^2 T}{\partial x^2}\right) + \frac{\left[A(T - T_e) + B(T^4 - T_e^4)\right]}{h}$$

which is the main equation describing the thermal behaviour of the specimen during the forming operation. The equation is a partial differential equation and has therefore to be solved using numerical methods.
The solver chosen is built in the software used for numerical analyses and uses finite difference approximation to approximate the values of temperature in the x coordinate and a variable order multistep solver based on the numerical differentiation formulas to evaluate the changes of temperature values on the time domain.
Since the boundary conditions evolves through time, the different imposed values are time dependent. The stamping can be divided into three main phases: soaking,

stamping and final cooling. During soaking and final cooling the boundary conditions are considered uniform throughout the specimen length and relative to the exchange with the environment case. When in stamping, A B and T_e are locally changed in correspondence of contact zones in order to account for the different heat fluxes. The problem therefore numerically stiffens both spatially and temporally and can require several additional iterations to come to an acceptable solution, in dependence to the required accuracy.

3.2.2 Convection coefficient evaluation

The evaluation of the convection coefficient is a critical aspect to correctly analyze the thermal behaviour of the specimen, and is also one of the most difficult parameter to evaluate. The fluid dynamic has been estimated as belonging to the natural convection case. The fluid motion has been evaluated as turbulent and the case of a hot surface upward facing has been applied to both the upward and downward facing surfaces of the specimen, both to simplify the model and to partly account for the motion of the specimen during the transferring from the furnace.
Considering the average values, the convection coefficient can be evaluated as:

$$\overline{\alpha}(T) = \frac{\lambda_a \overline{Nu}}{l}$$

Where λ_a is the thermal conductivity of the fluid, Nu the average Nusselt number and l the characteristic length of the plate. In the specific case, l has been evaluated, as suggested in literature, as the arithmetic average of long and short sides.
With the aforementioned simplification, Nu has been evaluated, following recommendations from literature[47], as

$$Nu = 0.14 Ra^{\frac{1}{3}}$$

Where Ra is the Rayleigh number and is defined as the product of the Grashof and Prandtl numbers:

$$Ra = Gr \,\mathrm{Pr}$$

Gr and Pr are defined from literature as

$$Gr = \frac{l^3 \rho^2 \beta g \Delta T}{\mu^2}$$

$$Pr = \frac{c_p \mu}{\lambda}$$

Where ρ is the fluid density, β is the isobaric thermal expansion coefficient, g the gravity constant and μ and c_p the dynamic viscosity and the specific heat at constant pressure respectively.
Density, specific heat at constant pressure and thermal conductivity of air can vary greatly with temperature. Therefore, the values in Table 3.4, derived from literature, have been use in order to evaluate, through linear interpolations, the values relative to a specific temperature.

Temperature [°C]	27	127	227	727
ρ [Kg/m^3]	1.1774	0.8826	0.7048	0.3524
c_p [J/Kg K]	1005.7	1014	1029.5	1141.7
λ_a [W/(m K)]	0.02624	0.03365	0.04038	0.06732
μ [Kg/(ms)]	$1.949\ 10^{-5}$			

Table 3.4: Thermal properties of air at different temperatures

3.3 Bidimensional model definition

The monodimensional model offers a good degree of accuracy, taking into account the major influencing factors, but lacks the ability to estimate the effects of die heating. When such high temperatures of the specimen are considered, it is indeed likely that the local increase of temperature on the dies can be elevated enough to significantly alter the thermal profile along the specimen length.
The bidimensional model addresses this problem taking into account not only the dimension along which the specimen primarily extends but also the one needed for the thermal modelling of die inserts sections. Taking into account the heating of the dies meant that a whole new set of data were required relative to their geometries and materials thermal properties.
The higher accuracy achievable through this model comes however at the expense of computational power required. The adding of another dimensions reflects in a dramatic increase of the number of equations that needs to be solved for every single time iteration, thus consequently increasing the time needed to obtain the solution. The computational time has been estimated as being two to three orders of magnitude higher than that needed to solve the corresponding monodimensional case.
The numerical analysis software used lacked the ability to solve partial differential equations in a bidimensional domain, therefore a new solver has been specifically developed.

3.3.1 Solver and model developed

In order to numerically solve the problem, two different codes have been developed: a model and a solver. The model describes the system and feeds the solver with the geometrical and physical quantities needed. In turn, the solver asks for them giving to the model an estimate of the temperatures along the different domains.

3.3.1.1 Solver development

The developed solver analyze the system and reduce the partial differential equation in a system of ordinary differential equations. The derivatives along the two different dimensions are approximated with the finite difference method using a direct approximation approach[48],[49]. To solve the system, a variable order multistep solver based on the numerical differentiation formulas has been chosen[50], in order to account for the elevate stiffness that can affect the problem.
The solving algorithm proceeds as follows: at first, the solver query the model for the matrix of point to be analyzed. This is a bidimensional matrix where spacing along the two different dimensions must remain constant throughout the entire domain. Then it enquires the model for the different domains to be analyzed, since every different object is assigned to a different subdomain, and for the initial temperatures at every point of the matrix. These latter values are directly fed to the ordinary differential equation solver as the initial values needed to solve the problem. It then proceeds to identify the boundaries of the various domains. The solver process then continues iteratively: for every iteration, the ordinary differential equation solver gives an estimate solution, the solver uses this estimate to query the model for local material properties and boundary correlations, then considers the general heat transmission equation and applies the finite difference method in order to obtain the values of temperature derivatives relative to time. These values are then passed to the ordinary differential equation solver, which in turn provides other estimates. This process continues iteratively till the convergence tolerances are met. The solving process is exemplified in Figure 3.11.

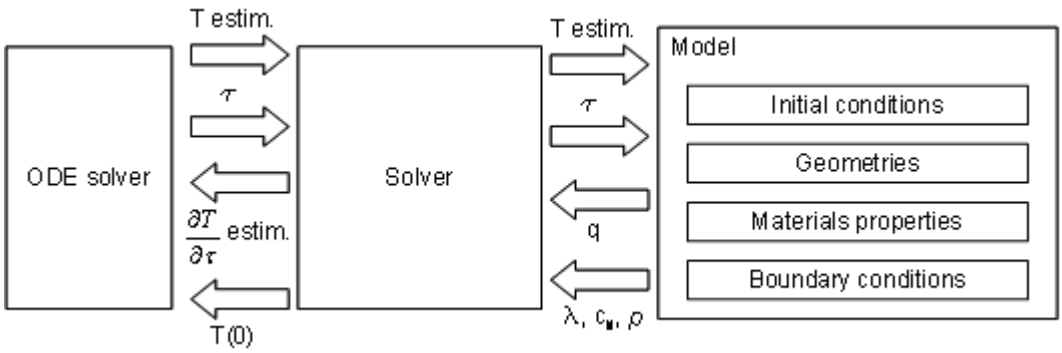

Figure 3.11: Bidimensional analyses process diagram

The heat transfer equation for a bidimensional domain, without taking into account heat fluxes normal to the solving plane and considering two orthogonal dimensions, can be written as:

$$\rho c_v \frac{\partial T}{\partial \tau} = \frac{(q_{xo} - q_{xi})}{\partial x} + \frac{(q_{yo} - q_{yi})}{\partial y}$$

Where q_{xo} and q_{xi} are respectively the outgoing and ingoing thermal fluxes along x dimension and q_{yo} and q_{yi} the outgoing and ingoing thermal fluxes along y dimension, as exemplified in Figure 3.12a.

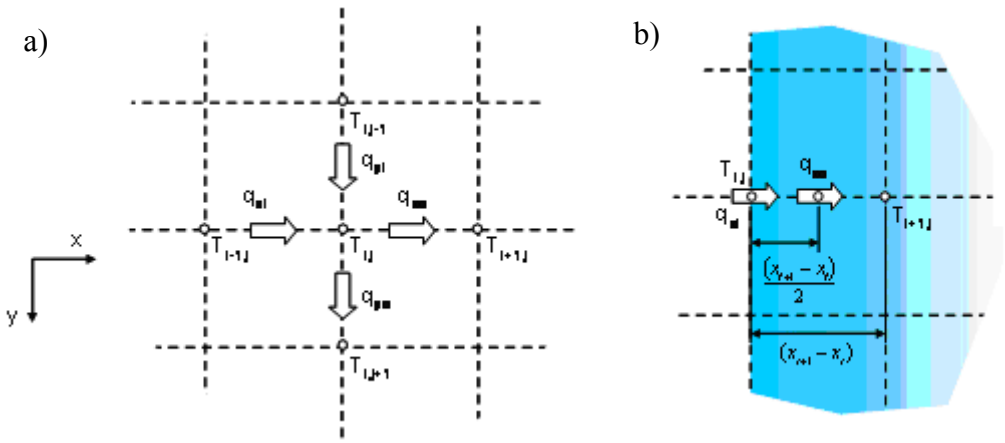

Figure 3.12: Thermal fluxes evaluated in bidimensional analyses: a) at domain internal points and b) at boundary points

Applying the finite difference method with a direct approximation approach the equation becomes:

$$\rho c_v \frac{\partial T}{\partial \tau} = \frac{(q_{xo} - q_{xi})}{\Delta x} + \frac{(q_{yo} - q_{yi})}{\Delta y}$$

Where ∆x and ∆y are the distances along the two dimensions of the points of application of the fluxes.
When the considered point is inside the integration domain and not on its boundary, the direct approximation approach can be applied directly to the equation, that then becomes:

$$\rho c_v \frac{\partial T}{\partial \tau} = \lambda \left[\frac{\left(T_{i+1,j} - 2T_{i,j} + T_{i-1,j}\right)}{\left(x_{i+1} - x_i\right)\left(x_i - x_{i-1}\right)} + \frac{\left(T_{i,j+1} - 2T_{i,j} + T_{i,j-1}\right)}{\left(y_{j+1} - y_j\right)\left(y_j - y_{j-1}\right)} \right]$$

Where i and j are the indices of the considered point along the two dimensions.
At the boundaries, the imposed external heat fluxes should be considered applied directly on the point taken into consideration, as explained in Figure 3.12b. Therefore, considering the case of a point placed on the left side of a boundary with a heat flux q_{xi} normal to the boundary plane applied, the equation becomes:

$$\rho c_v \frac{\partial T}{\partial \tau} = \left(\lambda \frac{\left(T_{i+1,j} - T_{i,j}\right)}{\left(x_{i+1} - x_i\right)} - q_{xi} \right) \left(\frac{2}{\left(x_{i+1} - x_i\right)} \right) + \lambda \frac{\left(T_{i,j+1} - 2T_{i,j} + T_{i,j-1}\right)}{\left(y_{j+1} - y_j\right)\left(y_j - y_{j-1}\right)}$$

Applying the same procedure for the other types of boundaries:

$$\rho c_v \frac{\partial T}{\partial \tau} = \left(q_{xo} - \lambda \frac{\left(T_{i,j} - T_{i-1,j}\right)}{\left(x_i - x_{i-1}\right)} \right) \left(\frac{2}{\left(x_i - x_{i-1}\right)} \right) + \lambda \frac{\left(T_{i,j+1} - 2T_{i,j} + T_{i,j-1}\right)}{\left(y_{j+1} - y_j\right)\left(y_j - y_{j-1}\right)}$$

$$\rho c_v \frac{\partial T}{\partial \tau} = \lambda \frac{\left(T_{i+1,j} - 2T_{i,j} + T_{i-1,j}\right)}{\left(x_{i+1} - x_i\right)\left(x_i - x_{i-1}\right)} + \left(\lambda \frac{\left(T_{i,j+1} - T_{i,j}\right)}{\left(y_{j+1} - y_j\right)} - q_{yi} \right) \left(\frac{2}{\left(y_{j+1} - y_j\right)} \right)$$

$$\rho c_v \frac{\partial T}{\partial \tau} = \lambda \frac{\left(T_{i+1,j} - 2T_{i,j} + T_{i-1,j}\right)}{\left(x_{i+1} - x_i\right)\left(x_i - x_{i-1}\right)} + \left(q_{yo} - \lambda \frac{\left(T_{i,j} - T_{i,j-1}\right)}{\left(y_j - y_{j-1}\right)} \right) \left(\frac{2}{\left(y_j - y_{j-1}\right)} \right)$$

3.3.1.2 Model definition

The chosen configuration considers a ceramic insert 75mm width surrounded on either side by two steel inserts 25mm wide each. A total length for the specimen of 200mm was chosen, with a thickness of 1.5mm.
A quarter symmetry has been used in order to reduce the total number of equations that had to be solved.
The boundary conditions impose null thermal flux on symmetry axes, in order to

represent symmetry, and also null thermal flux on the most external boundaries in order to represent the contact with an insulating surface. Contact heat transfer with appropriate HTC values is imposed for contacting surfaces during the time they are intended to came into contact, and for the remaining time domain convection and radiation are taken into account. These two effects are also imposed for the remaining surfaces that don't interact with the dies. The boundary conditions are summed-up in Table 3.5. The considered materials were USIBOR 1500P for the specimen, H11 for the steel die inserts and Zirconium dioxide for the ceramic insert. The forming process is similar to the one used in the monodimensional analyses and considers 5s of soaking time, three different closing times, 3s, 5s, and 10s, during which the specimen is pressed in the dies, and 50s of cooling in calm air after the extraction from the dies.

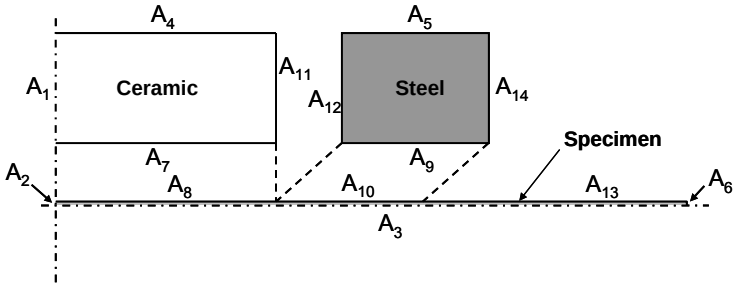

Figure 3.13: Bidimensional model geometries and boundaries relations

Boundary	Applied condition
Symmetry (all boundaries) (A_1, A_2, A_3)	q=0
Ceramic – external environment (A_4)	q=0
Steel die – external environment (A_5)	q=0
Specimen – external environment (A_6)	q=0
Ceramic die – Specimen (A_7, A_8)	$q = HTC_{cs}(T_c - T_s)$ $\tau_i < \tau < \tau_f$ $q = \alpha(T - T_a) + \sigma\varepsilon(T^4 - T_a^4)$ otherwise
Steel die – Specimen (A_9, A_{10})	$q = HTC_{ds}(T_d - T_s)$ $\tau_i < \tau < \tau_f$ $q = \alpha(T - T_a) + \sigma\varepsilon(T^4 - T_a^4)$ otherwise
Ceramic die – steel die (A_{11}, A_{12})	$q = HTC_{cd}(T_c - T_d)$
Specimen – internal environment (A_{13})	$q = \alpha(T - T_a) + \sigma\varepsilon(T^4 - T_a^4)$
Steel die – internal environment (A_{14})	$q = \alpha(T - T_a) + \sigma\varepsilon(T^4 - T_a^4)$

Table 3.5: Boundary conditions used in bidimensional analyses

3.3.1.3 Latent heat due to martensite transformation

In order to further improve the accuracy of the results obtained from the numerical models, the evaluation of the heat generated due to martensite phase

transformation has been introduced in a last set of numerical evaluations.
In most cases, the latent heat generated can be considered negligible if confronted to the other heat fluxes involved. Also, its evaluation can require much more computational power in dependence of the case considered. There are however some cases where the latent heat can impact the thermal profile in a significant way.
Being a diffusionless transformation[51], the martensitic phase change can be expressed as only dependent from temperature.
The heat internally generated due to martensite transformation can be expressed as:

$$H = r\frac{\partial m_m}{\partial \tau}$$

Where H is the heat internally generated due to phase transformation, r the latent heat for martensite transformation and m_m the transformed mass. Considering the volumetric expansion due to martensitic transformation negligible, the transformed mass can be evaluated as:

$$\frac{\partial m_m}{\partial \tau} = \frac{\partial Z_m}{\partial \tau}\rho\, dV$$

Where Z_m is the martensite transformed fraction and ρ the material density.
In order to evaluate the transformed fraction, the Koistinen-Marbuger equation has been used[52]:

$$Z_m = \left(1 - Z_b - Z_f\right)\left\{1 - e^{[a(M_s - T)]}\right\}$$

Where Z_b and Z_f are the fractions of transformed bainite and ferrite respectively, a a parameter specific of the given material and M_s the martensite start temperature.
Z_b and Z_f are considered identically zero in this case since bainitic and ferritic transformations are not considered.
In order to evaluate the thermal flux due to martensite transformation, the equation describing the transformed fraction had to be derived in the time domain, and since the only term that is dependent on time is T, the change in martensite fraction can be expressed as:

$$\frac{\partial Z_m}{\partial \tau} = -a\frac{\partial T}{\partial \tau}e^{[a(M_s - T)]}$$

The heat internally generated can therefore be expressed as:

$$H = r\frac{\partial Z_m}{\partial \tau}\rho\, dV = -r\, a\, \rho\frac{\partial T}{\partial \tau}e^{[a(M_s - T)]}dV$$

And the general heat transmission equation can be written as

$$\frac{\partial T}{\partial \tau} = \left[\frac{(q_{xo} - q_{xi})}{\partial x} + \frac{(q_{yo} - q_{yi})}{\partial y}\right]\frac{1}{\rho\left\{c_v + rae^{[a(M_s - T)]}\right\}}$$

This equation can be easily used in the bidimensional model.
From literature[44], the latent heat has been evaluated as:

$$r = 135\,KJ/Kg$$

while the a constant has been set as

$$a = 0.011K^{-1}.$$

3.4 Analytical models results

3.4.1 Monodimensional model

As already stated, the first analysis was performed without taking into account the dies, letting the specimen cool in air. The obtained temperature profile is visible in Figure 3.14 along with the CCT curves of USIBOR1500P.

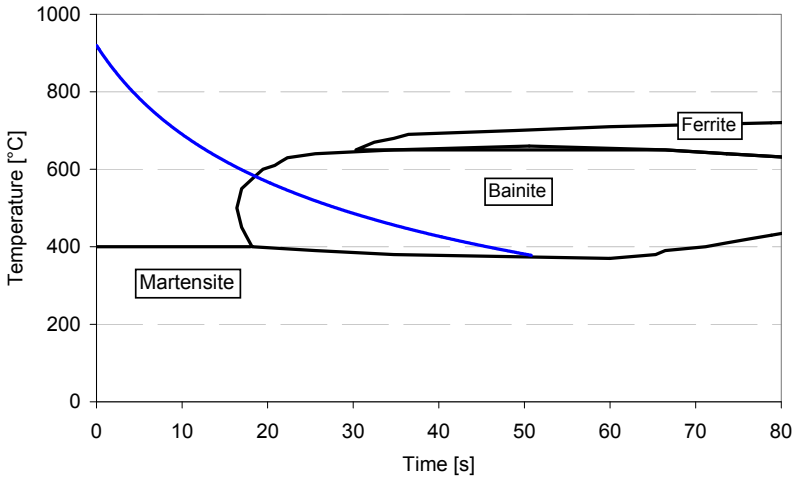

Figure 3.14: Cooling in calm air numerical results

From this first analysis, it was possible to verify that, in limit conditions, a cooling rate as low as 18.2 °C/s can be achieved, that enables to enter the upper bainite field at about 18.6s from the extraction from the furnace. This should enable a minimum hardness of about 38 HRB[53]. It has to be noticed that the thermal profile after the onset of the phase transformation lacks physical trustfulness since the heating due to transformation latent heat is not taken into account. Therefore the real overall cooling speed is expected to be lower than the value obtained from this analysis, as well as the resulting hardness. The value obtained is however enough to justify further investigations in order to find methodologies to locally control the thermal profile during forming, with useful effects on the stamped components.
The results for the second category of analyses, where an air gap is considered among two steel dies, are presented in Figure 3.15.

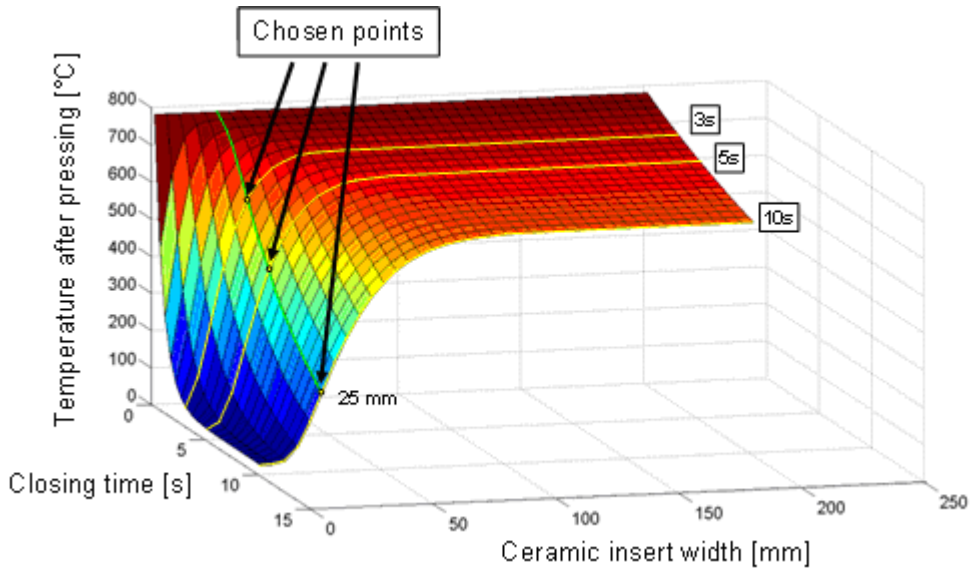

Figure 3.15: Air gap width and closing time influences numerical results

From these results it is possible to see that, when the air gap is wider than 50mm, the influence of the width itself is negligible as it doesn't influence significantly the temperature after pressing, whether the width considered. It is then possible to affirm that the presence of the steel dies creates a transition zone that can be predicted to be about 50mm wide, after which their presence can be considered not influencing. This also reflects on the sensitivity to the variation of the closing time. With air gaps wider than 50mm, since the influence of the dies themselves is very weak, different closing times don't affect the temperature after pressing and the thermal profile basically follows the same profile obtainable directly cooling in air. For a width less than 50mm, however, the closing time plays an important role in determining the temperature after pressing. A geometrical configuration with 25mm of air gap width has therefore been chosen to be analyzed through

experimental testing. In this geometrical configuration a great variation of the temperature after pressing is evident in dependence of the closing time. Three of these were consequently chosen as most significant cases: 3s, 5s and 10s.
In Figure 3.16 and Figure 3.17 are presented the results that shows the effects of steel die insert width and of total specimen length on the temperature after pressing for different closing times, with an air gap 25mm wide.

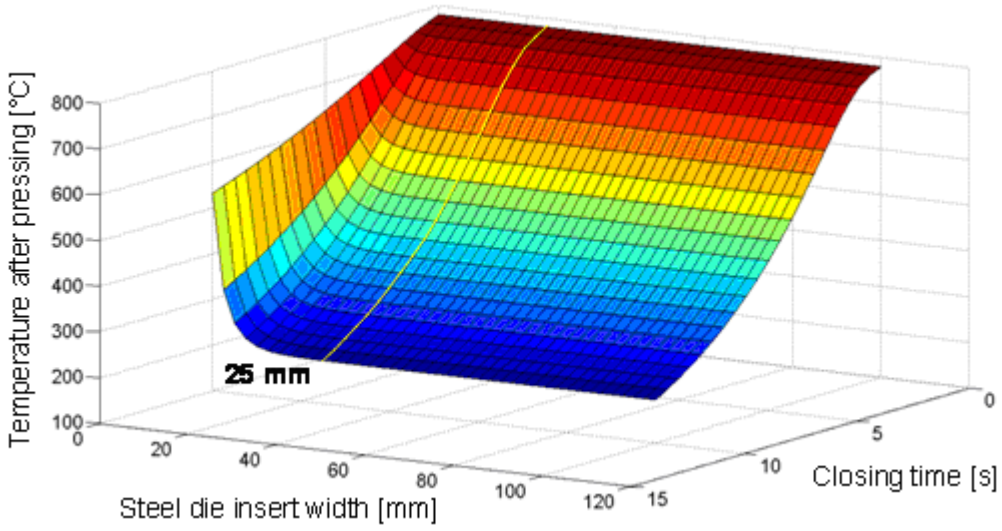

Figure 3.16: Steel die width and closing time influences numerical results

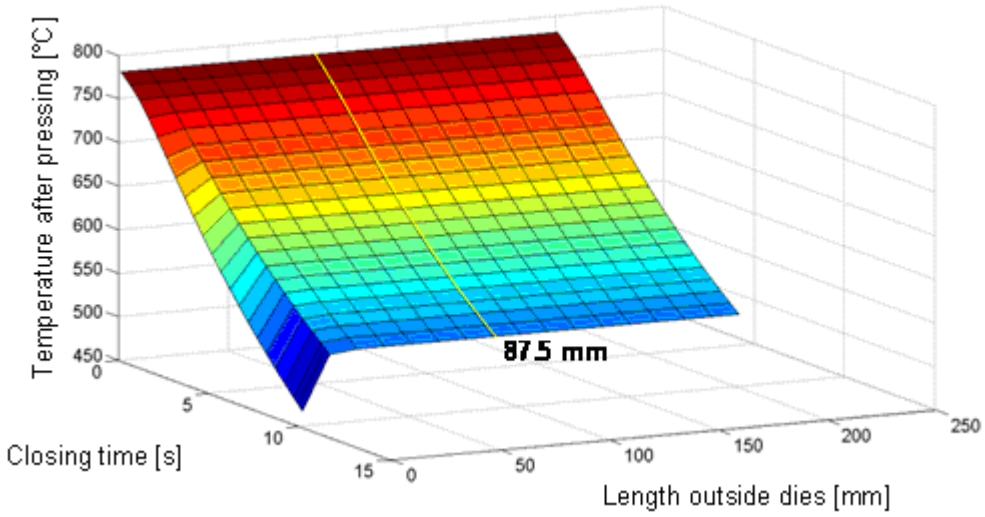

Figure 3.17: Length outside the dies and closing time influences numerical results

From these results it is visible that the influence of steel die width plays a significant role only for dimensions less than 15mm. With wider inserts it is therefore safe to say that the geometrical configurations are, with a good degree of

confidence, equivalent to one another. The variation of total specimen length seems to play an even smaller role in determining the cooling profile. Only for lengths left outside the dies smaller that 13mm an effect is indeed visible. It has to be underlined however that these analyses takes into account only the temperature after pressing, therefore no analyses are performed on the cooling profiles after the pressing operations, and it is safe to state that in those conditions the length of specimen could have a greater influence.
The results relative to the third configuration are visible in Figure 3.18.

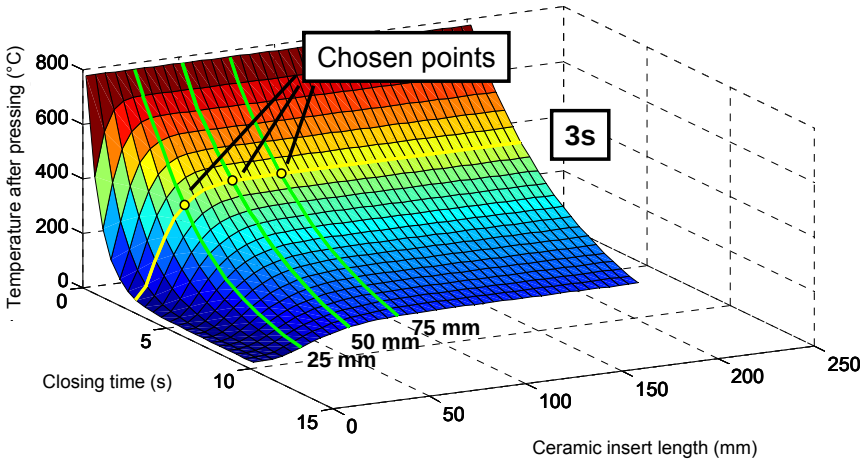

Figure 3.18: Ceramic insert width and closing time influences numerical results

In this case it is possible to see that a significant influence of the presence of the ceramic insert can be noted only when the latter is at least 25mm – 50mm wide. More than this, every geometrical configuration is greatly dependent on closing time, that in fact plays a heavy role in determining the final cooling speed. In particular, it is visible that closing times longer than 3s, which should be considered a limiting value due to the dynamics of a real process, brings to final temperatures lower than 430°C which is the martensite start temperature. Therefore, it has been decided to concentrate the experimental analysis on 3s of closing time. In order to study the effect of geometric configuration, three different width have been chosen for the ceramic insert: 25mm, 50mm and 75mm. These are marked in Figure 3.18.

3.4.2 Bidimensional model

3.4.2.1 Die temperature dependence

The dependence of the cooling profile, evaluated at point T_1 as described in Figure 3.8, from the die temperature are displayed in Figure 3.19, Figure 3.20,

Figure 3.21, where the profiles are evaluated for every different closing time.

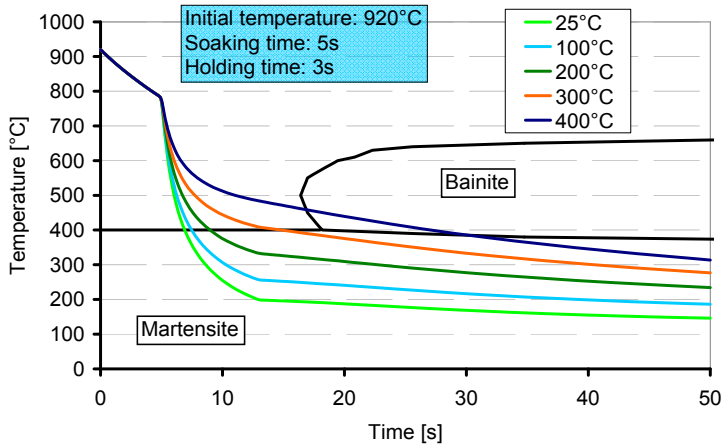

Figure 3.19: Thermal profiles obtained from the bidimensional model with 3s of holding time

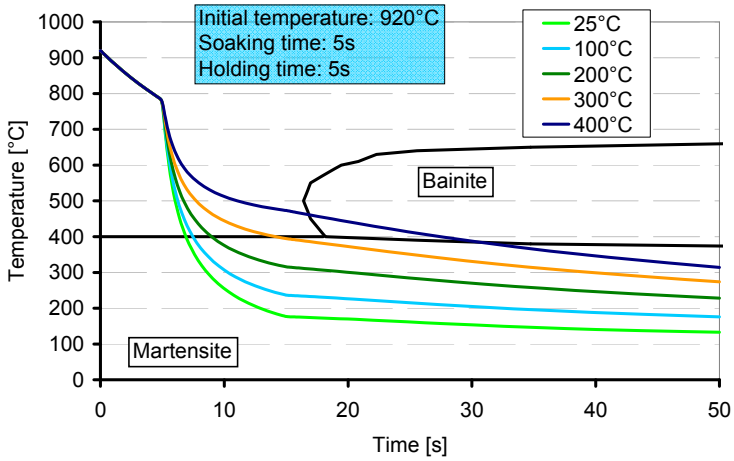

Figure 3.20: Thermal profile obtained from bidimensional model with 5s of holding time

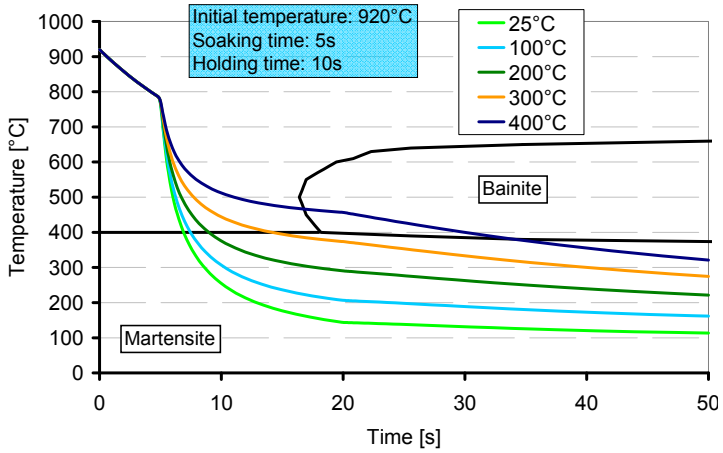

Figure 3.21: Thermal profile obtained from the bidimensional model with 10s of holding time

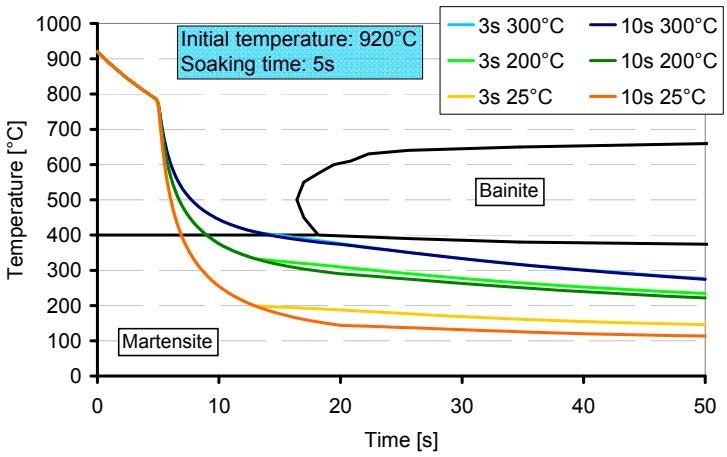

Figure 3.22: Thermal profile obtained from the bidimensional solver at different die temperatures

As it is possible to see, die temperature can have a significant effect on decreasing the cooling rate, with an influence on the final temperature that can almost be considered linear. In these results, as in the one relative to the monodimensional case, the heat generated due to phase transformation is not taken into account. The results also shows that, even if the use of heated dies can indeed decrease the cooling speed significantly, it isn't until die temperatures of about 300°C are reached that the martensite transformation can be inhibited and lower bainite can develop. This observation can be applied to all the case analyzed, whether the closing times taken into account.
The effect of different closing times for the same die temperatures are displayed in Figure 3.22. These results shows that the influence of closing time reduces as the die temperature increase. This is due to the fact that, at higher die temperatures, the specimen tends to reach the thermal equilibrium with the die sooner, as the initial temperature of the latter is closer of that of the specimen at the beginning of the pressing operation. When close to equilibrium, the heat exchanged lowers to values close to those typical of air to surface conditions, and can even get lower of those as it is possible to see comparing 3s and 5s cases with initial die temperature of 300°C.
Considering these results, other than with the dies at room temperature, it has been decided to perform the experiments with the dies at 200°C and 300°C, the latter being the maximum temperature applicable in real condition without incurring in severe drawbacks.

3.4.2.2 Latent heat evaluation

The analyses have been repeated for the different die temperatures and closing times. The results are visible in Figure 3.23 and Figure 3.24.

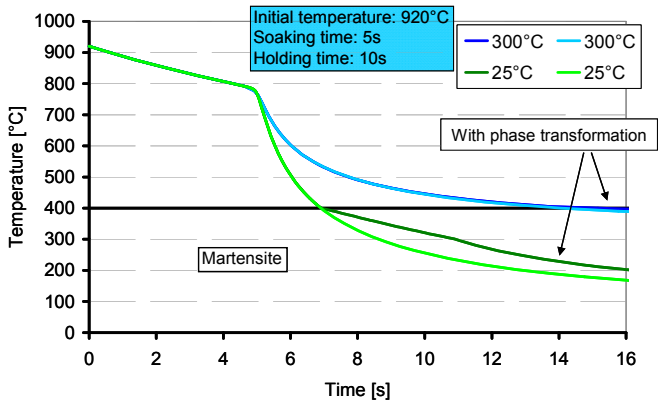

Figure 3.23: Thermal profiles evaluated with the bidimensional taking into account martensite phase transformation for 10s of holding time and different die temperatures

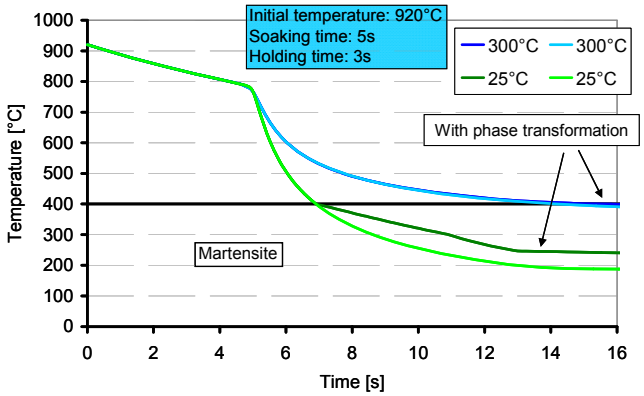

Figure 3.24: Thermal profiles evaluated with the bidimensional taking into account martensite phase transformation for 3s of holding time and different die temperatures

The results shows that, since with the dies at 300°C the profile enter only slightly into the martensite transformation area, little differences can be noticed between the results with and without phase transformation heat evaluation.
With the dies at room temperature, on the other hand, the two profiles differs significantly in the area of martensite transformation, and at 3s the influence of latent heat is greater than that evaluated at 10s. This is due to the fact that some areas at 3s remains in the middle of the transformation after the opening of the dies, therefore reducing the slope of the thermal profile in the other areas of the specimen.
Even if, considering the heat generated due to phase transformation, the cooling rates at lower die temperatures are lower then those evaluated without taking into account latent heat, the differences aren't big enough to change the considerations already illustrated in the previous chapter.

3.5 Conclusions

Using a number of analytical descriptions of different thermal phenomena, two different numerical models have been developed. The monodimensional model, while simple, is able to estimate the thermal behaviour of the specimen if interfacial conditions can be considered not dependent from blank temperature. The bidimensional model, on the other hand, is more complex and therefore requires an higher number of evaluations in order to produce the results, but it can account for the effects of heat exchanged with the dies on the temperature profile of the dies themselves, and therefore aim at more accurate results. The models were then used to evaluate geometrical configurations and test parameters most meaningful for the experimental testing, evaluating both the possibilities of using ceramic inserts and air gaps on dies. The most influencing parameters were found to be the closing time, the geometrical configuration, the soaking time and the dies temperature.
The possibility to evaluate heat due to martensite phase transformation has also be incorporated in the bidimensional model. This, at the expense of an increase in the computations required to obtain the solution, produce results that are expected to be even more close to the experimental results.

Chapter 4

Experimental Equipment

4.1 Introduction

In this chapter, the different experimental equipment used for the evaluation of formability and of the influence of different process parameters on the thermal evolution of a blank are illustrated.
To perform the Nakajima tests, due to the particular nature of the conditions on which they were performed, an experimental setup was specifically developed. Its design was conceived taking into account all the specific necessities and aiming at maximizing the repeatability of tests, therefore minimizing the influence of external sources of error.
To perform plane pressing tests, on the other hand, at first a tribological test equipment was used in order to choose the ceramic material best suited for the use as an insert in hot forming operations.
The equipment needed to perform plane pressing tests themselves was then designed, including a set of modular dies used to recreate the different geometrical configurations that needed to be studied. The setup included a modified version of the same equipment used for to perform Nakajima tests.
In the following chapters, these equipment will be described along with the choices that were followed for their design.

4.2 Nakajima test equipment

The test equipment needed to perform Nakajima tests at elevated temperatures was developed at the Chair of Manufacturing Technologies at the University of Padua, and is based on an earlier prototype built in order to assess the feasibility

of such kind of tests[54]. The equipment, and therefore all its different components, were designed or chosen specifically for the particular application, in order to optimize quality and repeatability of the results, set-up easiness and procedure soundness.
The choices made during the design phase were aimed at recreating on the specimen the various mechanical and thermal conditions that could represent those found on blanks in real hot forming conditions. The realized prototype along with the designed counterpart are visible in Figure 4.1a and in Figure 4.1b. The following chapters describes the different sub-systems built, underlining the design choices made.

a) b)

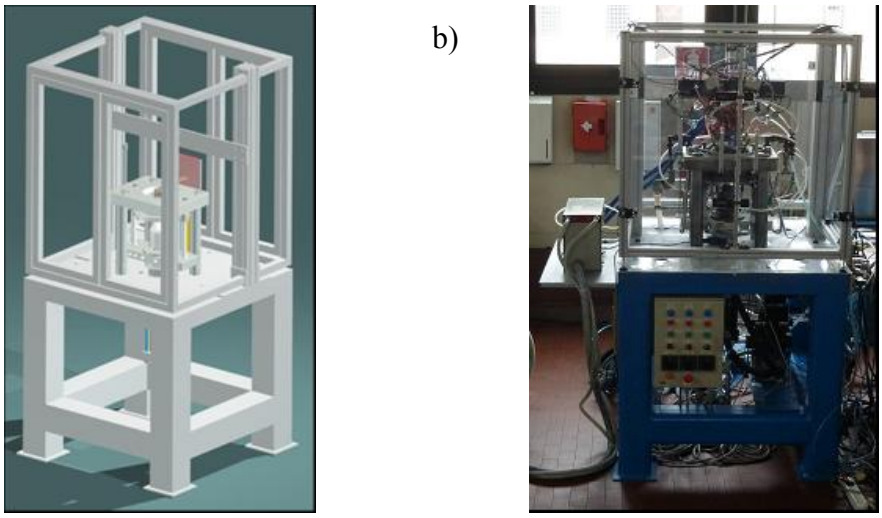

Figure 4.1: Experimental equipment to perform Nakajima tests a) as designed and b) as realized

4.2.1 Base structure

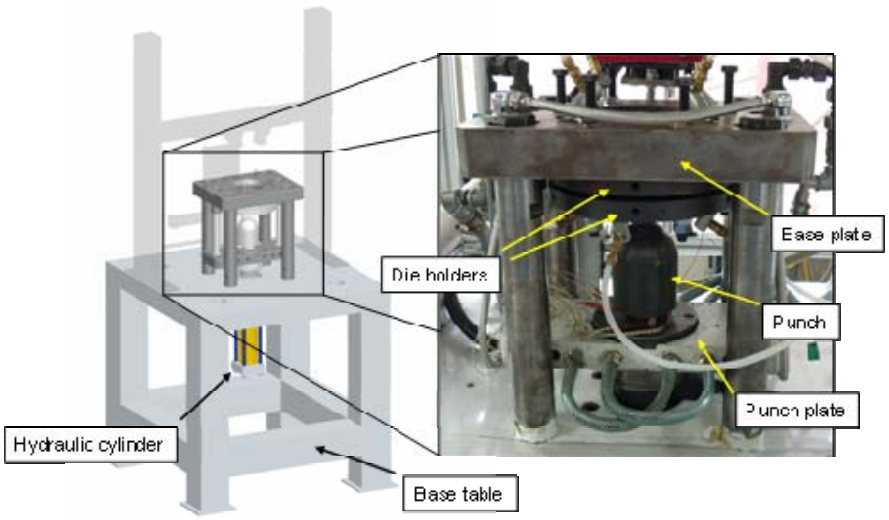

Figure 4.2: Base structural components

The base structure, as visible from Figure 4.2, is composed of the hydraulic cylinder, the die holders, the base plate, on which the blank holders are fixed, the punch, the punch plate, on which the latter is fixed, and of the base table.
The hydraulic cylinder was the first component to be considered since all others structural elements are dependent from its choice. It was dimensioned taking into account the results from preliminary tests performed on the earlier prototype, the capabilities of the available hydraulic circuit and focusing on replicating the range of strains as close as possible to that encountered in a real hot forming process. This task was performed following ISO 6020/2 guidelines[55]. The chosen characteristics and main cylinder dimensions are visible in Table 4.1.
.

Feature	Value
Bore	100 mm
Mounting style	Head rectangular flange
Rod diameter	45 mm
Stroke length	220 mm
Maximum working pressure	230 bar
Maximum push force	165 kN
Maximum rod speed	200 mm/s

Table 4.1: Hydraulic cylinder main properties

Using the cylinder dimensions as the base for frame design, this was designed so that the punch could move upward when deforming the specimen. The base plate was then designed in order to house the blank holders on its lower side. This configuration was chosen in order to maximize accessibility to the upper side of the specimen, maximizing its visibility for the optical analysis system used for strain measurements, while having a very stiff structure and avoiding to load the bolts used to close the blank holders, thus maintaining the clamping force constant throughout the tests. The blank holders were made of hardened steel with a drawbead ring embedded into them in order to fix the specimen and, as already mentioned, featured a set of bolts placed along a circumference of the blank holders themselves. The four columns that support the base plate that in turn supports the blank holders were designed in order to withstand the maximum load applicable through the punch, while the base table was designed to support both the overall equipment weight and the stresses derived from the equipment use. The table design was verified through the use of FEM simulations, with ANSYS software, as visible in Figure 4.3.

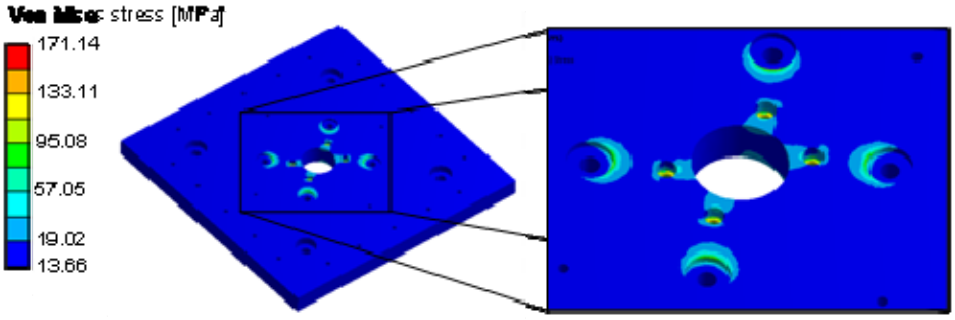

Figure 4.3: Structural analysis results of the upper plate of the base table under maximum load conditions

In order to improve structural stiffness and avoid the possible arise of misalignments between the specimen and the punch, the latter was fixed on a plate connected to the hydraulic cylinder rod and which features two columns that moves on bearings placed on the upper plate, where the die holders are fixed. The rod isn't directly fixed to the plate but through three elements: the connecting flange, the load cell and the hemispherical joint, as illustrated in Figure 4.4a.
The load cell was chosen so it could fit directly on the cylinder rod. The flange was designed in order to house it and discharge the load applied on its sensing surface, maintaining the alignment between the cylinder rod and the upper hemispherical joint. The latter was used to decouple punch plate lateral and rotational movements from those of the load cell, thus applying the load always in the proper direction and avoiding the arise of unwanted bending moments on the rod. The results from static analyses performed for the dimensioning of the flange using ANSYS FEM software are illustrated in Figure 4.4b.

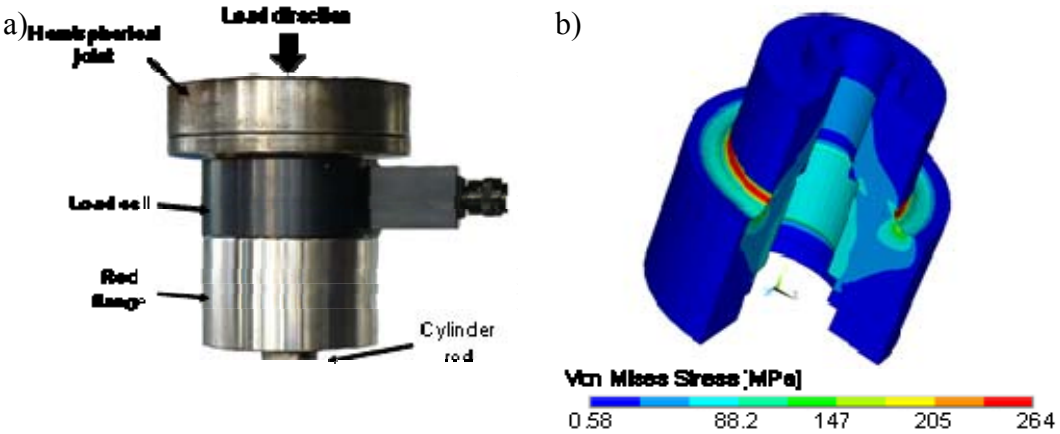

Figure 4.4: a) Elements of the connection chain from cylinder rod to punch plate and b) Stress analysis at maximum load for the rod flange component

In order to prevent access to the test area during the tests and to support the acquisition equipment, an upper lightweight aluminum structure has been

prepared that features doors with opening sensors and guides for acquisition system positioning.

4.2.2 Punch control system

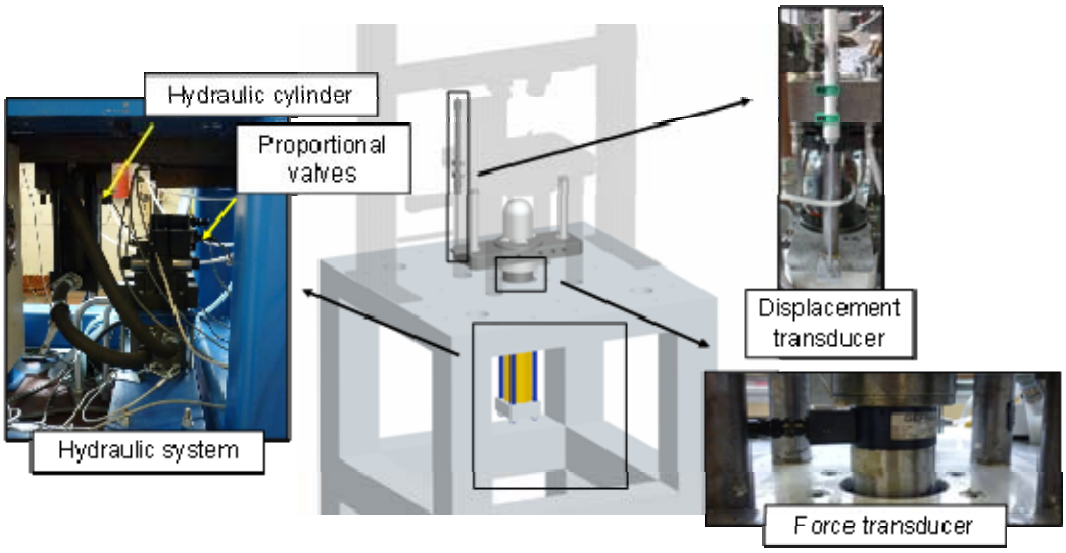

Figure 4.5: Punch control system components

The punch control system is composed of the hydraulic valves, the displacement transducer, the load cell and of the controlling software.
In order to control the punch movements and the applied loads, the entire acquisition and control chain have been specifically designed. To control the flow of oil inside the cylinder, two proportional hydraulic valves have been prepared. These where chosen and arranged on the hydraulic circuit in series, so that accurate control of both flow rate and pressure is possible. Their position on the hydraulic system as well as their main properties are presented in Figure 4.6 and in Table 4.2 and Table 4.3.

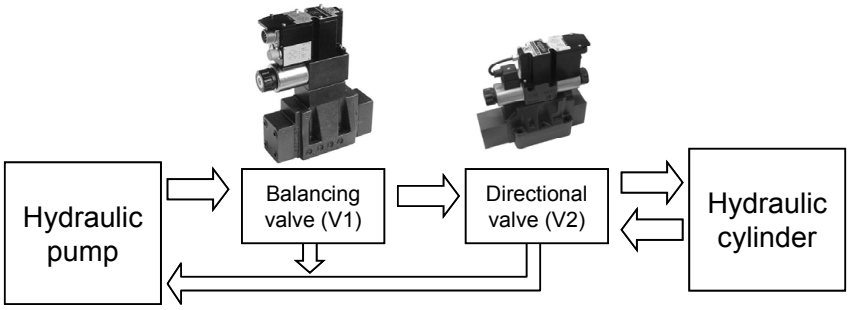

Figure 4.6: Position of proportional valves along the hydraulic system

Balancing valve (V1)	
Feature	Value
Maximum operating pressure [bar]	350
Maximum flow [l/min]	300
Piloting flow requested [l/min]	1.4
Pressure control range [bar]	210
Hysteresis	Less than 2% of maximum flow
Repeatability	Less than 4% of maximum flow

Table 4.2: Balancing valve main properties

Directional valve (V2)	
Feature	Value
Maximum operating pressure P – A – B ports [bar]	350
Controlled flow with 10 bar pressure on P – T [l/min]	150
Hysteresis	Less than 2% of maximum flow
Repeatability	Less than 2% of maximum flow

Table 4.3: Directional valve main properties

V1 is a balancing valve with proportional control that can reduce the incoming pressure of a given fraction while maintaining an almost constant flow rate in the standard operating window while V2 is a pilot operated directional valve with proportional control that can reduce and change the direction of the outgoing fluid flow in relation to the control signal applied and to the pressure difference among the ingoing and outgoing ports of the valve. Both the valves have integrated electronics and can be controlled remotely[56][57].
In order to acquire the movement of the cylinder rod, a linear position transducer potentiometer was used, its most important characteristics visible in Table 4.4, while in Figure 4.7 are displayed its main dimensions.

Feature	Value
Useful electrical stroke [mm]	250
Theoretical electrical stroke [mm]	251
Maximum displacement speed [m/s]	3 m/s
Resistance at theoretical electrical stroke [kΩ]	10
Independent linearity on useful electrical stroke	0.1%
Maximum applicable voltage [V]	60
Class of protection	IP67

Table 4.4: Linear position transducer properties

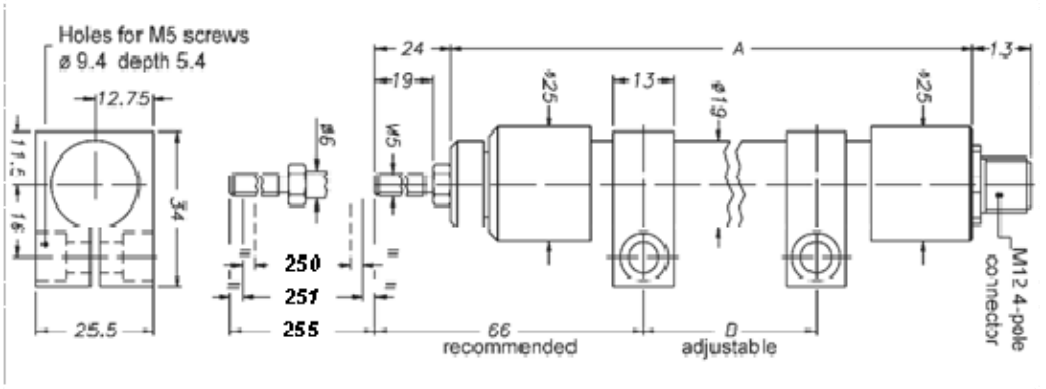

Figure 4.7: Linear position transducer main dimensions

This transducer was chosen for its ability to withstand harsh test conditions and, being a potentiometer, its resolution can be raised arbitrarily in relation to powering and acquisition equipment[58]. More than this, its nature makes it particularly resistant to the electric noise that is generated by the induction equipment that has been chosen for the heating of the specimens. The potentiometer is powered using an external stabilized power supply whose output is constantly monitored by the acquisition software in order to correct displacement measurements.

To measure the load applied to the rod of the hydraulic cylinder, a toroidal force transducer was used, its main characteristics listed in Table 4.5, while its dimensions are visible in Figure 4.8. This transducer uses strain gauges in a Wheatstone full-bridge configuration[59]. The cell is directly powered from the acquisition equipment.

Feature	Value
Nominal full scale load [kN]	500
Accuracy	0.5%
Nominal output at FSO [mV/V]	2
Output tolerance at maximum load	<2% of FSO
Combined errors	<1% of FSO
Creep after 30 min at maximum load	<0.12% of FSO
Zero load out of balance signal	<2% of FSO
Grade of protection	IP65

Table 4.5: Load transducer main properties

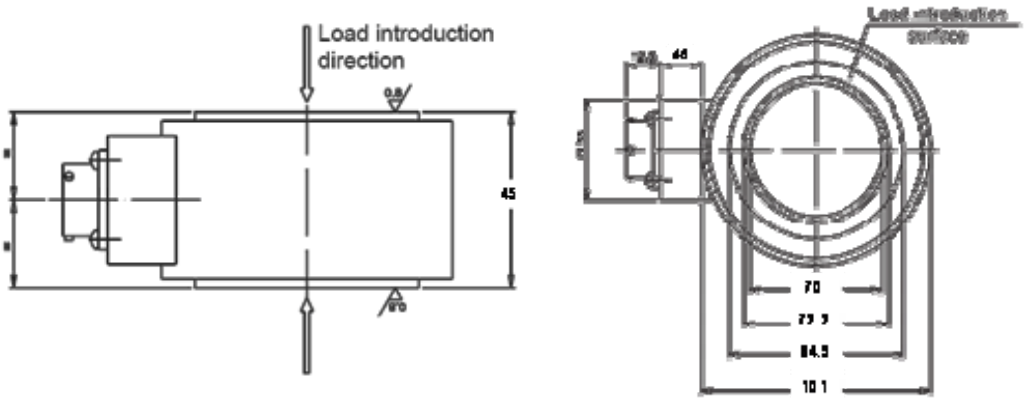

Figure 4.8: Load transducer main dimensions

In order to acquire correct values of the load applied, the load cell had to be calibrated using appropriate equipment. A number of preliminary tests showed a great dependence of the calibration curve on the geometrical configuration used to house the load cell. Therefore, the cell was calibrated with all the housing equipment using a dedicated press and a comparing the results to those of an high precision calibrated cell placed in the same press. A number of load ramps have been applied in order to analyze the response at different loads applied and also taking into account whether the load was being added or subtracted. The obtained calibration curve is visible in Figure 4.9.

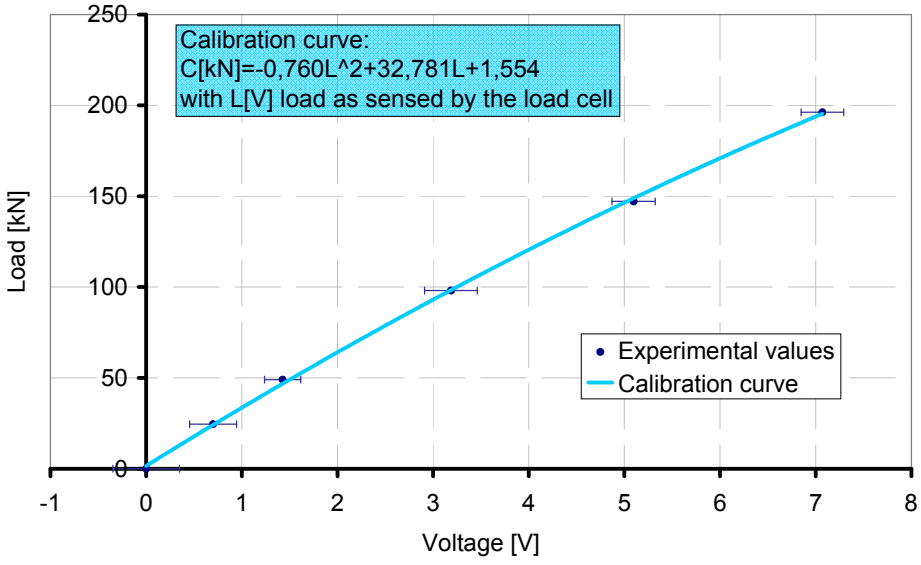

Figure 4.9: Obtained calibration curve of load transducer

The software control chain was specifically developed for the particular application and is illustrated in Figure 4.10.

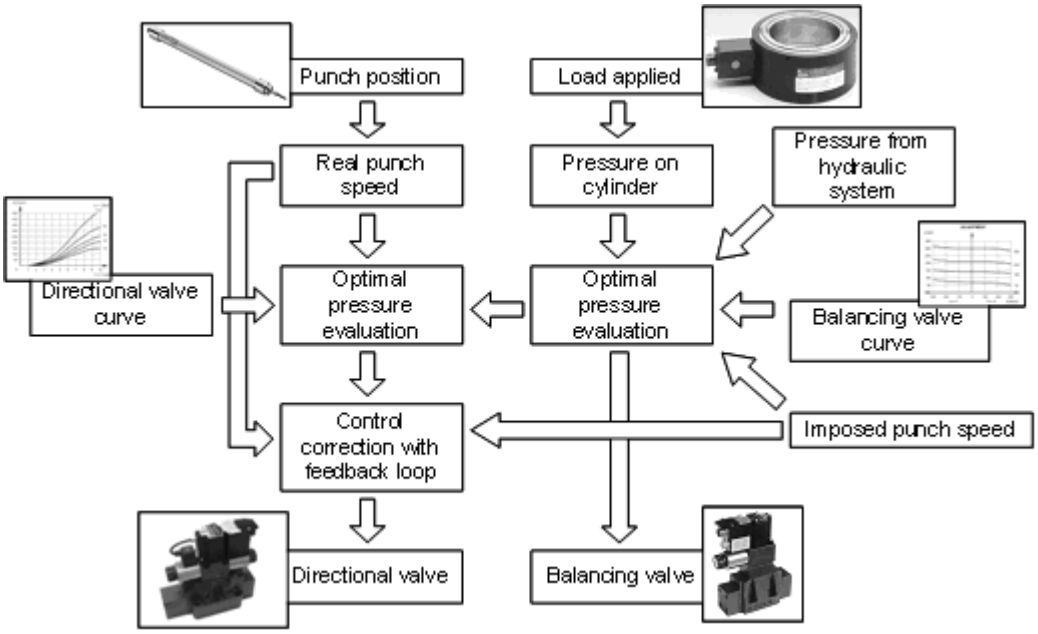

Figure 4.10: Diagram of the punch movement control chain

The punch position is acquired at high frequency and its speed calculated in real time. The speed is averaged in a 50Hz period in order to cancel low frequency electrical noise. Given the needed motion parameters, the characteristic response curves of the valves, visible in Figure 4.11a and Figure 4.11b, and the evaluated optimal control conditions are used in order to obtain the uncorrected control values to be applied at the two valves. The pressure at the exit of the pilot operated directional valve is estimated from system characteristics and load applied on the cylinder rod. The control to be applied to the balancing valve is then evaluated considering the pressure at the entrance of the valve itself, dependent from the hydraulic pump characteristic and evaluated to be 190 bar, and the optimal pressure difference among entrance and exit points of the directional valve, which has been evaluated to be 15 bar. The uncorrected control value to be applied to the directional valve is, on the other hand, calculated considering the imposed pressure difference, the set punch speed, the system characteristics and the response curve of the valve itself. The value obtained is then sent to an high speed feedback system that compares the real punch speed with the requested value and correct the control before sending it to the valve. This also enable to account for dynamic variations of hydraulic system characteristics such as oil properties and inertial effects.

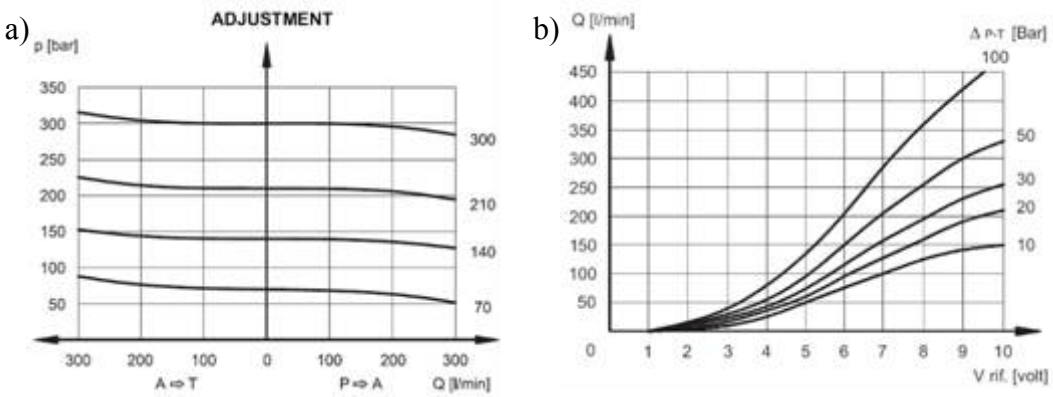

Figure 4.11: Characteristic response curve of a) the balancing valve and b) the directional valve

4.2.3 Heating

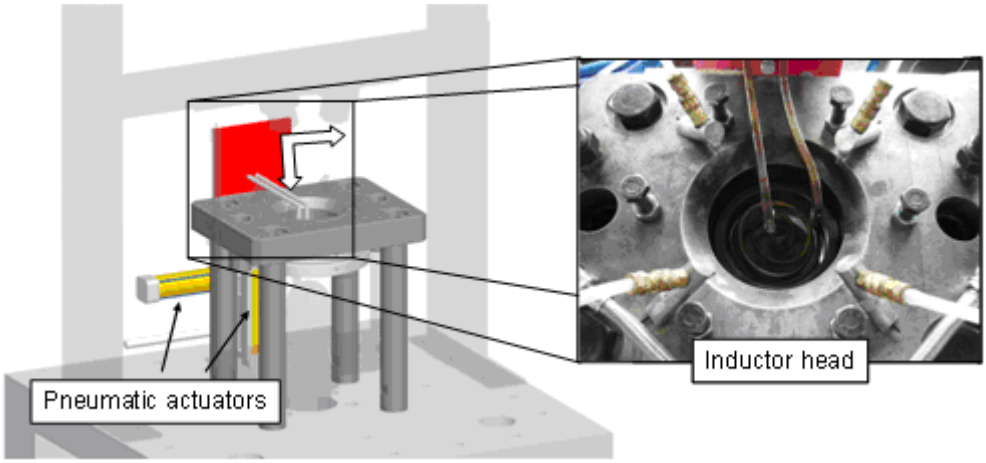

Figure 4.12: Induction heating system

In order to perform the tests applying the needed thermal profile on the specimens, two heating systems have been developed. The specimen itself is heated using an induction furnace through an induction head that can be moved near the specimen surface or outside the test area, in order to enable the use of the optical analysis system, as visible from Figure 4.12. Induction head movements are performed through the use of two automated compressed air cylinders. The main characteristic of the induction furnace are visible in Table 4.6 while the placement of the inductor head, along with its movement path, is visible in Figure 4.13.

Feature	Value
Powering voltage	400 V
Maximum powering current	66 A
Maximum output power	30 kW
Working frequency	70 – 250 kHz
Range of controllable power	20 – 100 %

Table 4.6: Main characteristics of the induction furnace

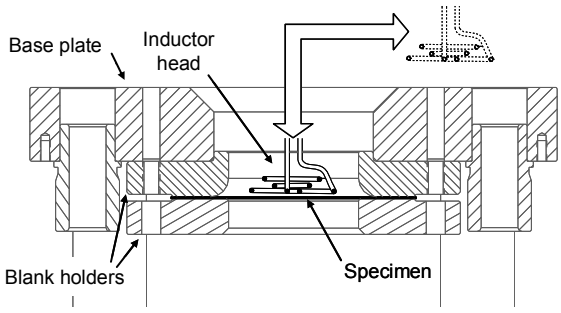

Figure 4.13: Inductor head placement in relation to specimen and blank holders

Different induction heads can be used in order to optimize the thermal profiles for the different specimens used in Nakajima tests, in accordance to their different dimensions. Since induction heating can be very localized, the induction head geometry must closely follow that of the specimen. Too much difference of the two geometries could indeed cause or unwanted eddy current concentrations on the specimen, thus causing very localized, very elevated overheating, or the presence of areas at temperatures so low that austenitic transformation cannot take place.

The heating profile is controlled through software with a feedback loop, using proportional, integral and derivative gains, that evaluate the power to be applied to the inductor head comparing the real temperature on the specimen acquired using k-type thermocouples and the wanted temperature in accordance to test procedure. The feedback control was calibrated considering the thermal profiles that would have been applied in real testing conditions for the different specimen geometries. Therefore, the calibration procedure was performed for every one of these, so that every different specimen has its own optimal values. Figure 4.14a shows a comparison of the real heating profiles, obtained using those calibration parameters, with the imposed ones. The heating profiles along specimen geometries were also analyzed by the means of a thermal camera that acquired a maximum difference of 50°C on the area that would be used in subsequent computations considering all the different geometries, as displayed in Figure 4.15a and Figure 4.15b.

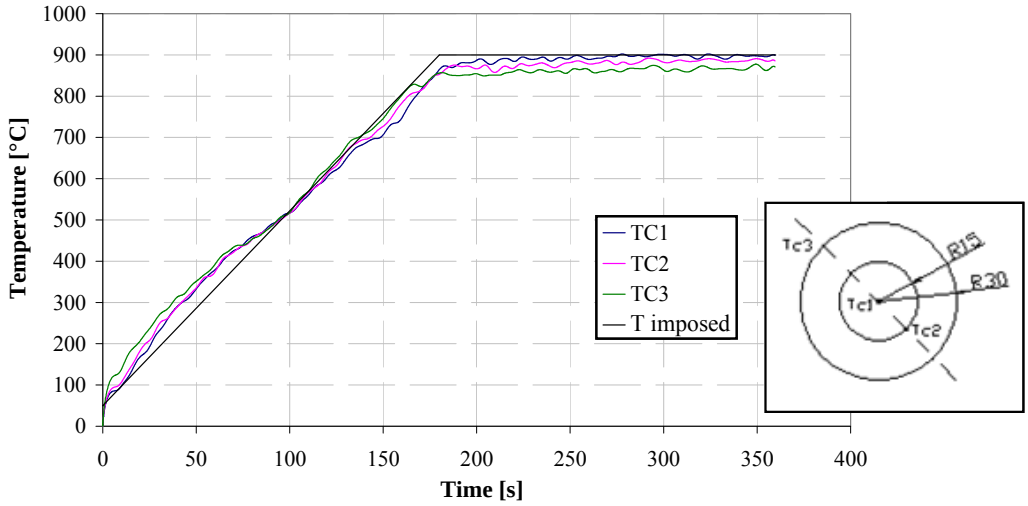

Figure 4.14: a) Thermal profile in a 200mm x 150mm specimen with thermocouple positioned as visible in relation to surface center

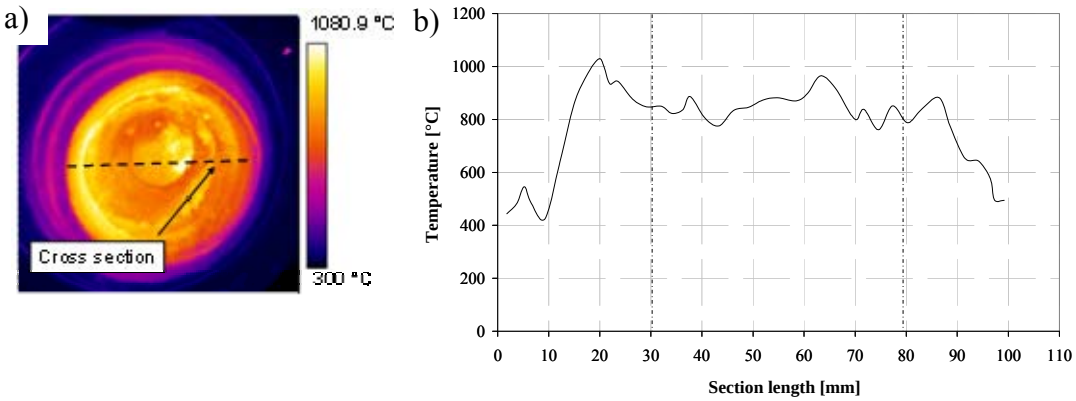

Figure 4.15: Thermal profile on a P type specimen as acquired from the thremal camera: a) on the whole surface, b) on a cross section

In order to maintain isothermal conditions during forming, also the punch has to be heated to test temperature. This was performed through the use of four heating cartridges placed on holes bored directly on the punch itself, as explained in Figure 4.16.

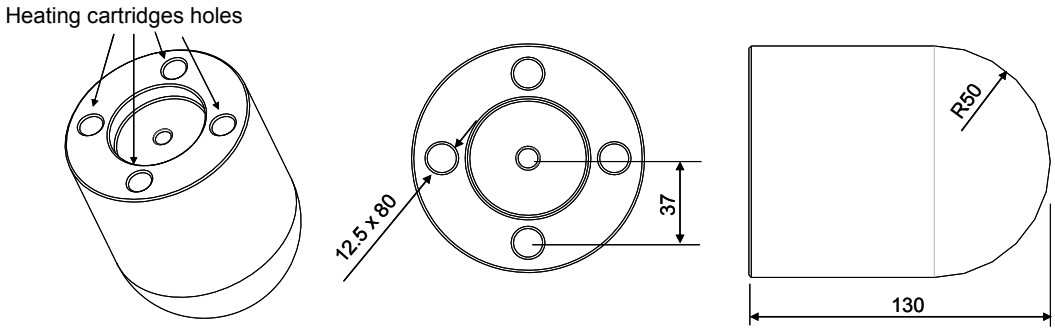

Figure 4.16: Punch heating cartridges position and punch main dimensions

These cartridges are able to apply a total heating power of 3kW and are able to heat the punch at temperatures over 700°C. The die holder can be also heated in case of necessity using two other independent sets of heating cartridges that can apply a total power of 1.8kW.
The elevated heat generated by the punch heating equipment would cause major problems with the load cell, which is placed directly below it and cannot withstand temperatures above 85°C. Also, the values of the load acquired can be altered significantly by thermal fluctuations. In order to avoid these drawbacks, a cooling circuit using water was prepared on the moving plate with the aim of absorbing heat and effectively thermally insulate the load cell.
Similar problems can verify in correspondence of the guides on the base plate, which can fall out of acceptable geometric tolerances due to thermal deformations interfering with the motion of the punch. Therefore these are continually cooled using the same cooling circuit of the moving plate.

4.2.4 Specimen cooling equipment

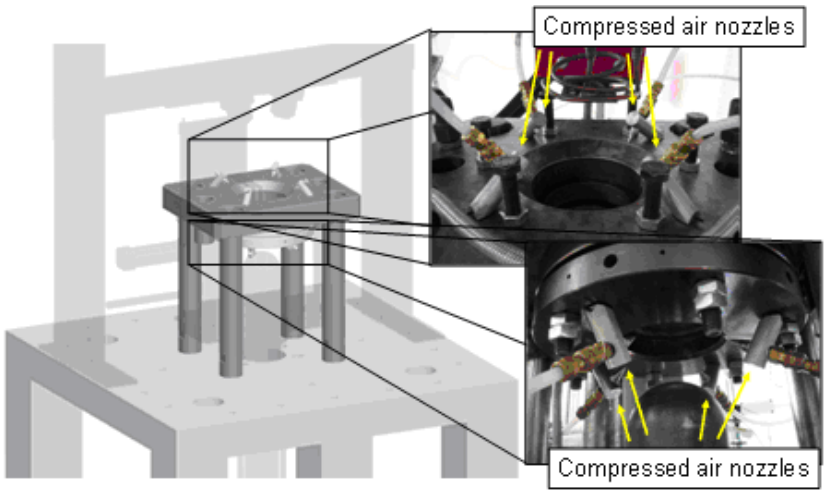

Figure 4.17: Position of compressed air nozzles that belongs to the specimen cooling system

In order to perform the tests maintaining a fully austenitic microstructure on the area that will be used as reference for subsequent strain analyses for the whole duration of the deformation, the test temperatures have to be reached as fast as possible. As visible from the CCT diagram of 22MnB5 of Figure 4.18, faster cooling times enables to have longer times to deform the specimen before the onset of bainitic phase transformation, thus amplifying the range of punch speeds usable. In order to achieve such elevated cooling rates, 8 compressed air nozzles have been arranged on the base plate and on the lower blank holder, directed toward both major sides of the specimen. These are positioned as visible in Figure 4.17 and controlled by the software in consideration of test procedure and temperature measured by the thermocouple welded on the centre of the specimen. They enable to reach cooling rates of approximately 50°C/s, thus allowing about 10s to deform the specimen till fracture.

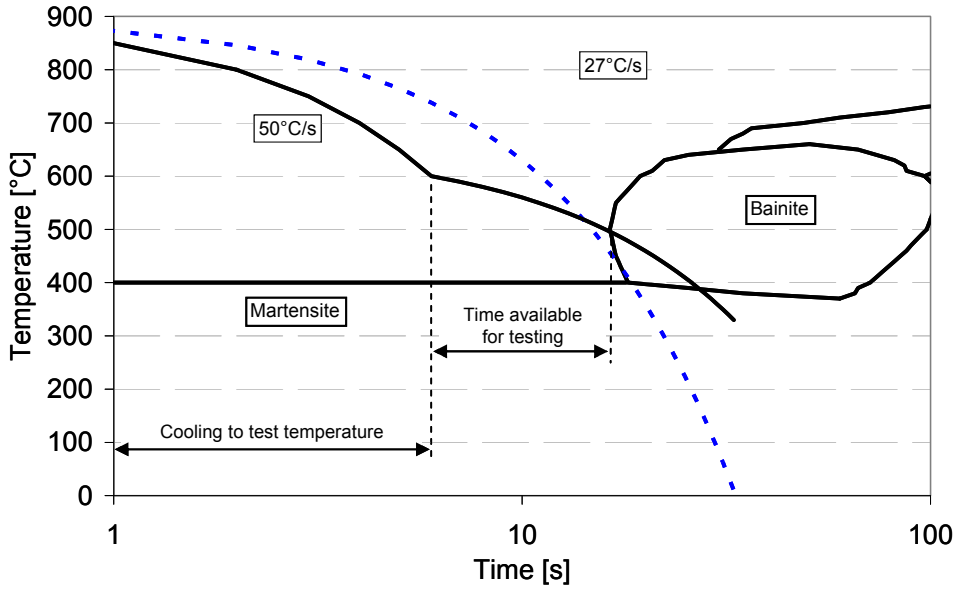

Figure 4.18: Cooling profile used in a Nakajima test performed at elevated temperature

4.2.5 Strain analysis equipment

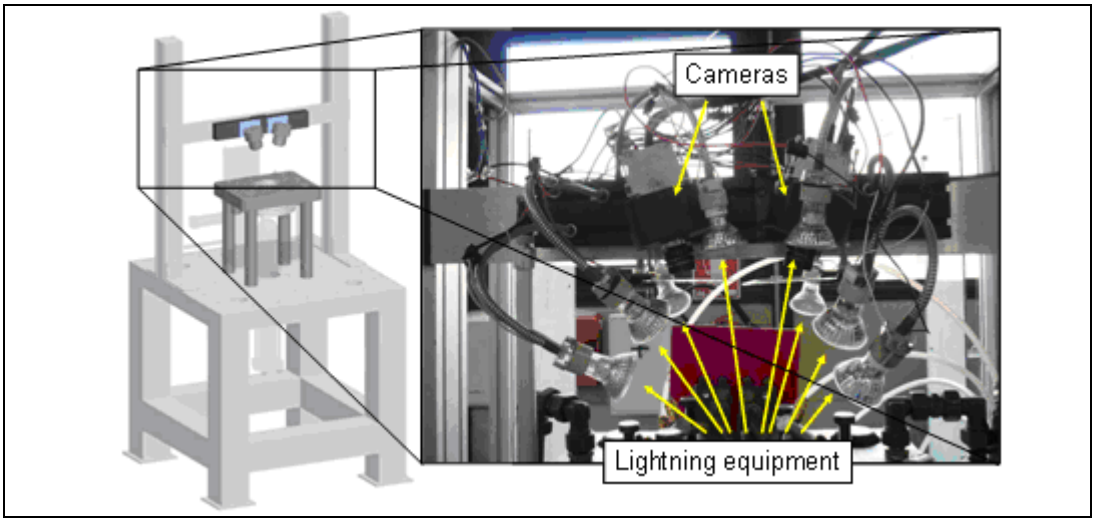

Figure 4.19: Position of optical acquisition equipment for strain evaluation and of the correlated lightning equipment

In order to analyze the deformation of the specimen, an inline optical acquisition system, ARAMIS from GOM, has been used. It is based on the analysis of a stochastic pattern printed on the deforming surface and utilizes two cameras in order to obtain a stereoscopic view and therefore evaluate deformations in all three dimensions. In order to determine strain values, it couples a matrix of points of definable geometry defined in the software to different features recognized on the pattern. Once the latter deforms, the system follows the relative displacements of the recognized features and therefore of the associated points, enabling the calculation of strains along the whole surface analyzed[60]. The pattern is made of white dots that are sprayed on the surface of the specimen and contrast with the dark coloring that the coatings develop during the thermal cycle. The cameras are also provided with flat glasses in front of the objectives in order to protect the optics from debris coming from the surface of the specimen.
A set of lights are placed near the cameras and pointed to the surface to be analyzed. Since the ability to perform a correct strain analysis is heavily dependent on the ability to distinguish the different features of the pattern, an elevated contrast ratio must be assured during the acquisitions. However, over about 650°C-700°C, the thermal radiation emitted increase and shift toward higher frequencies, enough to interfere with acquisitions reducing the contrast ratio until the inversion of the pattern eventually happens. The lights are calibrated in order to prevent this effect from happening assuring that the light reflected from the white dots of the pattern is always greater than the light emitted from the uncovered areas.

4.2.6 Controlling code

The software for the control of the equipment and the acquisition of test parameters was also specifically developed for this particular application. This system uses CompactRIO programmable automation controller from national instruments, which also provides the programming environment, LabVIEW, used for the development of the software itself. In order to improve performance and reliability, the software is divided into three main layers, that are illustrated in Figure 4.20 along with the interactions with each other and with the test equipment.

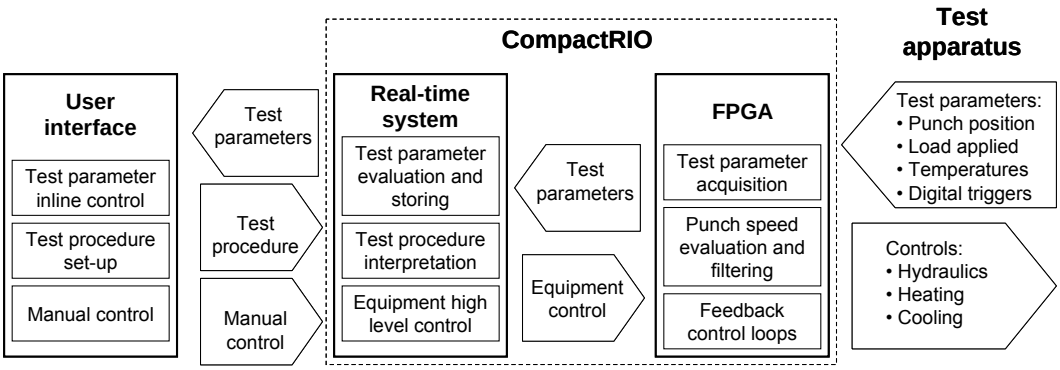

Figure 4.20: Controlling code overview

The layer closest to test equipment was programmed in order to run on the field programmable gate array (FPGA) hosted on the compactRIO system. It features the code needed to retrieve the data from the acquisition modules and send them to the second layer that runs on the real time system, also running on the comapactRIO system. It also provides real time punch speed estimation and filtering and feedback control on two separates control loops simultaneously. Due to the nature of the platform on which the code has been developed, it can run at very elevated speed, therefore enabling a particularly accurate control of the equipment, and is particularly reliable.

The code residing on the real time system on the compactRIO receives the data coming from the code on the FPGA and provides it the values needed to control the equipment. It can simply forward values coming from the user interface during test setup or can follow and interpret encoded programs also coming from the user interface and there defined from test parameters. It also gives the appropriate values to the feedback controls on the FPGA. More than this, it acquires and stores experimental data at frequencies up to 100Hz and send those to the user interface once the test is over.

The third layer provides the direct interface with the user. It also allows inline experimental data visualization.

4.3 Tribological tests equipment

The equipment setup used to perform tribological test on the evaluated ceramic materials is visible in Figure 4.21. The equipment used was a Universal Testing Machine (UTM) microtribometer provided by CETR, whose characteristics are visible in Table 4.7. This test machine was set-up in order to perform pin-on-disc type of tests. It also has an heating chamber that can be used to heat the discs at desired temperatures.

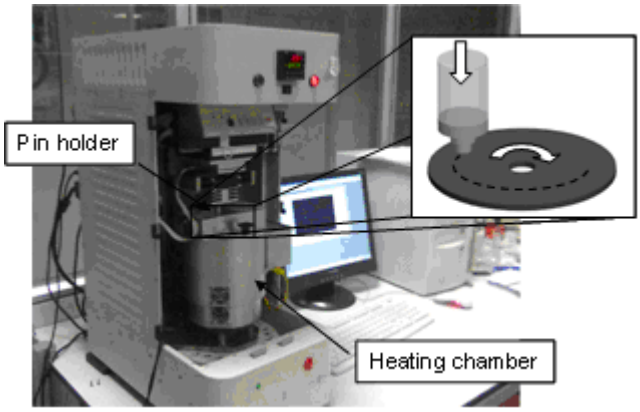

Figure 4.21: Equipment setup for tribological analyses

Feature	Value	
	Positioning system	
	Vertical	Lateral
Position resolution [mm]	1	2
Maximum travel [mm]	150	75
Speed [mm/s]	0.001 – 150	0.01 – 10
	Spindle	
Speed [rpm]	0.1 – 3000	
Maximum load [N]	500	
	Heating chamber	
Max. temperature [°C]	1000	
Heating speed [°C/s]	0.43	

Table 4.7: Main properties of the equipment used for tribological analyses

4.4 Plane pressing tests

4.4.1 Equipment setup

The equipment setup was prepared taking into account all the different process parameters that have to be changed during testing. A configuration where inserts of different materials but same geometry could be arranged on an insert holder was chosen in order to evaluate the different geometrical configurations.
In order to improve flexibility and exploit the ability of the Nakajima setup to operate at elevated temperatures, the latter was adapted to house the two insert holders.
Their main characteristics and dimensions are illustrated in Figure 4.22. They can house up to eight inserts of different materials. Particular attention has been also given in defining geometric tolerances so that the inserts can form a smooth planar surface when placed together and be parallel to the inserts placed on the opposing die, therefore avoiding local discontinuities in pressure distribution. Specimen and inserts dimensions used are visible in Figure 4.23 and in Figure 4.24.

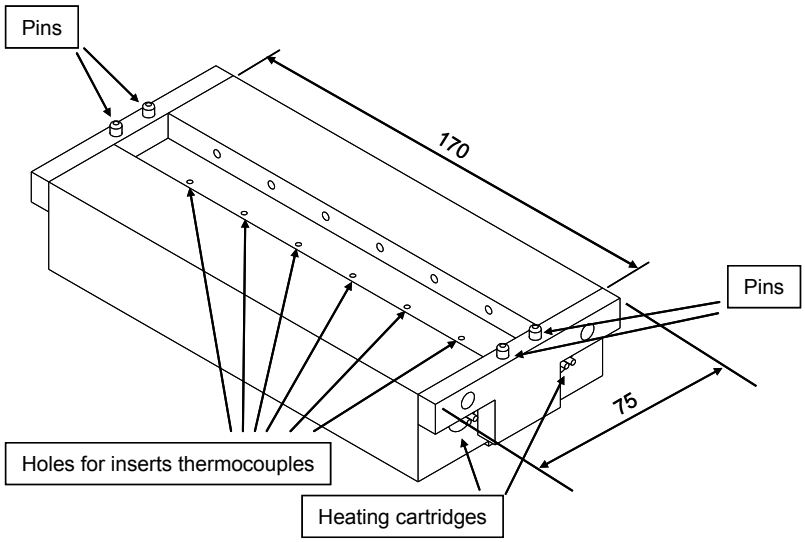

Figure 4.22: Insert holders dimensions and principal features

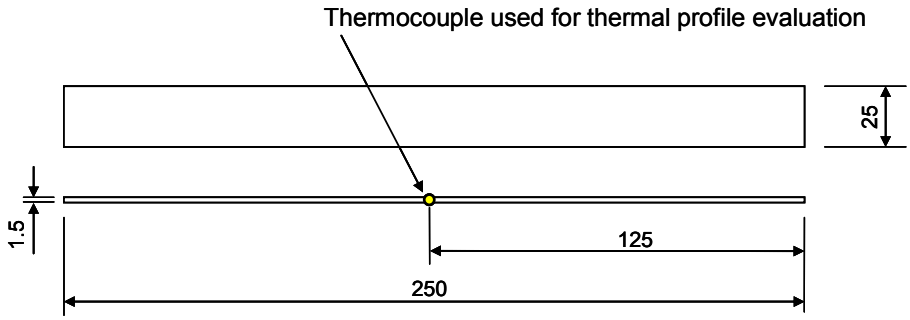

Figure 4.23: Specimen dimensions and thermocouple position in mm

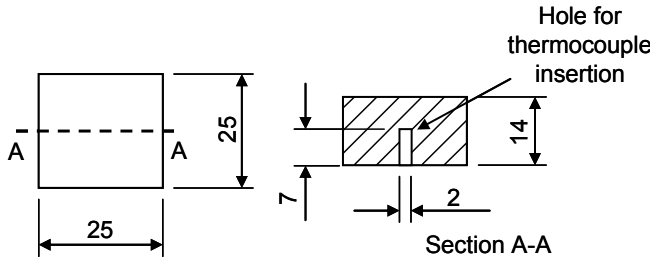

Figure 4.24: Insert dimensions in mm

In order to analyze the thermal profile achieved on the specimen, a k-type thermocouple was spot welded on its side, along its thickness, halfway across its length. When the dies close the thermocouple is placed in the middle of the area under the air gap or the ceramic inserts and, since its welded on the side, do not interfere with the contact between specimen and die surfaces. The general test configuration is illustrated in Figure 4.25.

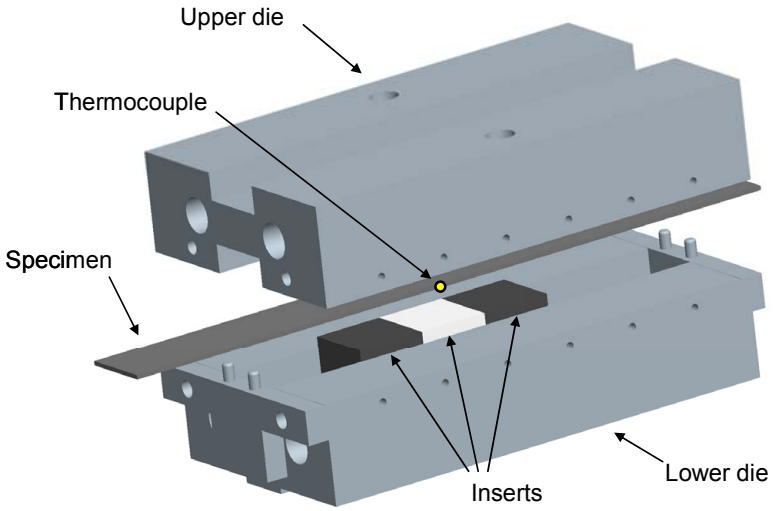

Figure 4.25: General test configuration used in plane pressing tests

The inserts have a hole, bored on the face opposite to the one facing the specimen,

that goes halfway through their thickness and enable the insertion of a k-type thermocouple in order to analyze the heating of the insert itself.
The insert holders have two drilled holes on each of their side which enable to fit a total of eight heating cartridges to heat the inserts at the different temperatures. Each side of the lower holder has also a plate that house two spring seated pins placed in holes so that the top of the pins remain 2mm above the top surface of the lower inserts. This enables to maintain the specimen separated from the lower inserts both before and after the pressing. The two insert holders can be fixed on the die holders using guides or holes so that they can be aligned during the set-up of the equipment.
As already mentioned, in order to applied the apply the move the dies and apply the desired load on the specimen, the insert holders were placed on the press used to perform Nakajima tests, adapting some of its components. The equipment configuration used in these tests is illustrated in Figure 4.26. The figures shows a case where ceramic inserts are used, but the setup is equivalent when the presence of air gaps is considered.

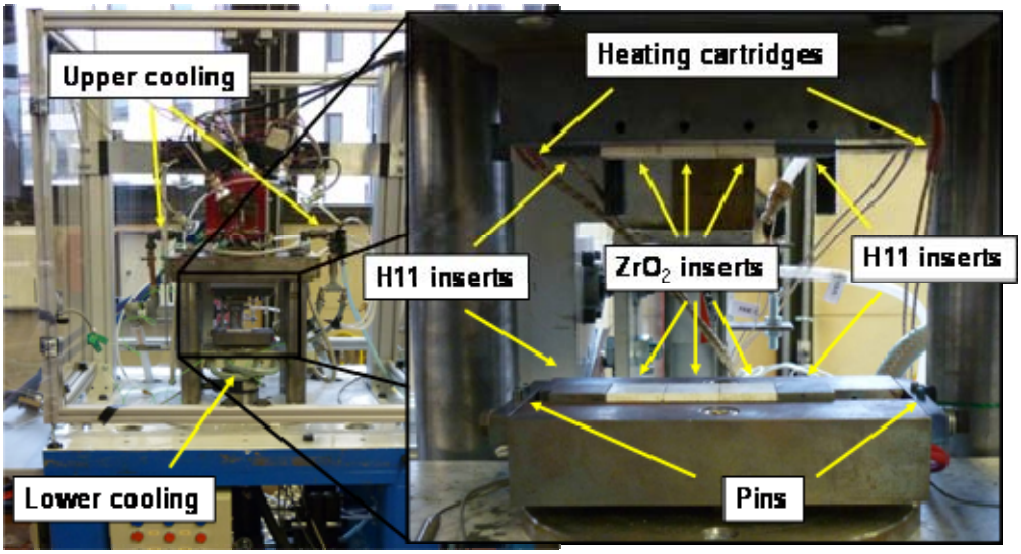

Figure 4.26: Equipment setup for plane stamping tests with hot dies

The press is capable of applying a maximum pressure of 45MPa on the dies. It is also capable of moving at speeds over 200mm/s, and this enables to contain the time spent for the closure of the dies under 1s.
When performing tests with heated inserts, four heating cartridges in every die were used, each of them capable of applying 400W of thermal power, thus enabling to reach temperatures of about 350°C. The dies were also fitted with three k-type thermocouples each, that were placed in the expressly bored holes on die inserts, two inserted on the opposed outermost inserts and one in the central one. The die heating was controlled considering only the temperature of the central insert, but both the other temperatures were also evaluated during test

preparation in order to assure the symmetry of test conditions and homogeneity of thermal profiles.
A load control routine was expressly coded. It evaluates the load applied in real time and uses a feedback control loop in order to control the balancing valve aperture and therefore the pressure of the oil going into the directional valve, which was controlled in the same ways used for speed control of the moving plate. The feedback control loop used one of the PID controls in the FPGA program and enables very fast load correction. More than this, proportional and integral gains for this control are set to zero until a certain load threshold is crossed, so pressure difference among entrance and exit points of the directional valve is kept constant during die approach and the speed of the closing die can be particularly elevated.
This equipment configuration also exploit the presence of a water cooling system in correspondence of the bases of the two insert holders, used to cool the most critical mechanical parts, to improve die thermal conditioning.
In order to heat the specimen over austenitization temperature, a furnace was used that was capable of maintain the desired temperature with an uncertainty of 5°C. Since the thermocouple was welded directly on the side of the specimen before the test, ceramic tubes made of mullite were to be used on each thermocouple wire to assure proper insulation even in the furnace.

Chapter 5

Experimental results

5.1 Introduction

All the results illustrated in the following chapters refers to the most commonly used material employed in hot forming operations, the 22MnB5. this has been provided from Arcelor-Mittal under the commercial name USIBOR1500P and therefore features the particular Al-Si coating used in this product.
At first, the formability of this material have been evaluated using the experimental equipment illustrated in Chapter 4.2. Two test campaigns were performed at two different temperatures, chosen as representative of the thermal states applied on a blank during hot forming. These enabled to evaluate two FLC curves, which were analyzed and compared with a FLC evaluated at room temperature available from literature.
Then, the most appropriate ceramic material to be used as an insert in hot forming operations has been chosen analyzing the results of pin-on-disc tests performed on two different materials, deemed the most appropriate among all the common ceramics materials.
The results of plane pressing tests, performed following the directions obtained from analytical analyses, are then presented. All the three main different configurations illustrated in Chapter 3 have been considered. The obtained thermal profiles were analyzed and the influence of the different test parameters assessed. This enabled to individuate the process conditions through which martensite transformation can be locally inhibited, thus achieving softer microstructures. The results of these tests were then used to critically evaluate the reliability of the numerical models.

5.2 Formability evaluation

5.2.1 Test procedure

Not being available in literature standards with guidelines on performing Nakajima tests at elevated temperatures, the test procedure was defined in accordance to existing ISO 12004 standards that refers to tests to be performed at room temperature[36], taking however into account the particular necessities needed to perform the tests at elevated temperatures. The test procedure is illustrated in Figure 5.1.

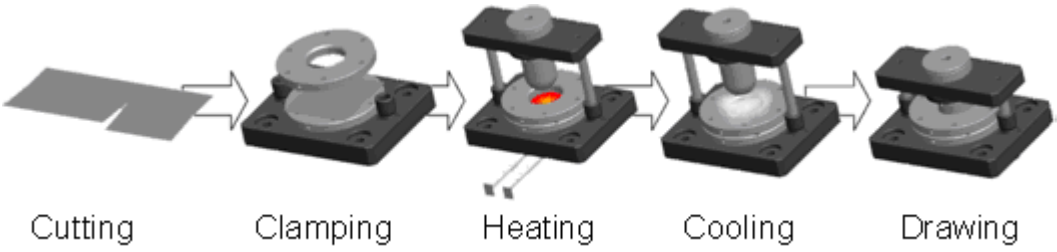

Figure 5.1: Testing procedure for a Nakajima test at elevated temperatures

The specimen is cut to the desired dimensions from the batch of 22MnB5. Several different specimen geometries have been used since every geometry correspond to a couple of major and minor strain in the FLC diagram. The different configurations are listed in Table 5.1. A total of seven different points defining the FLC diagram are therefore expected to be found.
The specimen is then prepared for the test: it's polished with petrol ether to avoid unwanted chemical interactions with elements at elevated temperatures, one k-type thermocouple is welded on the centre of the face not exposed to cameras and the pattern is sprayed on the other using a boron-nitride lubricant as the painting agent.

Specimen	Dimensions	
	L1 (mm)	L2 (mm)
P1	200	200
P2	200	150
P3	200	125
P4	200	100
P5	200	75
P6	200	50
P7	200	30

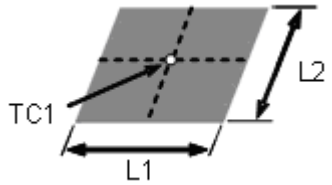

Table 5.1: Specimen dimensions used in Nakajima tests and thermocouple positioning

The specimen is then clamped on the die holders and their bolts tightened using

dynamometric torque wrenches in order to apply a load of 60kN on every bolt. The equipment is prepared fixing the appropriate inductor head and verifying its alignment relatively to specimen position. Its distance from specimen surface is also carefully set in order to optimize the power consumption of the heating furnace and the homogeneity of the heating profile.
After everything has been set-up, the punch is heated to test temperature and covered with a graphite foil in order to reduce friction when in contact with the specimen. The die holders are usually not heated since previous studies[4] showed that their influence on thermal profiles obtained on the specimen is negligible.
The test procedure was then encoded using the software and sent to the controlling software of the experimental equipment. In order to analyze the material in the condition most close as possible to those found in a real hot stamping process, the thermal profile explained in Figure 5.2 was used.

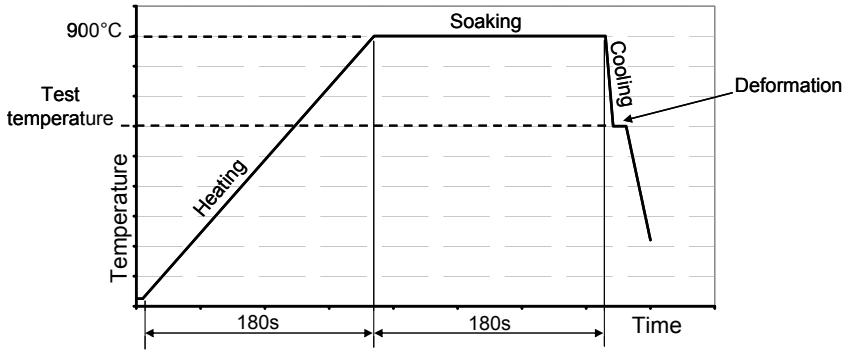

Figure 5.2:Temperature profile applied in Nakajima tests

The specimen was heated in 180s to 900°C, with an average heating rate of 5°C/s in order to avoid degradation of the Al-Si coating and allowing the Fe in the base steel to properly diffuse into it. Another 180s at 900°C follows in order to homogenize the thermal profile along specimen surface and to allow complete austenitic phase transformation to take place. More than one thermocouples are used at regular intervals on the specimen in order to verify the quality of the heating profile. During this phase the temperatures of both the specimen and the equipment are acquired at a frequency of 5Hz.
After the heating is completed, the induction head is extracted from the test area in order to clear the area framed by the cameras of the optical strain acquisition equipment and to avoid interferences with the cooling equipment. The specimen is then cooled to test temperature at an approximate rate of 50°C/s. As soon as the specimen reach that temperature, the cooling stops and the punch moves at a constant speed of 10mm/s till fracture occurs. During deformation, temperatures, load applied on punch and its position are acquired at 50Hz, while the optical acquisition equipment records specimen deformations at 12Hz.
The acquired images are then processed using the Aramis software, excluding non interesting areas and defining the appropriate dimensions for the analysis grid.

These dimensions depend on pattern quality and on environmental conditions.
After major and minor strains are evaluated on the whole specimen surface for all the different times, the strains at the image just before fracture are evaluated. In accordance to ISO 12004 standard, three different sections parallel to each other are defined on the specimen surface, with their direction normal to necking direction, 5mm apart from each other and centred on the centre of the necking region. Major and minor strain profiles are evaluated along these sections.
This data is then analyzed following two different methodologies, which are represented in Figure 5.3b. In one case, the procedures defined in standards were followed. These implied that the areas where necking is most prominent were left out of the evaluating procedure. The remaining points where then fitted using an inverse parabolas in order to calculate the values to be used in FLC diagrams. This procedure therefore don't consider post necking deformations, which could lead to excessively conservative evaluations. At elevated temperatures local instabilities develops indeed quite early and post necking deformations are therefore usually exploited in order to achieve the desired geometries.
On the other case the strains used in FLC computations were manually evaluated as the highest values reached on the strain profiles. This led to two different FLC diagrams to describe every single process condition.

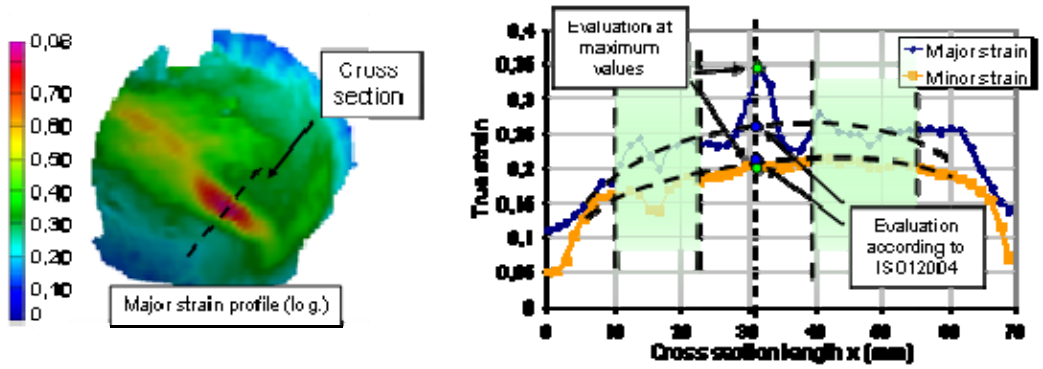

Figure 5.3: a) Strain profile as evaluated by the ARAMIS system and an analyzed cross section and b) Evaluations performed on strain profiles along a cross section

The tests were performed at two different temperatures, which represent the range where most deformations develops in an hot stamping process.
A summary of test parameters is visible in Table 5.2.

Parameter	Value
Heating temperature	900 °C
Heating time	120 s
Soaking time	120 s
Test temperatures	500 °C – 600 °C
Average cooling speed to test temperature	50 °C/s
Punch speed	10 mm/s

Table 5.2: Experimental parameters used in Nakajima tests

5.2.2 Results

In Figure 5.4 are visible the results relative to evaluation in accordance to ISO12004, confronted with FLC values as evaluated from Lechler et al.[61].

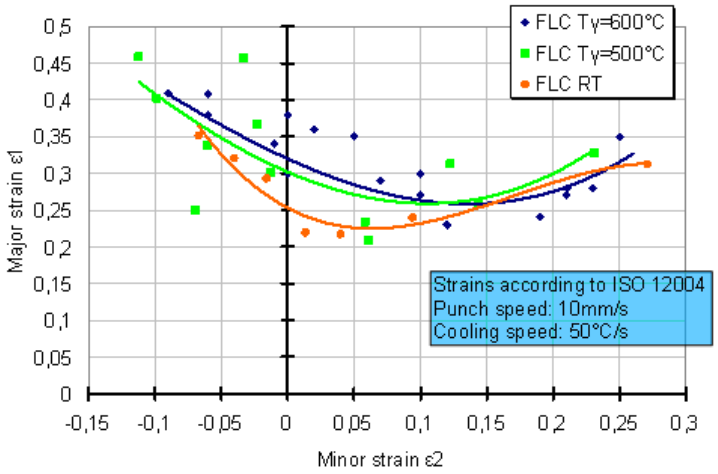

Figure 5.4: FLC determined for USIBOR 1500P at 500°C and 600°C in comparison to those relative to the same material before heat treatment as described from literature[61]. All data evaluated using ISO 12004 procedure.

The diagram shows that, evaluating the strain profiles using ISO 12004 procedure, an appreciable increase in formability can be noticed at both 500°C and 600°C if compared to room temperature results. A certain increase, of much lower magnitude, can also be noticed at 600°C if confronted to the 500°C case.
In Figure 5.5 are visible the results considering the maximum values reached in correspondence of the necking region just before failure.

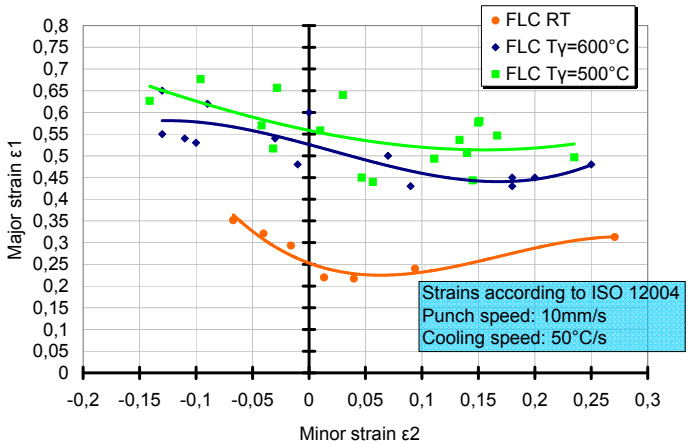

Figure 5.5: FLC for USIBOR 1500P at 500°C and 600°C evaluated considering the maximum values reached on the strain profiles and confronted to values evaluated at room temperature

These results shows in fact a considerable increase in formability if confronted with the results at room temperature. This is consistent with the increase of post necking deformations that is typical of a high temperature deformation.
The two result shows also that the values at 600°C seems lower than that achieved at 500°C when strains are evaluated at their maximum values. This is in direct contradiction with previous evaluations. It should be noticed, however, that results analysis, in this case, was performed by hand by taking the values on the strain profile closest to fracture. After instability has set in, the deformations becomes concentrated in the necking region, where therefore elevated strain gradients are achieved. So, many other parameters can significantly influence the results since little differences in the position of the point considered for strain evaluation can reflects in major differences in the evaluated values. Parameters such as strain grid dimensions and position, pattern quality and section position can therefore play a major role in assessment of the strain values. This is also reflected in the increased scattering of these results when confronted with the previous ones. They then cannot be considered a solid base for usage in FEM codes, but hints at the fact that newer more advanced standards are needed for a proper and useful evaluation of material formability at elevated temperatures.

5.3 Tribological tests results

In order to evaluate the use of ceramic inserts on hot forming dies, an appropriate material has first to be individuated. The ceramic employed has indeed to resist to harsh conditions, with sudden changes thermal conditions while assuring mechanical properties comparable to those of the die steel used. The choice of the wrong material, given also the brittle nature of most ceramics, could lead to frequent failures, with all the correlated drawbacks.
Among the different commonly used ceramics materials, the two deemed as the most appropriate for this particular application due to their mechanical and thermal properties were: Macor, a glass ceramic, and Zirconium dioxide Yttrium stabilized, whose properties are listed in Table 5.3 in comparison to those of a common die steel.

	H11	Macor	Zirconium dioxide [ZrO_2]
Young's Modulus [GPa]	210	66.9	186
Density [Kg/ m^3]	7750	2520	6000
Thermal conductivity [W/m K]	42.2	1.46	2.70
Heat capacity [J/Kg K]	460	790	400
Thermal expansion [10^{-6}/°C]	13.3	11.4	10.3

Table 5.3: Main thermal and mechanical properties of H11 steel and Macor and Zirconium dioxide ceramics

Macor was chosen because it featured very low heat conduction capabilities, which enable the surface temperature to rise significantly in respect to the temperature on the rest of the die, thus lowering the heat exchanged at the interface. It is also machinable with standard tools, and this would make the production of complex geometries particularly simple. It is also relatively cheap and its mechanical properties seems suited for the application even though no data can be obtained from literature that evaluates them at elevated tempeatures.
Zirconium dioxide Yttrium stabilized was evaluated as a good candidate due to its elevated mechanical and thermal properties. Its heat conduction is a bit higher than that of Macor but still very low compared to that of H11. It has very high hardness and therefore wear resistance. It also has a thermal expansion coefficient that is very close to that of the die steel and this could prove critical in the tests were the dies have to be heated.
In order to evaluate the suitability of these two materials to act as die inserts, their tribological capabilities were investigated using pin-on-disc tests performed at elevated temperatures on the equipment described in Chapter 4.

5.3.1 Test procedure

In order to replicate real forming conditions, it has been chosen to use the ceramics as the materials for the pins, and to apply to the 22MnB5 sheets, used for the discs, a thermal profile close to that applied to hot stamped blanks. The disc is therefore heated up to 900°C and then cooled till it reaches test temperature, when the test is actually performed. The ceramic pin is maintained at room temperature during the heating of the disc and inserted into the heating chamber only when needed, in order to replicate the case of a cold die coming in contact with a hot sheet.
After pin insertion into the heating chamber, the desired pressure is applied and the disc put in motion at constant angular speed. As in hot stamping operations performed on USIBOR 1500P, no lubricants have been used.
The tests were performed at 700°C applying a pressure of 36MPa and with a disc rotating at the speed of 3 or 5 revolution per minute. More than this, the tests continues since conditions are considerable stable.
To evaluate tribological capabilities, normal and tangential forces applied on the pins are acquired along with time and disc position. This enable to evaluate the friction coefficient and its evolution throughout time.

5.3.2 Test results

The results in terms of friction coefficient for the two cases as acquired from the

measuring equipment throughout the tests are visible in Figure 5.6a and Figure 5.6b.

a)

b)

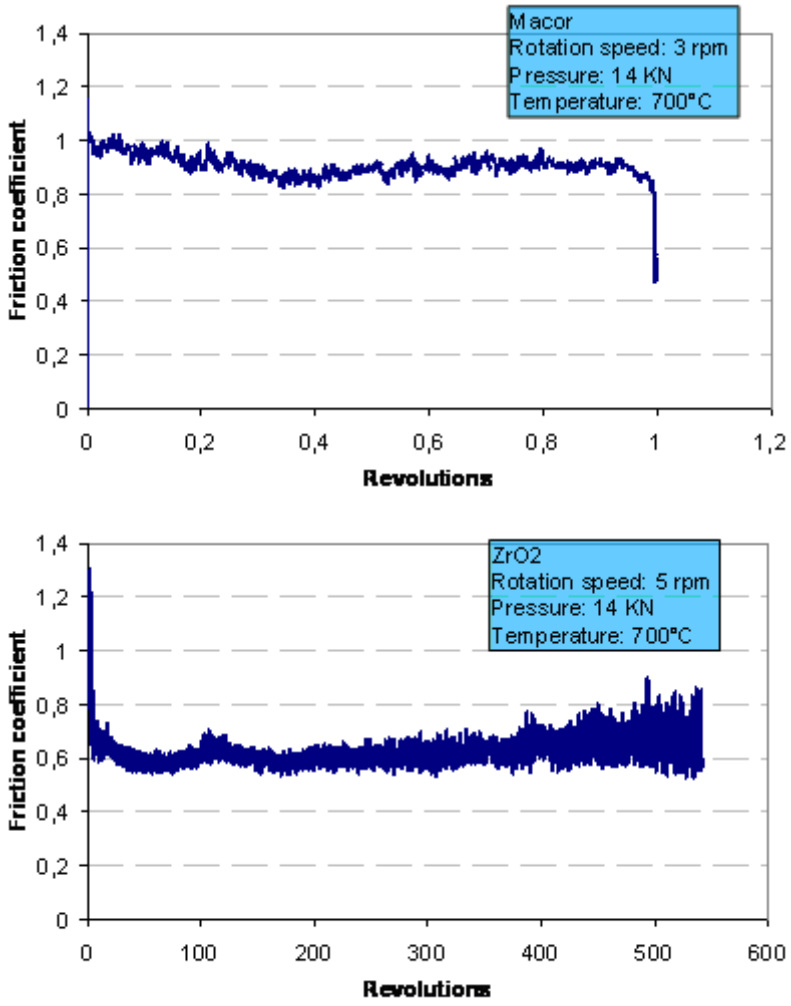

Figure 5.6: Friction coefficient evaluated for a) Macor and b) Zirconium dioxide

From these results it is possible to see that Macor pin didn't go over one total revolution, and this was due to the great quantity of material being transferred from the pin to the sheet, as visible in Figure 5.7a, which shows a 22MnB5 specimen after the test. This was probably due to chemical affinity of the glass ceramic in relation to the steel, which was made more prominent by the high temperature. When the pin went on an area where transferred material was already present, therefore after one complete revolution, the sudden increase of the friction coefficient stopped the testing equipment, preventing the continuation of the test. The effects of this mechanism are also visible in the pin surface that after the tests shows prominent wear, as visible in Figure 5.7b.

a) b)

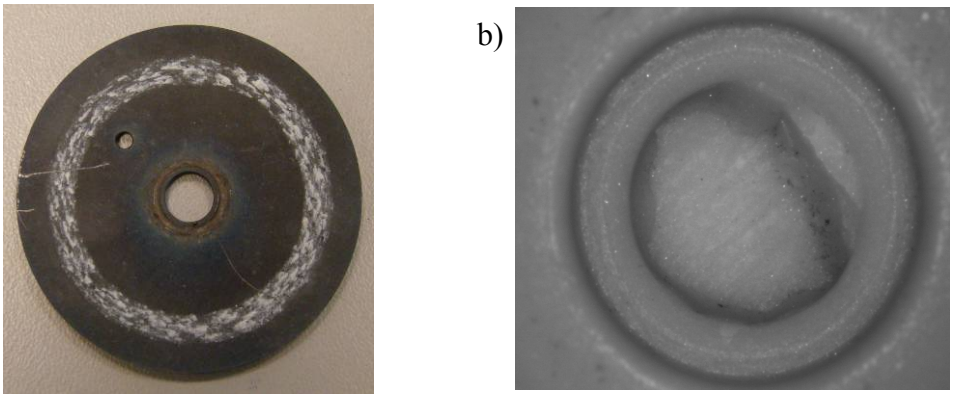

Figure 5.7: a) Metal disc surfacae conditions and b) Pin surface conditions after testing with Macor

It is also possible to see that, while stable throughout the test, the friction coefficient for the Macor is particularly elevated, being near to one, and this is not an acceptable value for its use as a die insert.
On the other hand, the results for Zirconium dioxide pins shows acceptable values of the friction coefficient, which remained stable till about 400 revolution, where the system began to show some instability. This performances are due to the elevated mechanical properties of the material, which therefore has very elevated hardness and thus wear resistance, even at elevated temperatures.
After the test both the pins and the 22MnB5 disc showed no particular alterations worth noticing.

5.3.3 Conclusions

The tests results shows that Macor ceramic material cannot withstand numerous stamping cycles without altering its superficial geometrical characteristics in a critical way. Zirconium dioxide, even if more difficult to use in actual applications, being not machinable after heat treatment, is preferable due to its elevate wear resistance.
Through these considerations it has been decided to use Zirconium dioxide as the preferred material to be used for ceramic inserts.

5.4 Plane pressing tests

5.4.1 Test procedure

The test procedure was basically the same whether the tests were performed with cool or heated dies, with differences acknowledgeable only in test parameters. The test procedure is illustrated by Figure 5.8.

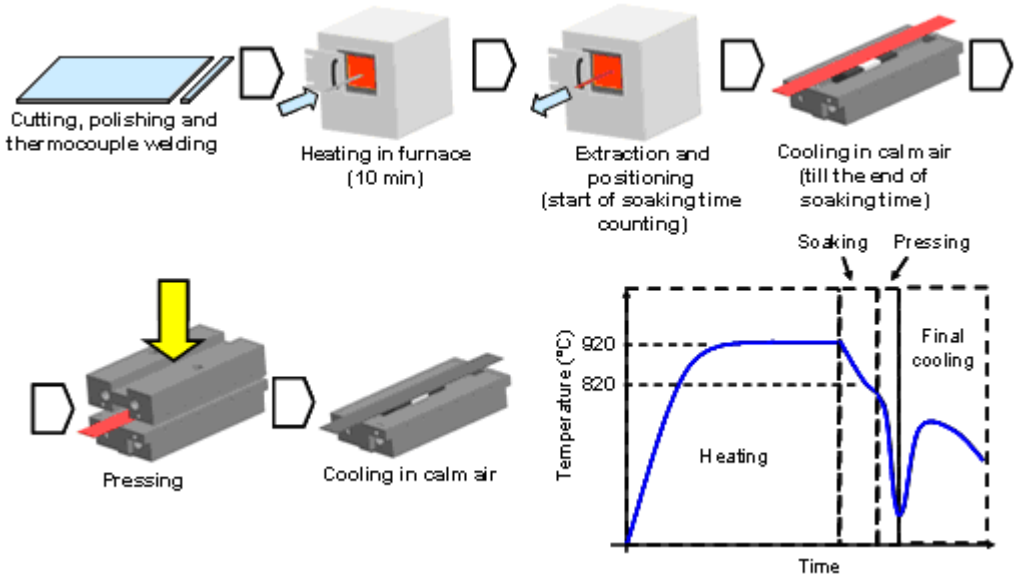

Figure 5.8: Test procedure for plane pressing tests

The specimen is cut from larger sheets with the dimensions defined from previous numerical analyses. Then it is polished using petrol ether and the k-type thermocouples is spot welded on its side. The specimen is then inserted into the furnace and there maintained for ten minutes, in order to mimic the heating performed in a real hot forming processes. Then it is manually extracted and let cooling in calm air or placed on the pins on the lower die, depending on the test procedure. In the latter case, the end of the decided soaking time is eventually awaited, then the dies are closed with the imposed load for the defined closing time. The dies then open and the specimen is left cooling in calm air till it reaches temperatures lower than 100°C.

Since the thermocouple are welded in the centre of the specimen, they measure the temperature profile in correspondence of the symmetry axis of the dies. This makes the results of these tests directly comparable to the results obtained from the numerical analyses.

In order to evaluate the obtained microstructures, after the test the coating on the specimens surfaces is mechanically taken off and Rockwell hardness measurements are performed following grids of points spaced 5 mm from each other along the specimen length and 10 mm along its width. This enabled to calculate the hardness in correspondence of every insert as an average of 15 different measurements.

For all the specimens, micrographic imaging was also used in order to evaluate the microstructures in the section of the specimen where the thermocouple was placed.

5.4.2 Experimental plans

The test campaigns were defined taking into account the results of the numerical analyses. Therefore, three different cases are analyzed: the cooling of the specimen in calm air, the cooling in dies where an air gap is present and the cooling in dies with ceramic inserts.
The first type of test consisted essentially in only one test and is necessary in order to evaluate the limits of a differentiated cooling process and the quality of the assumptions made on numerical analyses for the evaluation of the heat exchanged with the open environment. The test parameters for this test are listed in Table 5.4.
For the second type of test, the cooling in dies with an air gap, the geometrical configuration evaluated as the most interesting through numerical analyses, where two steel inserts are placed 25mm apart from each other, is used. The only changed parameter is closing time, which is varied as explained by Table 5.4, which also illustrates the other test parameters. The material used for the dies was H11, whose thermal properties are visible in Table 5.3. These tests represented a good performance bench for the study of numerical analyses reliability and enable to evaluate the effects of different holding times if grooves are used on dies to locally slower the cooling rate. The use of these is however limited to indirect hot stamping operations since freeforming conditions are reached in correspondence of the grooves.

Parameter	Value	
	Cooling in calm air	Air gap pressing
Heating temperature [°C]	940	920
Soaking time [s]	180	5
Holding time [s]	-	3 – 5 – 10
Air gap width [mm]	-	25
Steel insert width [mm]	-	25

Table 5.4: Test parameters for cooling in calm air and plane pressing tests with air gap

The third type of test is considered the most important for the design of an hot stamping process where the control of the thermal profile is performed along with forming. The material used for the ceramic inserts, as already stated, is Zirconium dioxide Yttrium stabilized, while the material used for the steel ones is the same used in the air gap tests, H11.
The test parameters whose influence was deemed of interest are: geometrical configuration, soaking time, die temperature and closing time. The test plans, defined in accordance to the results of the numerical analyses, are explained in Table 5.5.

Parameter	Value		
	Cool dies		Hot dies
	Geometry dependence	Soaking time dependence	Holding time and die temperature dependence
Heating temperature [°C]	920	920	910
Soaking time [s]	5	5 – 10 – 25 – 30	7
Holding time [s]	3	3	3 – 5 – 10
Ceramic insert width [mm]	25 – 50 – 75	75	75
Steel insert width [mm]	25	25	25
Die temperature [°C]	25	25	25 – 200 – 300
Repeatability	2	2	3

Table 5.5: Test parameters for plane pressing tests with ceramic inserts

5.4.3 Test results

5.4.3.1 Cooling in calm air

For this test, the thermocouple was welded in the centre of the specimen length. The results are visible in Figure 5.9, where the CCT diagram of 22MnB5 is also represented.

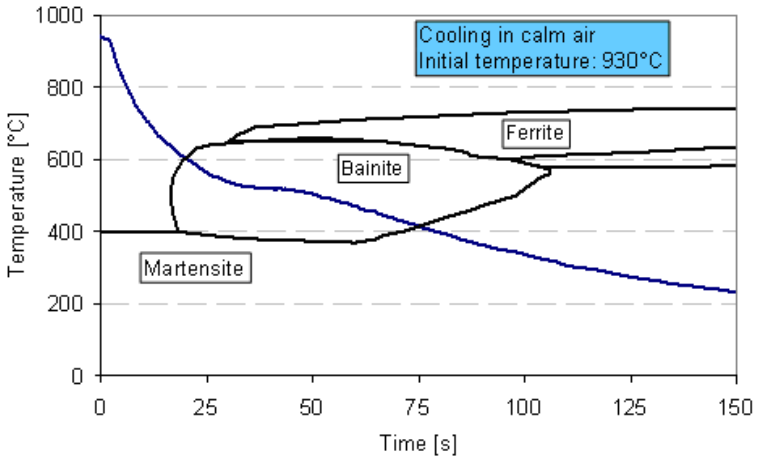

Figure 5.9: Thermal profiles resulting from cooling in calm air

The results shows an average cooling rate of 16.74°C/s which enables to enter the bainite transformation area on its upper half. The micrographies, presented in

Figure 5.10c, shows a fully bainitic microstructure as expected from the CCT diagrams. It shows indeed significant differences if confronted to the state of the material before the thermal treatment, which is shown in Figure 5.10a and has a ferritic-perlitic microstructure, and to the state of the material after quenching in water, that as visible in Figure 5.10b, which present a fully martensitic microstructure.

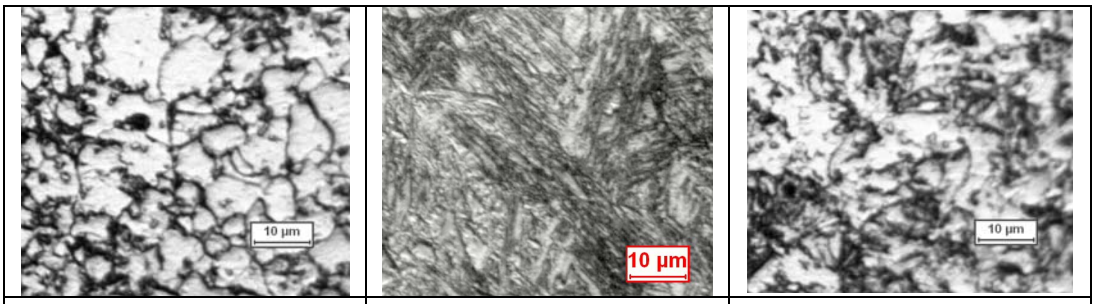

a) Base material	b) Water quenching	c) Air quenching

Figure 5.10: a) Microstructures of the material before heat treatment and b,c) after different quenching conditions

Hardness measurement performed on the specimen shows values around 50 HRA (150HV), which are compatible with an upper bainite microstructure.
Since all the other cases make use of air or mediums with higher heat exchange capabilities at relatively low temperatures, it is safe to say that this case represent the lower limit of obtainable cooling rates. Ferrite and perlite areas are thus not reachable through cooling in dies. Nevertheless, bainite can still provide enough softening to represent an advantage in a hot forming processes.

5.4.4 Cooling on dies with air gap

Since the chosen geometrical configuration should allow a great variation of the cooling rate in dependence of the closing time, as predicted by the numerical analyses, three of these were chosen and their influence evaluated.
The cooling profiles obtained can be seen in Figure 5.11.

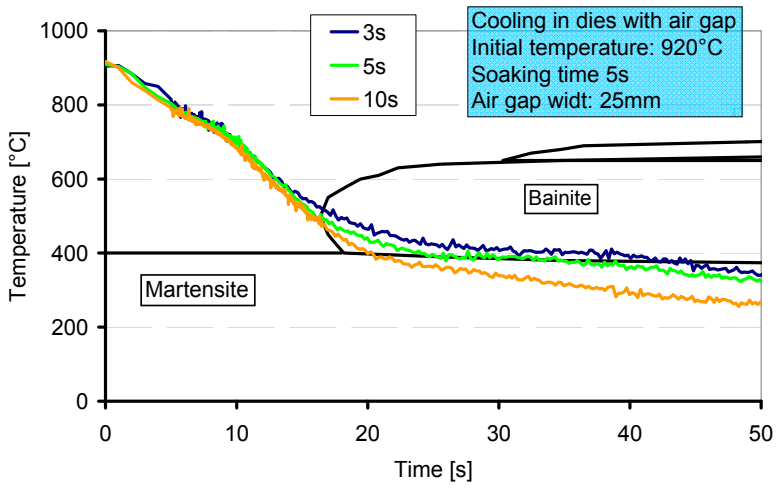

Figure 5.11: cooling profiles obtained from cooling in dies with air gap

As its possible to see, in all the three considered cases the thermal profiles enter the bainite transformation field. Even with 10s of closing time, a certain quantity of bainite is expected to be found in the specimen.
The results of hardness measurements along the length of the specimen are visible in Figure 5.12.

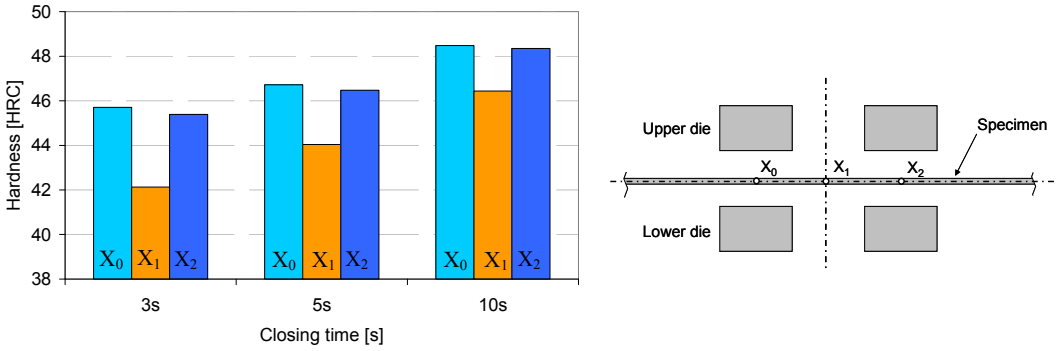

Figure 5.12: Hardness profiles along specimen length for air gap tests

The hardness results shows that, even if certain quantities of bainite certainly formed in the areas under the air gap, their contribute to the softening of the material is quite low. Only at 3s of closing time the reduction in hardness can be considered interesting. It should also be noticed that the difference between the hardness measured under the steel insert and that measured under the air gap increases as the closing time decreases.
The micrographies taken in the area of the specimen under the air gap are illustrated in Figure 5.13 for the cases with 10s and 3s of closing time.

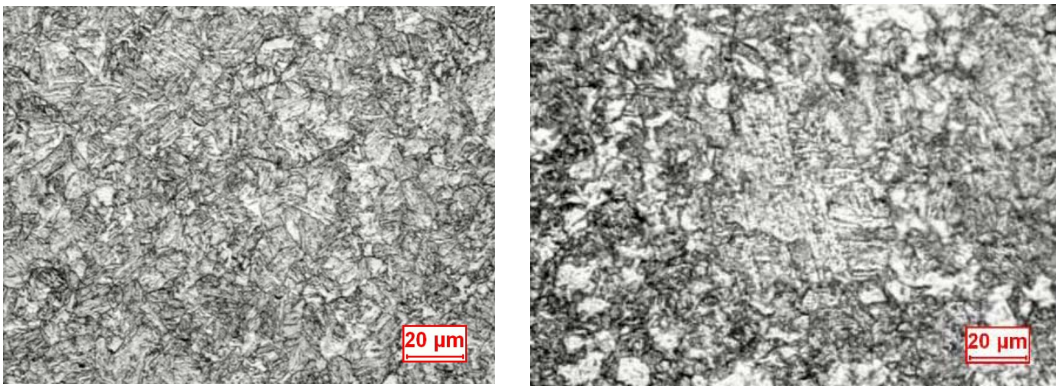

10s 3s

Figure 5.13: Micrographies for air gap tests

These shows that, in the first case, the obtained microstructure is almost completely martensitic, with only sparse areas of lower bainite. On the other hand, in the 3s case these areas are much larger, even if the martensite phase still constitutes the predominant one.
These results shows that using air gaps makes, at least for small dimensions, the choice of closing time a critical parameter that must be kept as low as possible.

5.4.5 Cooling on dies with ceramic inserts

The first case considered in order to evaluate the effects of the different process parameters on the obtainable temperature profiles, in the case where ceramic die inserts were used, was the geometrical configuration dependence. While maintaining the same dimensions for specimens and steel inserts used, three different width have been considered for the ceramic inserts. The other process parameters were kept constant and adherent to those used in numerical analyses. The temperature was always measured in the centre of the specimen. The obtained temperature profiles are described in Figure 5.14.

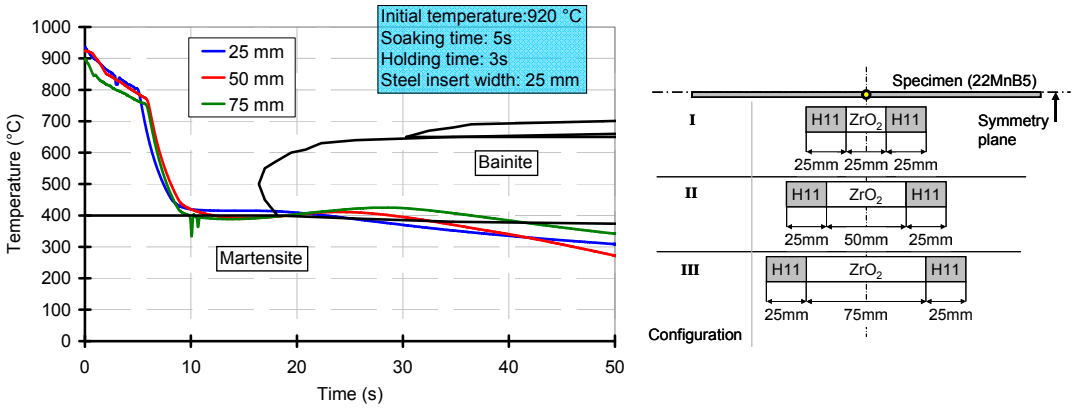

Figure 5.14: Thermal profiles for geometry dependence with ceramic die inserts

As it is possible to see from the results, the effects of wider ceramic inserts is subtle but noticeable mostly after 20s, where the case where 75mm insert was used has a sensible increase in temperature as it enters the bainitic transformation area if confronted with the other two cases. This is due to a slightly minor cooling rate that inhibits complete martensite transformation and allows the formation of lower bainite. The resulting hardness profiles are illustrated in Figure 5.15.

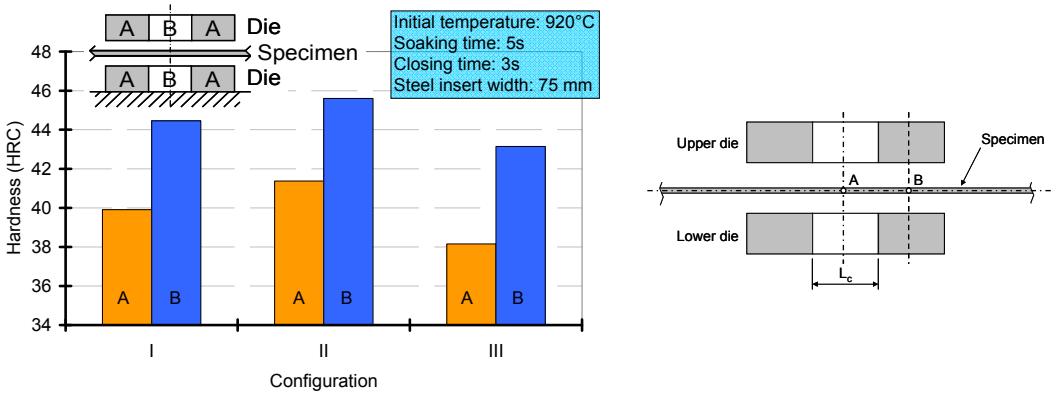

Figure 5.15: Hardness profiles along specimen length for ceramic insert width dependence

The results shows a slight decrease in the hardness of the area under the ceramic insert in relation to that evaluated under the steel inserts in all the three cases, with a more visible effect for the case with the 75mm wide ceramic insert. The micrographies obtained relative to point A for the first and the third configurations are visible in Figure 5.16.

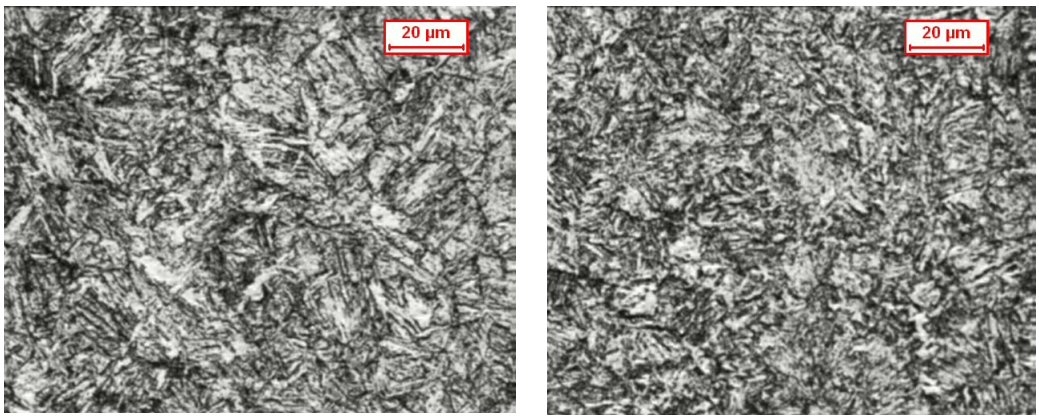

Figure 5.16: Microstructures at the centre of the specimen with a) a 25mm and b) a 75mm wide ceramic insert

This micrographies shows that, as suggested from hardness results, a slight increase of the fraction of obtained martensite phase can be noticed.
This case therefore shows that the simple use of ceramic inserts in standard

forming conditions is not sufficient to achieve microstructures that are soft enough to allow useful thermal profile control. Also, it shows that, even if different cooling profiles are achieved, microstructures comparable to those obtained using air gaps are achievable.
These results displays that softer microstructures are indeed achievable and that the geometrical configuration with 75mm wide ceramic insert is the one that has to be used in following analyses in order to obtain useful results.
The second case considered took into consideration the influence of soaking time on thermal profiles. The purpose of this test campaign was to analyze if different soaking times could amplify the effects of different cooling rates in different areas of the specimen.
In this case, four different soaking times have been considered: 5s, 10s, 25s and 30s. The resulting thermal profile are visible in Figure 5.17.

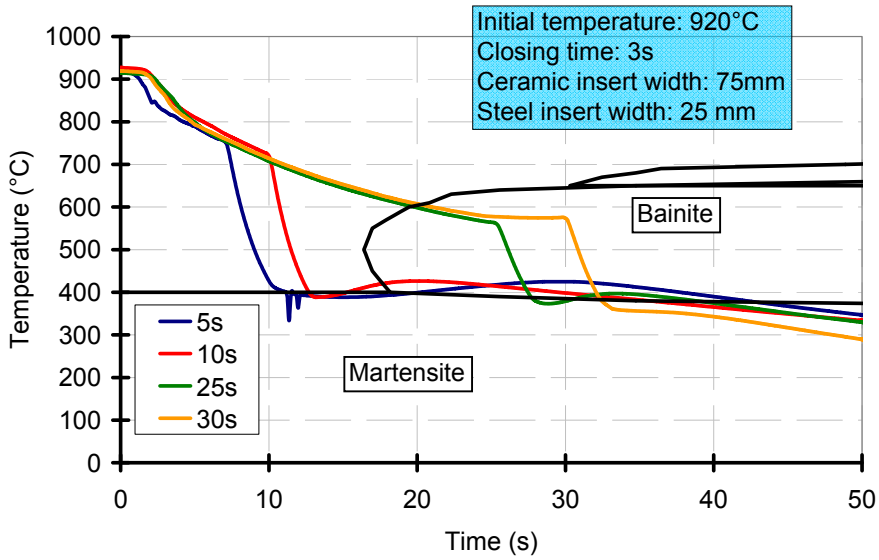

Figure 5.17: Thermal profiles for soaking time dependence tests

At the increase of soaking time, the cooling profile during pressing, which maintains throughout the tests about the same cooling rate, gets closer and closer to the bainite transformation until it eventually enters it for 25s and 30s.
The results of the hardness measurements for this case are reported in Figure 5.18.

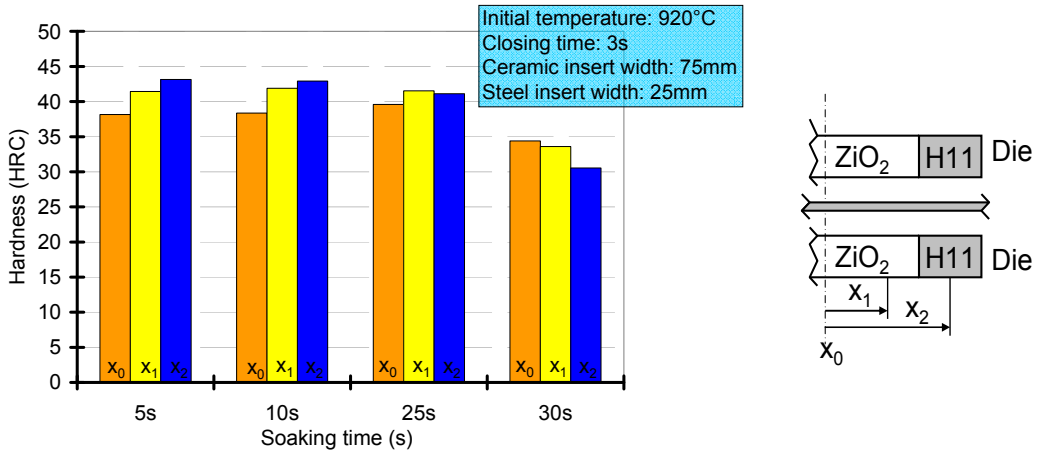

Figure 5.18: Hardness profile along specimen length for different soaking times

From these results it is possible to see that going from 5s to 10s doesn't show any particular effect. For 25s, a certain levelling of the hardness along the length of the specimen is noticeable but it isn't accompanied to a useful reduction in the overall hardness value. At 30s the bainitic transformation plays the major role in determining the final hardness and therefore the mechanical properties of the specimen, and it is possible to see an inversion in the hardness profile, probably due to heat exchanged with the pins used to sustain the specimen.
The micrographies relative to 10s and 30s as obtained for the area in correspondence of the point X_0 are shown in Figure 5.19.

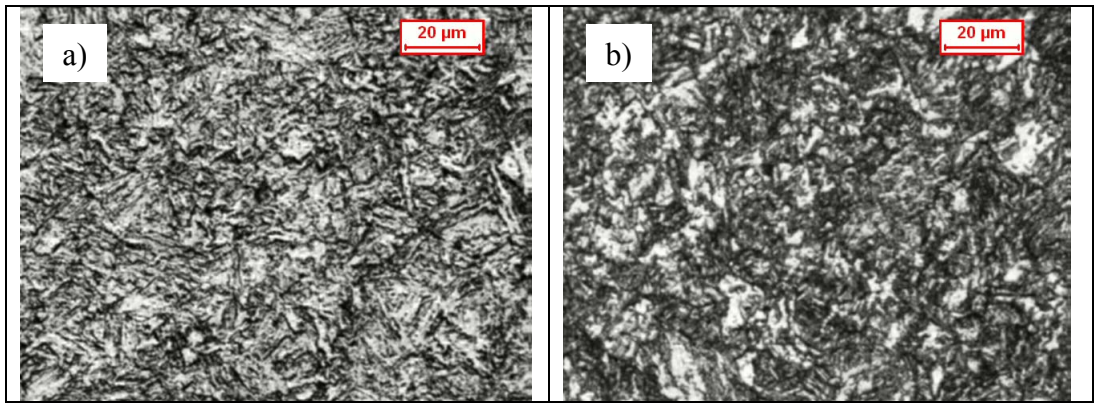

Figure 5.19: Microstructures evaluated in X_0 at a) 10s and b) 30s of soaking time

The micrographies are consistent with the results obtained from the hardness analysis. The microstructure with 10s of soaking time is fundamentally equivalent to that evaluated at 5s, while at 30s the bainite phase is the most prominent phase, with some presence of retained metastable austenite.
The results of this series of evaluations show that it is not possible to exploit the use of longer soaking times in order to amplify the effects of using different die materials. However, they also shows that a certain variation in soaking time

doesn't produce any noticeable effect on the specimen mechanical properties as long as the other parameters are kept constant.
The third case evaluate the effects of die temperature and closing times on the achievable thermal profiles. Three different die temperatures, 25°C, 200°C and 300°C, and three different closing times, 3s, 5s and 10s, have been considered, in accordance to the results of the numerical analyses.
Higher die temperatures reduce the heat flux at interfaces, thus reducing in turn the cooling rates on the specimen. The elevated HTC value at the contact with the steel inserts should however be enough to allow the formation of a fully martensitic microstructure, while the lower HTC value at the ceramic interfaces should inhibit that effect. This should also enable the use of higher closing times. The results in terms of temperature profiles evaluated in the centre of the area under the ceramic insert are visible in Figure 5.20.

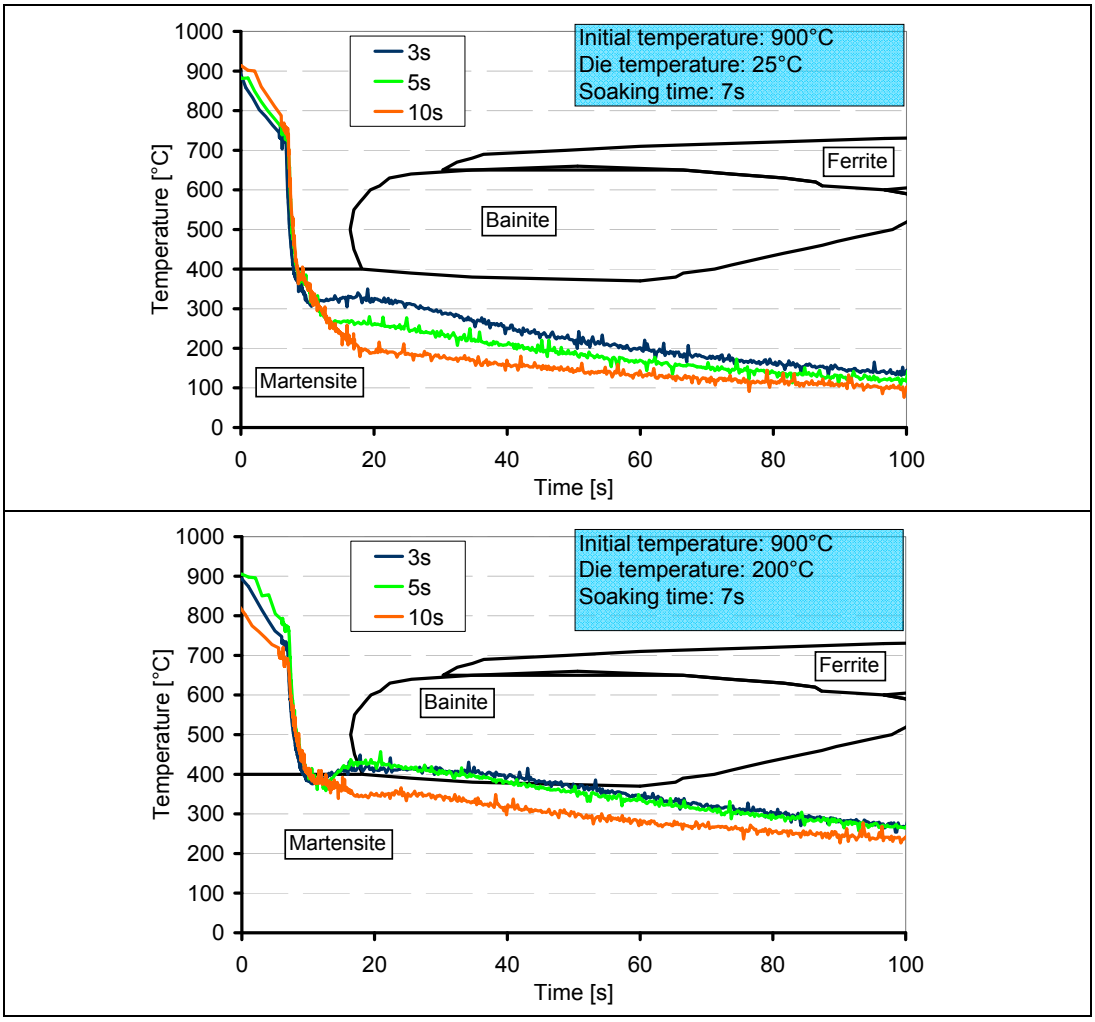

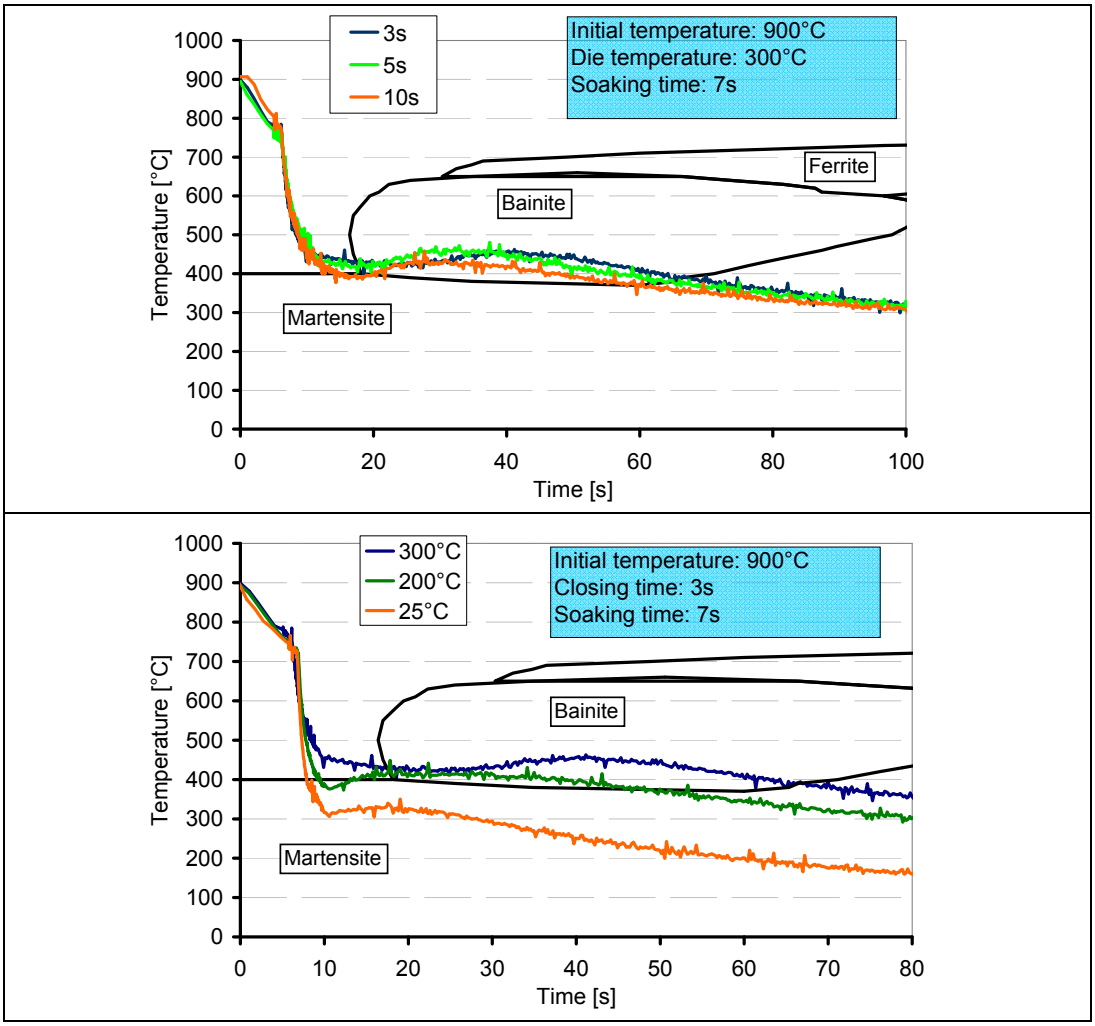

Figure 5.20: Thermal profiles for different closing times and die temperatures with ceramic inserts

These results shows that, at the increase of die temperature, the average cooling rate decrease considerably. While with dies at ambient temperature the final microstructure should be completely martensitic, at 200°C only with 10s of closing time the profile is similar to those obtained with the previous case. At 3s and 5s of closing time, the profiles enter the lower bainite range and the formation of the relative phase, along with a certain quantity of martensite, is expected. With the dies at 300°C the average cooling rates obtained are even slower and temperatures pass completely in the lower bainite range. A completely bainitic microstructure is therefore expected, regardless of the closing time considered. It should also be noticed that the influence of closing time diminish as higher die temperatures are considered, in accordance to the results obtained with the numerical analyses.

The hardness measured along the length of the specimens for the tests performed at 300°C and for the ones with 3s of closing time are reported in Figure 5.21a and Figure 5.21b.

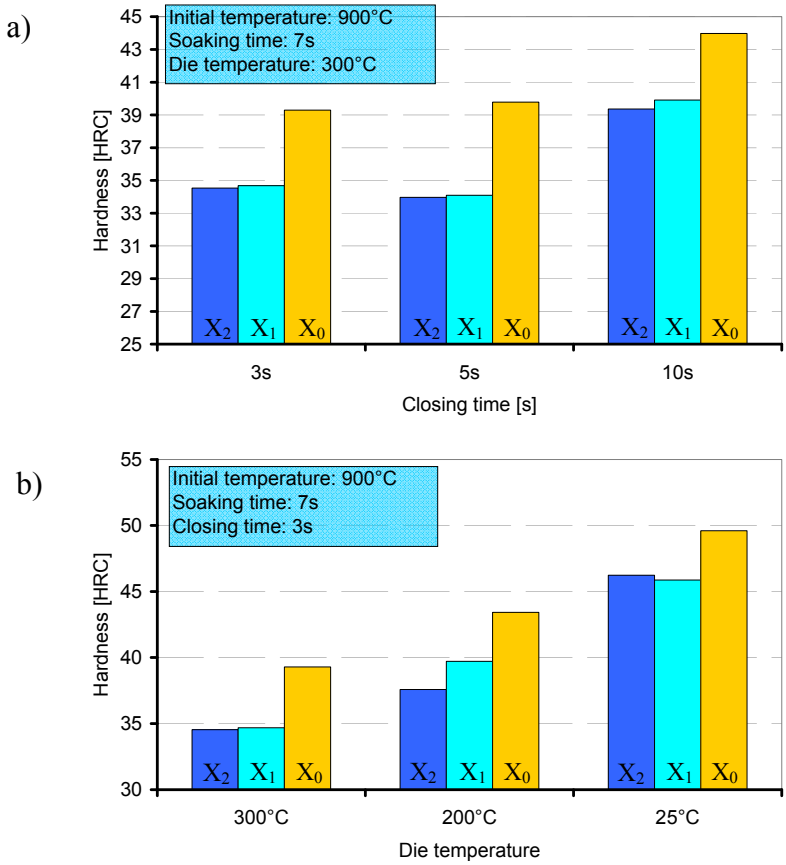

Figure 5.21: Hardness profiles along specimen length a) with dies at 300°C at different closing times and b) at 3s of closing time at different die temperatures

These results shows that higher die temperatures significantly reduce not only the hardness of the areas under the ceramic insert but also that of the areas under the steel inserts. However, the difference between these two values increase as well and, even if the hardness under the steel inserts can lower down to 40 HRC, it is still enough to be considered has having almost completely transformed into martensite, while a hardness of about 35 HRC, as that found on areas under the ceramic insert, is low enough predict a decisive decrease of the mechanical properties due to increased presence of bainite. These results also shows that the influence of closing time at 300°C can be neglected if times lower than or equal to 5s are considered.

The micrographies in figures shows the microstructures in the area X_0 for 3s and 10s of closing time and for 200°C and 300°C of die temperature.

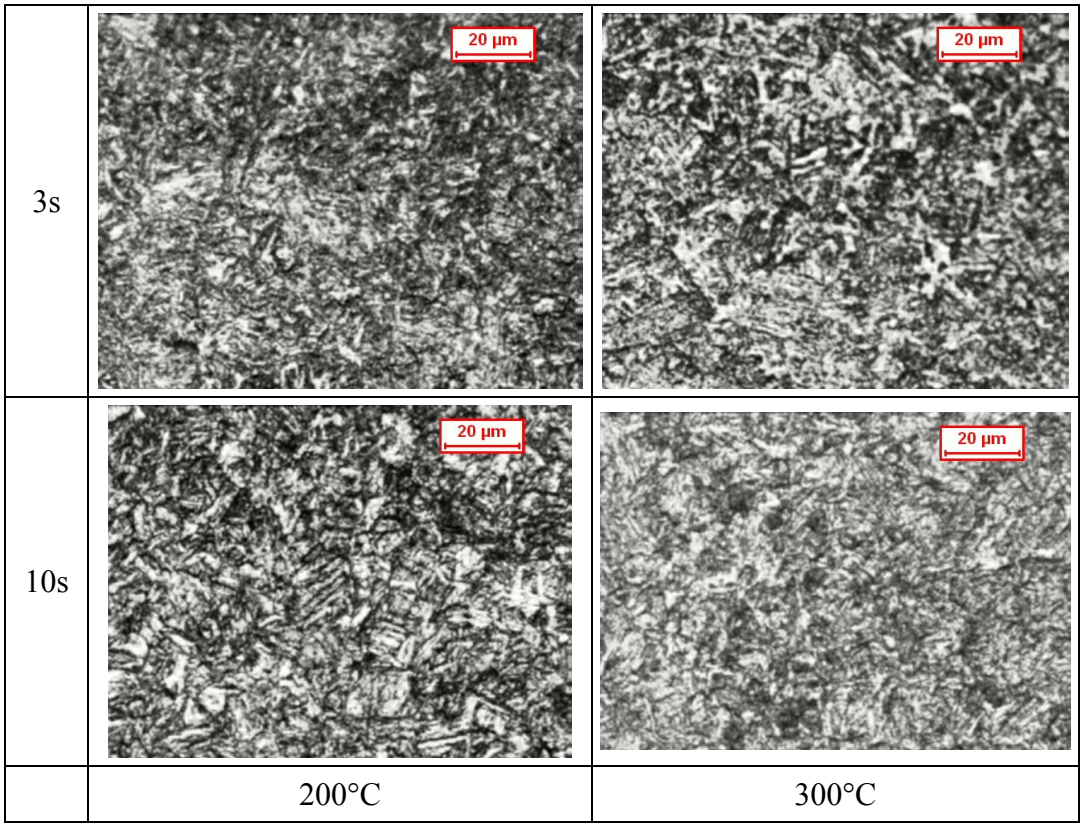

Figure 5.22: Microstructures evaluated in X_0 at 3s and 10s of closing time with dies at 200°C and 300°C

The micrographies show that only at 3s and 300°C a significant fraction of bainite can be noticed, while at 10s and 300°C much lesser amounts can be found. At 200°C in both cases the main phase is still predominantly martensite with probable traces of retained metastable austenite. Traces of lower bainite can still be seen in the 3s case.
The best conditions for the obtainment of a properly graded microstructure, where the difference in mechanical properties at the different points evaluated is maximized, can therefore be found at 300°C if closing times lower than 5s are considered or at 200°C if the closing time is maintained at 3s.
A minimum die temperature of 200°C is therefore requested in order to obtain bainitic phase transformation under the ceramic dies. The results also shows that the die temperature has much more influence in the final obtained mechanical properties than the closing time.

5.5 Experimental and numerical results comparison

The thermal profiles obtained through numerical analyses where directly compared to those acquired with the experimental campaigns in order to understand type and magnitude of errors introduced due to the use of the different simplifications applied in the numerical models. These errors were considered not only relatively to temperature values themselves but also to the tendencies and mutual correlations of the different process parameters that were predicted by the models.

5.5.1 Cooling in calm air

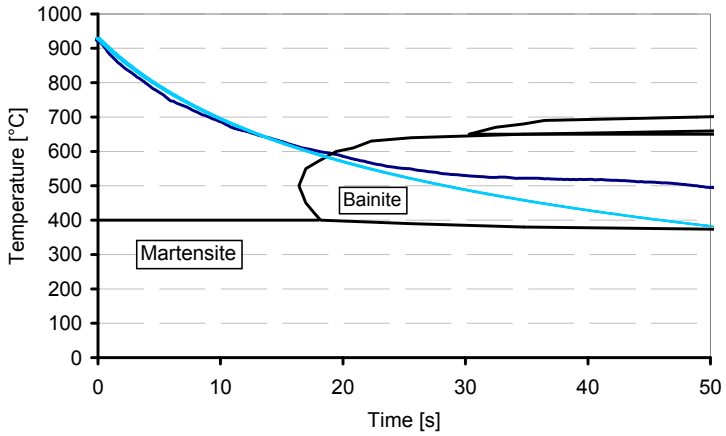

Figure 5.23: Comparison of experimental and numerical results for cooling in calm air

This comparison, visible in Figure 5.23, shows that numerical and experimental data are in good agreement as long as the area before the onset of phase transformations is considered. This is due to the fact that the model doesn't consider the latent heat generation and therefore the two results differs more as more austenite transforms into bainite. It however also shows that the assumptions made regarding heat exchanged with the environment during numerical model setup are correct.

5.5.2 Cooling on dies with air gap

The comparison between the thermal profiles predicted by the numerical model

and those obtained through experimental testing are visible in Figure 5.24.

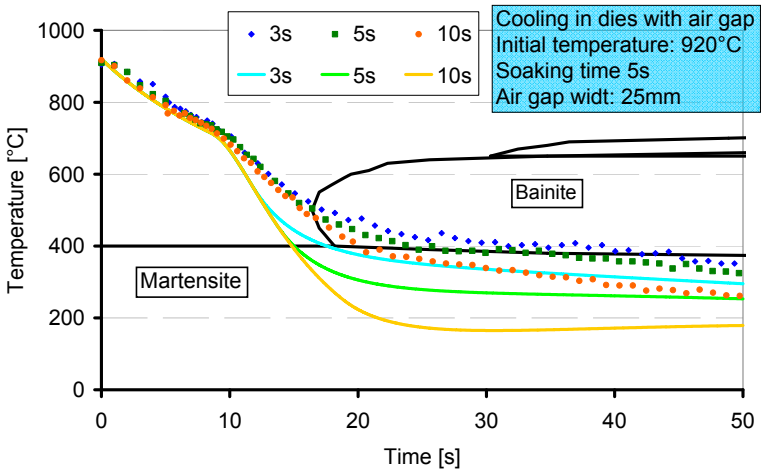

Figure 5.24: Comparison between calculated and experimental results for the case of dies with air gap

These comparison shows as there's a moderate difference between calculated and experimental results as soon as the dies closes. This is probably due to the abrupt change in convection regime in the air gap in the dies, since, due to the geometry of the air gap itself, the open boundaries approximation used for the definition of the convection coefficient is no longer valid.

5.5.3 Cooling in dies with ceramic inserts

5.5.3.1 Geometrical configuration dependence

The comparison is shown in Figure 5.26 for the cases with ceramic inserts 25mm and 75mm wide

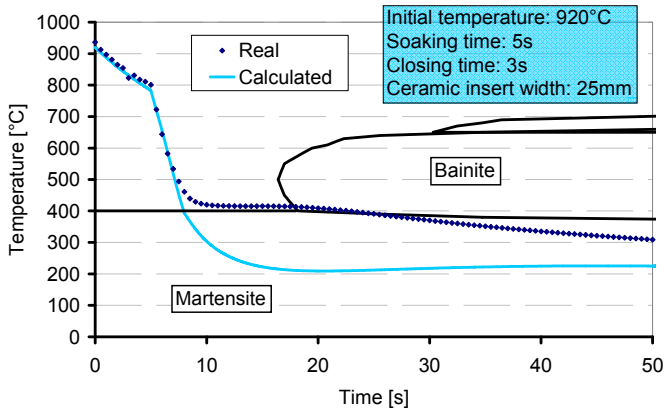

Figure 5.25: Comparison of experimental results with numerical results from monodimensional model for a ceramic insert 25mm wide

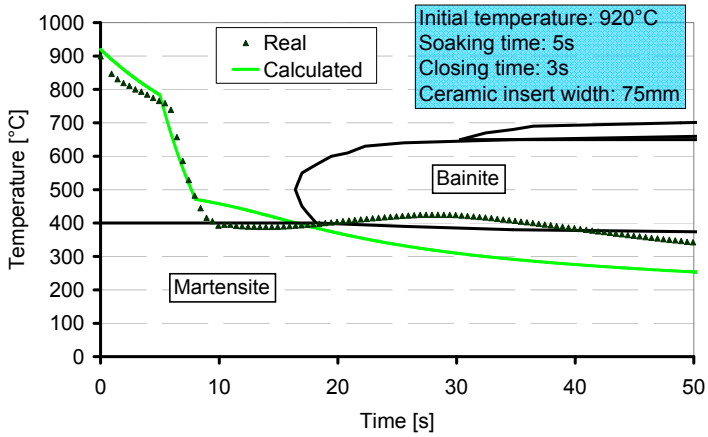

Figure 5.26: Comparison of experimental results with numerical results from monodimensional model for a ceramic insert 75mm wide

These results shows good agreement in the prediction of the slope of the thermal profile during pressing, meaning that the model can predict with good accuracy the heat exchanged at the different interfaces. The predictions depart from the real profile when the heat generated due to phase transformation become prominent in relation to the heat exchanged with the environment. This is visible as soon as the temperature reach martensite start value in the 25mm case and even before that for the 75mm case, meaning that phase transformation in the areas under the steel inserts can influence the temperature profile achieved under the ceramic insert.

5.5.3.2 Soaking time dependence

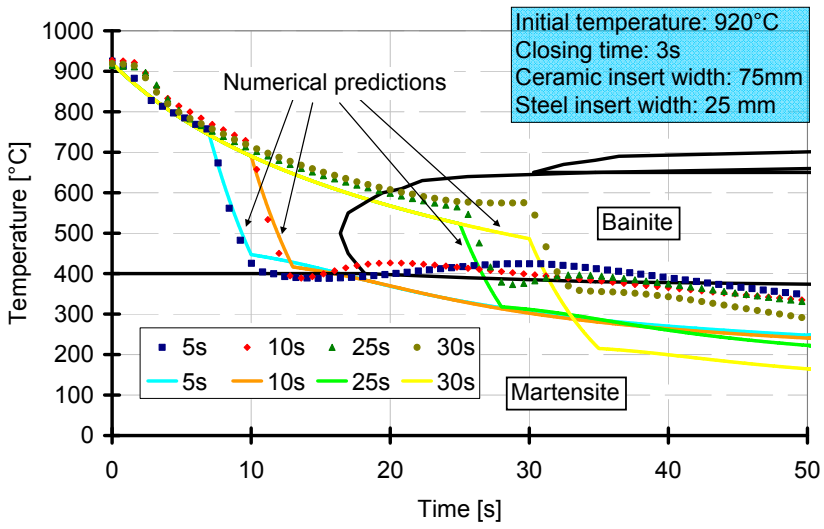

Figure 5.27: Comparison of experimental results with numerical results from monodimensional model for soaking time dependence

Also in this case the same trends seen in the previous cases are visible. The numerical predictions are close to the experimental behaviour as long as latent heat doesn't become elevated. In this case this is particularly visible since at the increase of the soaking time, and therefore as more material transforms into bainite before pressing, the error done by the model is increasing.

5.5.3.3 Die temperature and closing time dependence

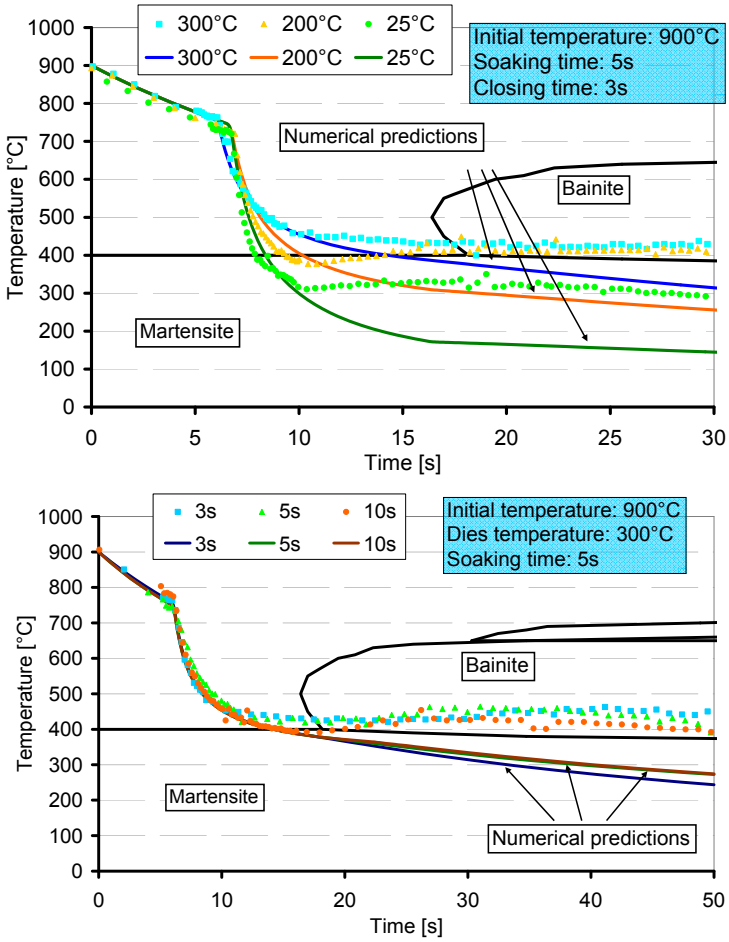

Figure 5.28: Comparison of experimental results with numerical results from bisimensional model for closing die temperature and soaking time dependences

These comparisons shows that the numerical predictions that were, unlike the other cases, obtained through the use of the bidimensional model, can predict the thermal behaviour of the system with a very good accuracy, higher than that obtained with the monodimensional model, until the latent heat due to phase transformation is contained. The variations in cooling rate due to increasing die temperature is also correctly predicted.

The comparison between real and calculated thermal profiles for the case with 10s of closing time and the dies at room temperature, where the effects of latent heat are most evident, is visible in Figure 5.29.

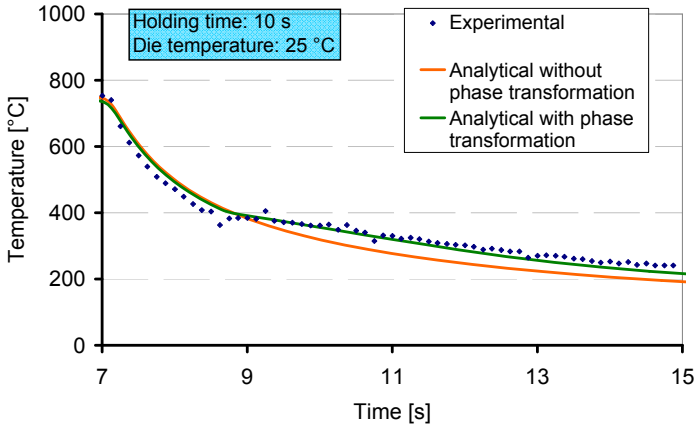

Figure 5.29: Thermal profile comparison between numrical models, with and without latent heat evaluation, and experimental results

This comparison clearly shows than, when introducing the latent heat into the bidimensional model, the predictions can become even more adherent to the results obtained from the experiments. It should also be noticed however that the increase in computational power needed is not negligible.

5.5.4 Conclusions

The results of these tests allow to develop a deeper understanding of the mechanisms that concur to define the thermal profile achieved on a hot stamped sheet. The results of test performed using air gaps shows that the only presence of grooves on dies used in hot stamping operations, at least for air gaps narrower than 25mm, is not enough to enable the formation of a microstructure soft enough to represent a concrete advantage in a real hot stamping process. The thermal profiles obtained through the use of ceramic inserts are aligned to those obtained using air gaps, but they enable to control blank deformations if used on hot forming dies.
When using ceramic dies, a minimum width of 75mm is advisable, while, among all the evaluated parameters, the die temperature showed to be the most influencing. In order to obtain a fully bainitic microstructure, a temperature of 300°C as die temperature is necessary along with closing times no longer than 5s. Similar results can also be found at 200°C if the closing time is contained at 3s. The decreased influence of closing time at the increase of die temperatures enable to use even longer closing time at the expense of higher material final mechanical properties.

6 Conclusions

In order to improve the ability to properly design an hot stamping process and to extend the knowledge of the mechanical properties of an ultra high strength steel and of the thermal behaviour of a blank under hot forming conditions, both formability and the thermal evolution during stamping of an Ultra High Strength Steel, the 22MnB5, have been evaluated.
In order to assess the formability of this material, an experimental equipment dedicated to performing Nakajima tests at elevated temperatures has been designed and calibrated. This was then used in order to perform two test campaigns, at different temperatures, representing conditions found in real hot forming processes. The test procedure was defined so that the test was performed with the specimen still in austenitic phase.
The strain profiles obtained through testing were analyzed using two different procedures, one adherent to ISO 12004 standard, which is commonly used to evaluate Forming Limit Curves at room temperature, and one considering the highest strain values reached along sections normal to fracture direction. This enabled to trace two different Forming Limit Diagrams for every temperature.
The results shows an increase in formability if confronted to the values achieved at room temperature, in accordance to rheological tests already performed in literature. This is clearly visible in the FLCs evaluated using standard ISO procedure, but is much more prominent in the FLCs evaluated using the maximum strain values approach. This method should also be considered more useful in actual process design since the majority of deformations, in a hot stamping process, are expected to take place after the onset of local instabilities.
However, these latter curves also exhibits higher scattering of the results, meaning that new standards for a sound evaluation of the formability limit in hot forming conditions are necessary.
The other major issue considered was the analysis of the thermal profile developed by the blank under the dies. The final goal was to exploit that knowledge in order to assess the possibility of obtaining functionally graded shapes locally reducing the heat transfer coefficient at the interface with the dies.
In order to evaluate the most influencing process parameters, a particular case study was proposed in order to analyze the influence of every single factor individually in the most controllable conditions.
Two different numerical models were at first developed. These enabled to

individuate the theoretical limits of the approach, to estimate the effects and the nature of the most influencing factors and to plan experimental testing. In these analyses, the possibility of using ceramic insert to locally alter the thermal profile of the blank to the point where softer microstructure can develop was evaluated.
The analytical results assessed the feasibility of the considered approach and were used to individuate the ranges of values of test parameters where their influence is most appreciable. These results were used to define the experimental campaigns.
In order to evaluate the most appropriate ceramic to be used as insert material in a hot stamping process, the tribological properties of two materials, that were chosen among the most commonly used for their particular mechanical and thermal properties, where tested. The best suited material was found to be Zirconium dioxide.
A number of experimental campaigns where then performed using a plane pressing configuration. Through these tests, the influence of different die materials, closing time, soaking time and die temperature was assessed.
The results from these tests show the geometrical limitations of such approach and demonstrate the advantages of using a combined approach where both different die materials and heating of the dies are used. These results were then used to assess the combination of process parameters which produce the best results for the obtainment of functionally graded shapes.
In the end, the results from experimental testing were also used to verify the reliability of the analytical results in describing the thermal evolution of the blank. Even the results of the most simple model were found to be in good agreement with the experimental results as long as the heat generated due to phase transformation is contained if confronted to the other heat fluxes involved. The bidimensional model is able to describe the thermal evolution of the blank even better, particularly if latent heat due to martensitic phase transformation is considered, at the expense of much greater computational times.
This work therefore shows that, through appropriate analysis of all the concurring effects of the different thermal phenomena involved, it is possible to design an hot stamping process controlling with elevated accuracy the thermal evolution of all the different areas of the blank so that its microstructural evolution, and therefore its final properties, can be accurately defined.

References

[1] Berglund, G., *The history of hardening of boron steel in northern* Sweden, 1st international conference on Hot Sheet Metal Forming of High-Performance Steel, Kassel (2008), Germany, pages 175-177

[2] Aspacher J., *Forming hardening concepts*, 1st international conference on Hot Sheet Metal Forming of High-Performance Steel, Kassel (2008), Germany, pages 77-81

[3] Stahl-Information-Zentrum. *Stahl im Automobil, Leicht und sicher*. www.stahl-info.de

[4] Turetta, A., *PhD Thesis* (2008), Padova, Italy

[5] *Usibor® 1500P and Ductibor® 500P the ultimate tool for weight and cost reduction*, www.arcelormittal.com

[6] Pferstorf P., *Manufacturing of high strength steel and aluminium for a mixed material body in white*, Sheet Metal 2005, Erlangen, Germany, pages 109-124

[7] Merklein M., Lechler, J., *Investigation of the thermo-mechanical properties of hot stamping steels*, Journal of Material Processing Technology 177 (2006), pages 452-455

[8] Lechler J., Merklein M., *Investigation on forming limits within hot stamping*, 1st international conference on Hot Sheet Metal Forming of High-Performance Steel, Kassel (2008), Germany, pages 55-61

[9] Karbasian H., Tekkaya A.E., *A review on hot stamping*, Journal of Materials Processing Technology 210 (2010), pages 2103-2118

[10] Picas I., Hernández R., Casellas D., Valls I, *Cold cutting of microstructurally tailored hot formed components*, 2nd international conference on Hot Sheet Metal Forming of High-Performance Steels (2009), Luleå, Sweden, pages 115-126

[11] So H., Hoffmann H., Golle R., *Blanking of press hardened ultra high strength steel*, 2nd international conference on Hot Sheet Metal Forming of High-Performance Steel (2009), Luleå, Sweden, pages 137-145

[12] Paar U., Becker H., Alsmann M., *Press-hardened components from Kassel – chances and challenges*, 1st international conference on Hot Sheet Metal Forming of High-Performance Steels (2008), Kassel, Germany, pages 153-163

[13] Lechler J., Merklein M., *Hot stamping of ultra strength steels as a key technology for lightweight contruction*, Materials Science and Technology (2008), Pittsburg, pages 1698-1709

[14] Borsetto F., *Tribological performance of environmentally friendly solid*

lubricant coatings for sheet metal forming, PhD Thesis (2010), Padova, Italy

[15] Kolleck R., Veit R., Hofmann H., Lenze F., *Alternative heating concepts for sheet metal forming*, 1st international conference on Hot Sheet Metal Forming of High-Performance Steels (2008), Kassel, Germany, pages 239-246

[16] Neugebauer R., Göschel A., Sterzing A., Shieck F., *Gas forming with integrated heat treatment for high performance steel – a solution approach for press hardened tubes and profiles*, 2nd international conference on Hot Sheet Metal Forming of High-Performance Steels (2009), Luleå, Sweden, pages 181-188

[17] Lindkvist G., Häggblad H., Oldenburg M., *Thermo-mechanical simulation of high temperature formblowing and hardening*, 2nd international conference on Hot Sheet Metal Forming of High-Performance Steels (2009), Luleå, Sweden, pages 247-254

[18] Casas B., Latre D., Rodriguez N., Valls I., *Tailor made tools materials for the present and upcoming tooling solutions in hot sheet metal forming*, 1st international conference on Hot Sheet Metal Forming of High-Performance Steels (2008), Kassel, Germany, pages 23-35

[19] Picas I., Hérnandez R., Casellas D., Casas B, Valls I., *Tool performance in cutting of hot stamped steels*, 1st international conference on Hot Sheet Metal Forming of High-Performance Steels (2008), Kassel, Germany, pages 179-189

[20] Somani M., Karjalainen L., Eriksson M., Oldenburg M., *Dimensional changes and microstructural evolution in a B-bearing steel in the simulated forming and quenching process*, Iron and Steel Institute of Japan (ISIJ) International, vol. 41 (2001), pages 361-367

[21] Borsetto F., Ghiotti A., Bruschi S., *Investigation of the high strength steel Al-Si costing during hot stamping operations*, Key Engineering Materials 410-411 (2009), pages 289-296

[22] Goedicke S., Sepeur S., Frezner G., Breyer C., *Wet chemical coating materials for hot sheet forming - anti scaling and corrosion protection*, 1st international conference on Hot Sheet Metal Forming of High-Performance Steels (2008), Kassel, Germany, pages 37-44

[23] Merklein M., Lechler J., *Determination of material and process characteristics for hot stamping processes of quenchable ultra high strength steels with respect to a FE-based process design*, SAE World Congress, Innovations in Steel and Applications of Advanced High Strength Steels for Automobile Structures (2008), Paper no. 2008-0853

[24] Durrenberger L., Wilsius J., Hein P., *Impact of the constitutive model on the hot forming numerical predictions of Usibor 1500P*, 2nd international conference on Hot Sheet Metal Forming of High-Performance Steels (2009), Luleå, Sweden, pages 51-58

[25] Hocholdinger B., Grass H., Lipp A., Hora P., *Modeling and determination of flow curves for the simulation of hot forming*, International Deep Drawing Research Group 2009 (2009), Golden, CO, USA, pages 659-669

[26] Kalpakjian S., Schmid S., *Manufacturing, Engineering and Technology*,

5th edition
[27] Keller S., *Circular grid system: a valuable aid for evaluation sheet forming*, Sheet Met. Ind. 45 (1969), pages 633-640
[28] Goodwin G., *Application of strain analysis to sheet metal forming problems*, Metall, Ital. 60 (1968), pages 767-771
[29] Arrieux R., Chalons J., Bedrin J., Bovin M., *Computer aided method for the determination of the FLD at necking*, CIRP annals 33/1 (1984), pages 171-174
[30] Nakazima K., Kikuma T., Asaku K., *Study on formability of steel sheet*, Yawata Technical report 264 (1968)
[31] Marciniak Z., Kuczynzky K., *Limit strains in the process of stretch-forming sheet metal*, International Journal of Mechanical Sciences 9 (1967), pages 609-620
[32] Swift H., *Plastic instability under plane stress*, J. Mech. Phys. Solids 1 (1952), pages 1-18
[33] Hill R., *On discontinuous plastic states with special reference to localized necking in thin sheets*, J. Mech. Phys. Solids 1 (1952), pages 19-30
[34] Banabic D., Bunge H., Pohlandt K., Tekkaya A., *Formability of Metallic Materials* (2000), Berlin
[35] Nie Q., Lee D., Matter J., *The effect of strain rate sensitivity on history dependent forming limits of anisotropic sheet metals*, Journal of Material Shaping Technology 9 (1991), pages 233-240
[36] Standard ISO 12004-2:1997, TC 164/SC 2
[37] Lamprecht K., Deinzer G., Stich A., Lechler J., Stöhr T., Merklein M., *Thermo-mechanical properties of tailor welded blanks in hot sheet metal forming processes*, International Deep Drawing Research Group (IDDRG) 2010, Graz, Austria, pages 37-48
[38] Saeglitz M., Bake K., Gernert U., *Microstructure and mechanical properties in the transition zone of a low carbon boron steel after partial hardening*, International Deep Drawing Research Group (IDDRG) 2010, Graz, Austria, pages 91-99
[39] Lenze F., Sikora S., Banik J., Sauer D., *Development tendencies as to processing of press gardening under application of coated steel*, 1st international conference on Hot Sheet Metal Forming of High-Performance Steels (2008), Kassel, Germany, pages 15-21
[40] Mori K., Okuda Y., *Tailor die quenching in hot stamping for producing ultra-high strength steel formed parts having strength distribution*, CIRP annals – Manufacturing technology 59 (2010), pages 291-294
[41] George R., Bardelcik A., Worswick M., *Localized die temperature control for tailored properties in hot forming of boron steels-numerical study*, International Deep Drawing Research Group (IDDRG) 2009, Golden, CO, USA, pages 131-139
[42] Laumann T., Picas I., Grané M., Casellas D., Riera M. D., Vaals I., *Hard cutting of tailored hardened 22MnB5*, International Deep Drawing Research

Group (IDDRG) 2010, Graz, Austria, pages 355-362
[43] Salomonsson P., Oldenburg M., Åkerström P., Bergman G., *Experimental and numerical evaluation of the heat-transfer coefficient in press hardening*, 1st international conference on Hot Sheet Metal Forming of High-Performance Steels (2008), Kassel, Germany, pages 267-274
[44] Hay B., Bourouga B., Dessain C., *Thermal contact resistance estimation at the blank/tool interface: experimental approach to simulate the blank cooling during the hot stamping process*, International Journal of Material Forming 3 (2010), pages 147-163
[45] Bonacina M., Cavallini A., Mattarolo L., *Trasmissione del calore*, Padova (1985)
[46] Merklein M., Lehcler J., Geiger M., *Determination of thermal and mechanical material properties for hot stamping processes of ultra high strength steels*, SAE International (2007), pages 7-22
[47] Burmeister L., *Convective heat transfer*, New York NY, USA (1993)
[48] Jaluria Y., Torrance K., *Computational heat transfer*, USA (1986)
[49] Mikhlin S., Smolitskiy K., *Approximate methods for solution of differential and integral equations*, Modern Analytic and Computational Methods in Science and Mathematics, New York (1967)
[50] *Matlab user's manual*, Mathworks (2009)
[51] Porter D., Easterling K., *Phase transformation in metals and alloys*, second edition, Padstow, Cornwall, Great Britain (1992)
[52] Zhao H., Liu X., Wang G., *Progress in modeling of phase transformation kinetics, Journal of Iron and Steel Research*, International 13 (2006), pages 68-73
[53] Naderi M., Durrenberger L., Molinari A., Bleck W., *Constitutive relationships for 22MnB5 boron steel deformed isothermally at high temperatures*, Materials Science and Engineering A 478 (2008), pages 130-139
[54] Bariani P.F., Bruschi S., Ghiotti A., Turetta A., *Testing formability in the hot stamping of HSS*, CIRP Annals – Manufacturing technology 57 (2008), pages 265-268
[55] ISO 6020-2:2006 standard
[56] DZCE7G, balancing valve with proportional control and integrated electronics, www.duplomatic.com
[57] DSPE7G, Pilot operated directional valve with proportioinal control and integrated electronics, www.duplomatic.com
[58] PZ67-S, Rectilinear displacement transducer with IP67 protection level, www.gefran.com
[59] CTBKN5C, Toroidal force transducerfor industrial applications, www.gefran.com
[60] *ARAMIS user's manual*, GOM
[61] Lechler J., Merklein M., *Determination of forming limit diagrams at elevated temperatures for failure prediction within hot stamping of*

quenchable ultra high strength steels, International Conference on Technology of Plasticity (ICTP) 2008, pages 1842-1847